Synthesis and Self-Assembly of Organometallic Semiconducting PMMA-*b*-PFS-*b*-PS-*b*-PFS-*b*-PMMA Pentablock Copolymers

Dem Fachbereich Chemie
der Technische Universität Darmstadt

zur Erlangung des akademischen Grades eines

Doctor rerum naturalium (Dr. rer. nat.)

genehmigte
DISSERTATION

eingereicht von

M. Tech. Chem. Uttam Datta
aus New Delhi (India)

Berichterstatter:	Prof. Dr. M. Rehahn
Mitberichterstatter:	Prof. Dr. E. Gruber
Tag der Einreichung:	Mai 9, 2005
Tag der Mündlichen Prüfung:	Juni 27, 2005

Darmstadt 2005

D17

In the loving memory of my papa

ACKNOWLEDGEMENT

As I sit here in front of my ThinkPad I realize that writing an acknowledgement is perhaps the most difficult part of a Ph.D. dissertation. How can you mention all of the people you have interacted with in a page or two? Therefore, the first thing I would like to say is ***THANK YOU*** to all the people with whom I have worked with over the past three years.

First and foremost I would like to express my deepest gratitude to my supervisor Prof. Dr. Matthias Rehahn (Dekanat, Fachbereich Chemie, TUD) whose sincere and invaluable guidance helped me in bringing this thesis work to a successful completion. Thanks for all the discussions and the ideas.

This work could not have been carried out without the help and support of Dr. Christian Kloninger (presently scientist in 3M, Neuse) who introduced me to the concept of anionic polymerization and got me started in the lab with the high vacuum line and the schlenk techniques. My sincere thanks to Dr. Roland Klein for the SAXS measurements at DESY and frequent little snags regarding the local area network, computers, printers etc.

I also thank my colleagues including Michael Roth, Stefan Tockner and Dr. Bellas for making the work atmosphere lively.

My heartfelt warm thanks to Frau Cornelia Gräfing (Conny) for everyday trouble shooting small and big problems associated with the formalities of TUD and my stay as a foreigner in Darmstadt.

My special thanks to Dr. Jianjan Xu for all the efforts with regard to the DRS conductivity measurements. I would also like to acknowledge the discussions with Prof. Dr. Volker Abetz regarding microphase separation and SAXS data interpretation. Thanks to Herr Christoph Brinkmann for the GPC analyses, Dr. Tilmann Ruhl for training me on TEM and Dr. Birgit Staben for TGA/DSC measurements.

At this moment I wish to acknowledge the blessings and good wishes of my family members. A special thanks to papa's grandson '*Hercules*'. Last but not the least, I have no words to acknowledge the contribution of my better half Dr. Anupama Datta whose constant emotional support and encouragement made all the difference and without whom I am sure I would not have made it.

Diese Arbeit wurde am Ernst-Berl-Institut für Technische und Makromolekulare Chemie der Technische Universität Darmstadt und am Deutschen Kunststoff Institut Darmstadt, unter der Leitung von Prof. Dr. M. Rehahn in der Zeit von Juni 2002 bis Juni 2005 durchgeführt.

TABLE OF CONTENTS

Chapter 1

Introduction

1. Block Copolymers

Block copolymers are a fascinating class of polymeric materials belonging to a big family known as "soft materials". This class of polymer is made by the covalent bonding of two or more polymeric chains that, in most cases, are thermodynamically incompatible giving rise to a rich variety of microstructures in bulk and solution. The length scale of these microstructures is comparable to the size of the block copolymer molecules (ca. 5-50 nm) and therefore the microstructures are highly coupled to the physical and chemical characteristics of the molecules. The variety of microstructures results in materials with applications ranging from thermoplastic elastomers and high impact resistant plastics to pressure sensitive adhesives, additives, foams etc. Further, block copolymers are very strong candidates for potential applications in advanced technologies such as information storage, nanolithography, drug delivery and photonic crystals.

1.1 Types of Block Copolymers

The architecture[1-4] of copolymers can be controlled by the synthetic strategies and it is possible to prepare diblock, triblock, multiblock, starblock and graft copolymers (**Fig. 1.1**).

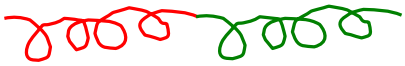

Diblock Copolymer (AB)

Triblock Copolymer (BAB)

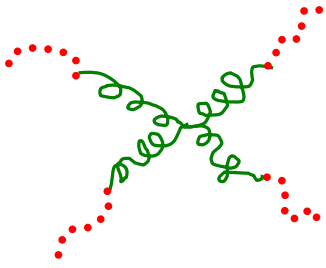

Four Arm Star Block

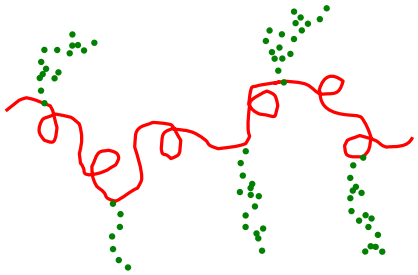

Graft Copolymer

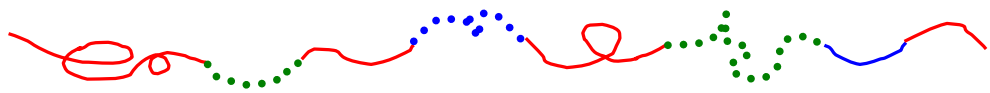

Random Multicomponent Multiblock

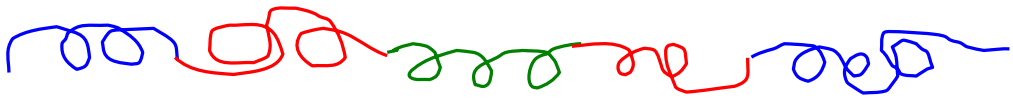

Linear AB_2C_2 Pentablock

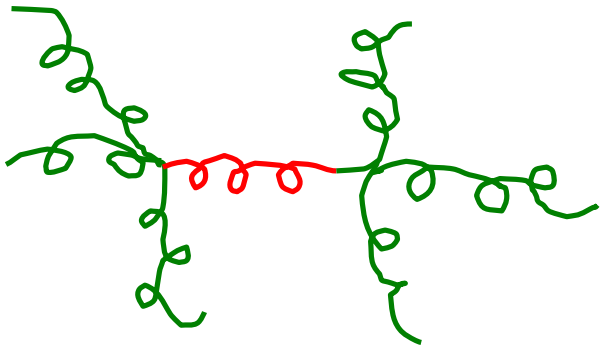

A_3BA_3 Super H-shaped Block Copolymer

Fig. 1.1 *Different possible architectures of block copolymers.*

1.2 General Methods for Synthesis of Block Copolymers

1.2.1 *Cationic Polymerization*

In the middle eighties with the discovery of true living cationic polymerization of vinyl ethers, Higashimura et al.[5] have shown their real potential for the synthesis of tailor-made macromolecules. In this type of polymerization chain propagation is achieved through a carbocation, which can be generated by a cationic initiator and a vinyl monomer.[6] Carbocations in general are very reactive and unstable, consequently they can

participate in a number of side reactions like termination, chain transfer and carbocation rearrangements. However, they can be stabilized by using an appropriate counterion or a carefully selected Lewis base.[7] The most common monomers used for cationic polymerization are isobutylene, vinyl ethers, styrene and its derivatives with electron donating groups, N-vinyl carbazole, furan and some other heterocyclic monomers.[8-10]

1.2.2 *Living Free Radical Polymerization*

Free radical polymerization is widely used for the industrial preparation of a large number of polymeric materials like LDPE, PVC etc.[11] This polymerization process is tolerant of protic and aqueous solvent media. However the disadvantage of the free radical mechanism is that the polymers produced are polydisperse in nature due to termination and chain transfer processes leading to little control over their molecular characteristics. Recent advances in free radical polymerization have led to the development of synthetic methods that suppress the undesired termination and chain transfer reactions[12] by using persistent free radicals like nitroxides as reversible terminating agents[13, 14] and transition metal complexes such as CuX/ bipyridine (X = halogen). Metal complexes with Ru, Fe, Ni, Rh and Pd are also employed which involve atom transfer in a reversible reaction, thereby lowering the equilibrium concentration of the radical intermediates tremendously [ATRP]. [15-18]

1.2.3 *Group Transfer Polymerization*

Group transfer polymerization (GTP) is a Michael type catalyzed addition reaction.[19] A silyl ketene acetal is usually used as the initiator. The silane group is transferred to the growing chain end after the addition of each monomer. Thus, the chain end remains active till the complete consumption of monomer. This type of polymerization has been widely applied for the polymerization of methacrylic monomers at room temperature, in the presence of various side groups, sensitive to ionic or radical polymerization reactions.[20]

1.2.4 *Ring Opening Metathesis Polymerization*

Ring opening metathesis polymerization (ROMP) has recently emerged as a valuable tool for the polymerization of a wide variety of strained cyclic alkene monomers.[21] ROMP is a transition-metal-mediated polymerization technique and can proceed in a living manner if the transition metal initiator and other experimental conditions are properly chosen. A typical characteristic example is the polymerization of norbornene with titanacyclobutane complexes.[22, 23]

1.2.5 *Living Anionic Polymerization*

Living anionic polymerization has been known for almost fifty years now.[24-26] The first insightful description of the "living" nature of anionic polymerization of styrene and diene monomers was given by Szwarc and co-workers. A *living anionic polymerization* is a chain polymerization that proceeds in the absence of the kinetic steps of *termination* or *chain transfer*.[27] It has emerged as the most powerful synthetic tool for the preparation of well-defined block copolymers with narrow molecular weight distribution and controlled molecular characteristics like composition, microstructure and architecture. Polydispersity index (PDI) as a function of the degree of polymerization, X_w and X_n, for a living polymerization is given by[28, 29] **eq. 1.2a**

$$PDI = X_w/X_n \qquad \textbf{1.2a}$$

where X_w is the weight average degree of polymerization and X_n is the number average degree of polymerization.

1.2.5a *Experimental Criteria for Living Anionic Polymerizations*

The following experimental criteria have been proposed for living anionic polymerizations:

(i) The rate of initiation (R_i) must be comparable (slightly more) to the rate of propagation (R_p) making it possible to prepare a polymer with a narrow molecular weight distribution. This ensures that all of the chains grow essentially at the same period of time.

(ii) The number average molecular weight M_n is a linear function of conversion.

(iii) No chain termination or chain transfer caused by side reactions of the monomers, impurities, water, oxygen etc.

(iv) There should only be one propagating carbanion active species. If there are more than one species then they must be in an open equilibrium so that on the time-average all the chains grow uniformly.

1.2.5b *Suitable Monomers*

Monomers suitable for anionic polymerization can be classified into two broad categories namely (i) vinyl, diene and carbonyl type monomers with bifunctionality provided by the double bonds and (ii) cyclic (e.g. heterocyclic) monomers where difunctionality is provided by a ring that can open by reaction with nucleophiles. Monomers based on styrene, dienes, vinyl pyridines and alkyl methacrylates represent the former categories[30-41] while epoxides, cyclic sulfides and lactones etc. represent the latter.[42-47]

1.2.5c *Initiators*

Generally the initiators employed are low molecular weight organometallic compounds e.g. alkyl lithiums. The main reason behind the employment of an organometallic compound as an anionic initiator is its rapid reaction with the monomer at the initiation step of the polymerization reaction particularly with a rate larger than that of propagation step. This leads to the formation of polymers with narrow molecular weight distributions as all active sites start to polymerize the monomer almost at the same time. The different kinds of initiators used in anionic polymerization are as follows:

(i) Alkali *Metals*: The direct use of alkali metals as initiators for polymerization of diene monomers is primarily of historical interest.[48] Initiation is a heterogeneous process on the surface of the metal (M_t) by transfer of an electron to adsorbed monomer.

(ii) *Radical Anions*: Many aromatic hydrocarbons react with alkali metals in polar aprotic solvents to form stable solutions of the corresponding radical anions e.g.

$$M_t + Ar \rightleftharpoons Ar^{\cdot -} M_t^+ , M_t = Li, Na, K, Rb, Cs$$

Subsequent initiation of chain propagation again proceeds via electron transfer followed by recombination of two intermediate radical anions. Monomers that can be polymerized with aromatic radical anions include styrenes, dienes, epoxides and cyclosiloxanes.[49] Difunctional initiators are of considerable interest for the preparation of triblock copolymers, pentablock and macrocyclic polymers. Aromatic radical anions, such as lithium naphthalide or sodium naphthalide are efficient difunctional initiators.[51-54]

(iii) *Alkyllithium Compounds*: A variety of simple alkyllithium compounds are commercially available in hydrocarbon solvents such as hexane and cyclohexane. The important differences between the various alkyllithium compounds are their degree of aggregation in solution and their relative reactivity as initiators for anionic polymerization of styrene and diene monomers. *n*-Butyllithium and *sec*-butyllithium are used commercially to initiate anionic homopolymerization and copolymerization of butadiene, isoprene and styrene with linear and branched structures.[50]

1.2.5d *Kinetics and Mechanism of Living Anionic Polymerization*

The term living polymers is often used to describe systems in which propagating chain ends remain active after polymerization, so that a new batch of monomer subsequently added would be incorporated to the existing chains and increase their degree of polymerization.

(i) *Initiation*: Initiation step is a reaction that generates reactive reaction intermediates, which then participate in a chain reaction.

$$I \text{ (Initiator)} \longrightarrow I^* \text{ (Initiating Species)} \qquad \textbf{1.2b}$$

$$I^* + M \xrightarrow{k_i} I—M^* \qquad \textbf{1.2c}$$

[* Represents an active reaction center]

(ii) *Propagation*: Propagation proceeds through nucleophilic attack of a carbanionic site onto a monomer molecule with reformation of the first anionic active center. Propagation step is the continuous regeneration of reactive intermediates as shown where 'i' is an index indicating the degree of polymerization of the growing polymer chain, P_i^*

$$P_i^* + M \xrightarrow{k_p} P_i\text{—}M^* \equiv P_{i+1}^* \qquad \textbf{1.2d}$$

(iii) *Termination*: This is the step in a chain reaction in which the reactive reaction intermediates are destroyed or rendered inactive thus ending the chain. Here 'P' is dead or inactive polymer with respect to chain growth.

$$P^* \longrightarrow P \qquad \textbf{1.2e}$$

(iv) *Chain Transfer*: This involves the transfer by the reactive intermediate end of a growing chain polymer, of an atom (or group) to or from another molecule (or polymer). Chain transfer reaction is illustrated below where A-X is the chain transfer agent and A* is a new reactive intermediate capable of continuing the chain growth reaction by reinitiating chain growth at a rate comparable to the normal chain propagation rate.

$$P^* + AX \longrightarrow P\text{—}X + A^* \qquad \textbf{1.2f}$$

$$A^* + M \longrightarrow A\text{—}M^* \qquad \textbf{1.2g}$$

The kinetics for a living polymerization follows relatively simple pseudo 1st order behaviour as shown **eq. 1.2h**

$$R_p = -d[M]/dt = k_p[P^*][M] = k_{obs}[M] \qquad \textbf{1.2h}$$

If the concentration of active propagating species is constant (i.e. no chain termination) integration of the above equation yields

$$\ln[M]_0/[M] = k_{obs}t \qquad \textbf{1.2i}$$

The diagnostic test for chain transfer is conducted by calculating the number average degree of polymerization that is defined as **eq. 1.2j**

$$X_n = ([M]_0-[M]_t)/[P^*] = ([M]_0-[M]_t)/[I]_0 \qquad \textbf{1.2j}$$

Similarly, the diagnostic test for chain termination is given by

$$-d[M]/dt = -k_p[P^*][M]_t = -k_p[I_0][M]_t \qquad \textbf{1.2k}$$

Finally, combining the above two equations namely **1.2j** and **1.2k** a relationship is obtained which provides a useful criterion for living polymerizations **eq. 1.2l**

$$\ln\{1-[I_0][X_n]/[M_0]\} = -k_p\,[I_0]t \qquad \textbf{1.2l}$$

Thus a linear plot of X_n vs. time indicates absence of chain termination and chain transfer.[55]

The role of ion pairs has been carefully and clearly elucidated for delocalized carbanionic systems (such as the allylic and benzylic species) involved as propagating species in anionic polymerization.[56] In addition to the aggregated (1) and unassociated (2) species that can exist in hydrocarbon solution, in polar solvents it is necessary to consider the intervention of free ions (5), the contact-intimate ion pair (3) and solvent separated (4) ion-paired carbanionic species as shown in **Scheme 1** where 'M_t' represents a metallic counter ion such as an alkali metal cation. In principle each of these types of intermediates can participate as reactive propagating species in anionic polymerization under certain experimental conditions. Thus the kinetics of propagation can be complicated by participation of more than one type of these carbanionic intermediates because each carbanionic species would be expected to react with monomer with its own unique rate constant as mentioned in **Scheme 1**.

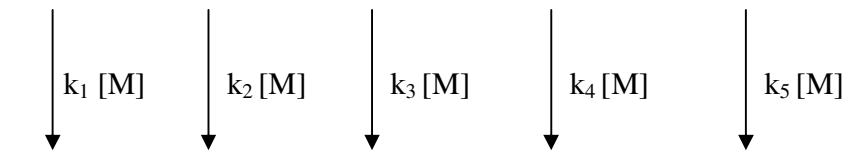

Scheme 1

1.3 Anionic Polymerization of Styrene

The anionic polymerization of styrene is very important from the industrial point of view. The methodology of living anionic polymerization, especially the alkyllithium initiated polymerization of styrene, is particularly suitable for the synthesis of functionalized polymers with well-defined structures. Since these living polymerizations generate stable anionic polymer chain ends when all the monomer has been consumed, post polymerization reactions with a variety of electrophilic species can be used to generate a diverse array of functional groups and copolymers. When present as one of the blocks in a block copolymer it makes the material transparent resinous thermoplastic. Thermoplastic elastomers (TPE) combine the flexibility and impact resistance of rubbers with the easy processability of thermoplastics. In addition they have frictional properties and hardness that are generally intermediate between those of conventional rubbers and thermoplastics. The TPE can be repeatedly processed and molded retaining their elastomeric properties all the while.

Styrene has been polymerized anionically by using various kinds of initiators among which alkyl lithium initiators are extensively used. The reactivity order of these initiators is as follows:

methyllithium > *sec*-BuLi > *i*-PrLi > *i*-BuLi > *n*-BuLi > *t*-BuLi

The kinetics of the alkyllithium initiation reactions for styrene polymerization in hydrocarbon solution has been investigated extensively.[57] *n*-Butyllithium is used commercially to initiate polymerization of styrene. Due to the high degree of association

(hexameric), *n*-butyllithium[50] initiated polymerizations are often carried out at elevated temperatures (> 50 °C) to increase the rate of initiation relative to propagation and thus to obtain polymers with narrower molecular weight distribution. Generally an excess of butyllithium (i.e. more than the stoichiometric amounts required to generate the molecular weight) is employed to destroy the impurities. The kinetics of the initiation reaction of *n*-butyllithium with styrene in benzene exhibits a first order dependence on styrene concentration and a one-sixth order dependence on *n*-butyllithium concentration as shown in **eq. 1.3a**

$$R_i = k_i K_d [BuLi]^{1/6}[M] \qquad \textbf{1.3a}$$

Since *n*-butyllithium is aggregated predominantly into hexamers in hydrocarbon solution, the fractional kinetic order dependency of the initiation process on the total concentration was rationalized on the basis that the species that reacts with styrene monomer must be the unassociated form of the initiator and this is formed by the equilibrium dissociation of the hexamer **eq. 1.3b**

$$(RLi)_6 \rightleftharpoons 6RLi \ (K_d, \text{the dissociation constant}) \qquad \textbf{1.3b}$$

Further *sec*-butyllithium[58] is the second most important organolithium initiator, which is used to prepare polystyrene blocks with relatively low molecular weight (10,000-15,000 $g \cdot mol^{-1}$) having stoichiometric control and narrow molecular weight distributions. The kinetic order for *sec*-butyllithium initiated polymerization of styrene is close to 0.25 in benzene solution. This reaction is also consistent with reaction of the unassociated alkyllithium form since *sec*-butyllithium is associated predominantly into tetramers in benzene solution.[8]

The use of aliphatic solvents causes profound changes in the observed kinetic behaviour for the alkyllithium initiation reaction with styrene. The rates of initiation in aliphatic solvents[59] were found to be in the range of (0.5-1.0, w.r.t. Reaction order) whereas in aromatic solvents[60] the reaction orders are in the range of 0.16 - 0.33. This difference in the reaction order can be attributed to the ability of aromatic solvents to promote dissociation of organolithium aggregates. Lewis bases and alkali metal alkoxides

have been used as additives to modify the initiation reactions with alkyllithium compounds.[61] Worsfold and Bywater have reported that in the presence of THF the initiation reaction of styrene with *sec*-butyllithium is first order. It has been discovered in a number of studies that Lewis bases such as ethers and amines when present in amounts comparable to the initiator concentration, dramatically increase the rate of initiation of styrene polymerization relative to propagation.[62, 63] The polymerization of styrene in benzene with *n*-butyllithium as initiator in the presence of 0.15 M THF, the initiation step is completed instantaneously on mixing of the reagents. Using small amounts of THF {[THF]/[Li]= 2-30} narrow molecular weight distribution polystyrenes (M_w/M_n< 1.1) have been prepared even with *n*-butyllithium in benzene.[62]

1.4 Anionic Polymerization of Methyl Methacrylate

The anionic polymerization of polar vinyl monomers such as acrylates is often complicated by side reactions between an existing chain and growing anionic chain ends (**Fig. 1.2**) along with chain termination[59] and chain transfer reactions.[64]

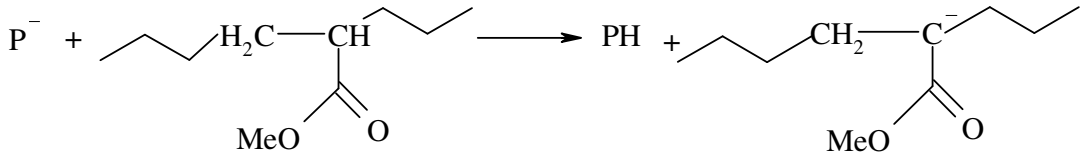

Fig. 1.2 *Proton abstraction/transfer process from the living chain end to an already existing chain.*

However synthesis of polymers with well-defined structures can be performed under carefully controlled conditions, often requiring the use of low polymerization temperatures to minimize or eliminate chain termination and transfer reactions. The acrylate monomers are more reactive than methyl methacrylate (MMA) because the polymer backbone has enolizable hydrogens that can react with the initiator to form chain ester enolate anions.

This will correspond to either termination or chain transfer reactions, depending on whether the resulting ester enolate anion reacts with monomer to initiate polymerization or branching. Further in addition to the desired Michael type addition reaction of the initiator with methyl methacrylate monomer, the initiator can react with the ester carbonyl group to form the corresponding ketone derivative (**Fig 1.3**).

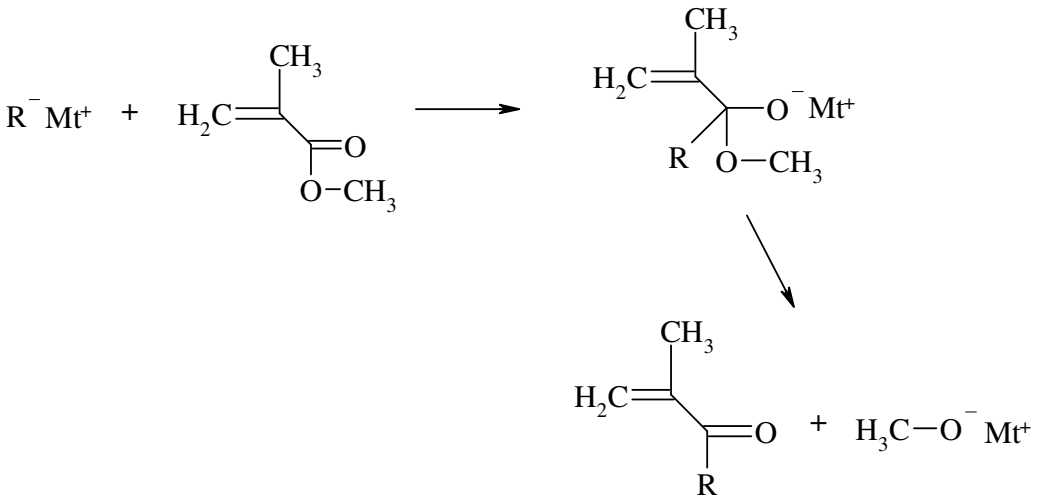

Fig. 1.3 *Side reaction of the initiator with the ester carbonyl group.*

The competition between these two modes of addition depends on the general reactivity of the initiator and also on the steric requirements of the initiator. As a general rule an initiator should have approximately the same reactivity/stability as that of the propagating chain end carbanionic species. The reaction of MMA with *n*-butyllithium in toluene at -78 °C produces approximately 51% of lithium methoxide by attack at the carbonyl carbon. The consumption of 50% of initiator by reaction at the ester carbonyl group is not acceptable generally. The most useful initiator for anionic polymerization of MMA[43] and other related acrylates is 1,1-diphenylhexyllithium, which is formed by the quantitative addition of butyllithium to 1,1-diphenylethylene (DPE).[65] The usefulness of 1,1-diphenylhexyllithium initiators to polymerize MMA efficiently with minimal attack at the ester carbonyl group is in accordance with the pKa of diphenylmethane (32), the conjugate acid of this carbanion, which is approximately the same as that of the

propagating ester enolate anion (30-31).[66] Further the increased steric requirements reduce the rate of addition to the ester carbonyl group. Alkoxide salts have been reported to initiate polymerization of methyl methacrylate with varying degrees of efficiency, which seems to depend on the counterion and solvent.[67] The potassium salt of the ω-alkoxide from poly(ethylene oxide) was reported to polymerize methyl methacrylate with high efficiency (> 92% yield) at room temperature in tetrahydrofuran.[68] The backbiting reactions during the propagation as shown below (**Fig. 1.4**) can be avoided by carrying out the polymerization at -78°C.

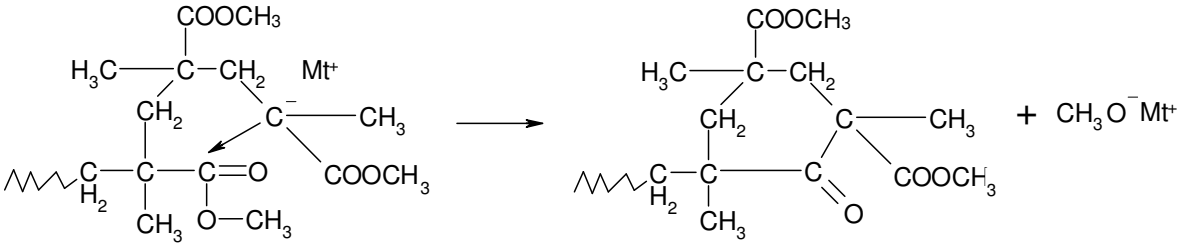

Fig. 1.4 *Backbiting reactions during polymerization of MMA.*

Organomagnesium compounds as initiators for polymerization of methyl methacrylate and related compounds have been investigated[47] in considerable detail as well.[69] Unfortunately, although it is possible to control stereochemistry and obtain either highly isotactic or highly syndiotactic PMMA using organomagnesium initiators, the mechanisms of these polymerizations are very complex. Part of the complexity arises from the schlenk equilibrium between various species in a typical grignard reagent as shown in **eq. 1.4a**

$$R_2Mg + MgX_2 \rightleftharpoons 2RMgX \qquad \textbf{1.4a}$$

Thus, as these systems have multiple active species with different reactivities and stereospecifities, the molecular weight is often not controllable and the molecular weight distribution tends to be broad or multimodal.

1.5 Ferrocene Containing Polymers

The incorporation of transition metals into a polymer chain offers unique potential for the preparation of processable materials with properties that differ significantly from those of conventional organic polymers. Over the past thirty years it has been well established that transition-metal complexes and metal containing solid-state polymeric materials possess a variety of interesting and useful redox, magnetic, optical, electrical and catalytic properties. Well-characterized, high molecular weight transition metal-based polymers are attractive materials because of their possible applications like antistatic coatings, polymeric semiconductors, electrochromic, magnetic ceramics and nanolithography. In addition, the diverse range of coordination numbers and geometries that exist for transition elements helps the polymer to access unusual conformational, mechanical and morphological characteristics.[70] The thermal stability and interesting physical properties associated with the ferrocene nucleus encouraged chemists to make extensive studies leading to the introduction of this organometallic unit into polymers.[71]

1.5.1 *Polymers Containing Ferrocene in the Main Chain*

As mentioned above the incorporation of inorganic elements into the main chain of high polymers provide access to some of the interesting (physical, electrical, magnetic and catalytic) properties characteristic of small molecule metal complexes and solid-state metal containing compounds.[72] This is especially the case if the metal atoms are in close proximity so as to allow metal-metal interactions. One of the good reasons for the synthesis of polymers with skeletal ferrocenyl units was provided by the observation that in molecular species where two ferrocene units are linked together in close proximity the iron atoms can often interact to yield delocalized, mixed-valent species on one-electron oxidation. For e.g., the mixed valence cations derived from biferrocenylene **(1)**, the acetylene-bridged species **(2)** and the biferrocenes such as **(3)** had been shown to be delocalized on the IR and/or Mössbauer time scale.[73-75] These results suggested that macromolecules with skeletal ferrocene units might provide access to materials with interesting electronic and magnetic properties.

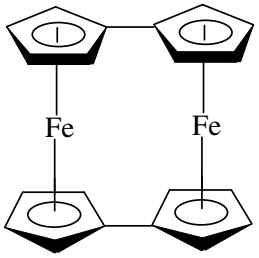

(1)

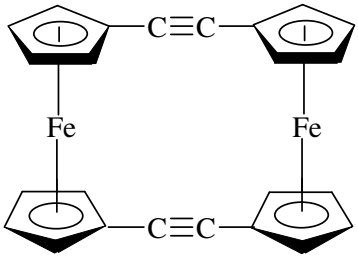

(2)

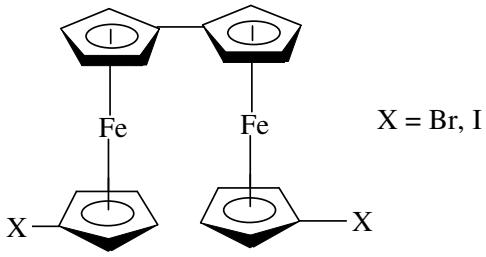

(3)

The first attempt to polymerize ferrocene so as to give polyferrocenylene was made by Rosenberg and Neuse[76] where soluble oligomeric compounds were prepared at 200 °C using *tert*-butyl peroxide as the free radical initiator by polyrecombination (**Scheme 2**). Unfortunately materials obtained by this method could not attain molecular weight of more than 7000 $g \cdot mol^{-1}$ and the products were constitutionally highly inhomogeneous. Similarly, a wide variety of [2]ferrocenophanes with different elements in the bridge structure have also been reported in the late sixties and early seventies.[77-79]

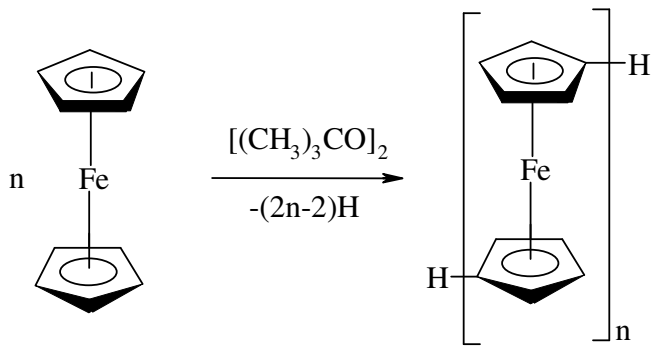

Ferrocene **Polyferrocenylene**

Scheme 2

The reduced ability of such species to polymerize has been attributed to the low ring strain present, which is reflected by the very small cyclopentadienyl ring tilt angle of only about 4°. Poly(ferrocenylmethylene) **(4)** was reportedly prepared via the $ZnCl_2$/HCl-catalyzed polymerization of (dimethylamino)methylferrocene.[80] However all the methods used yielded mainly low molecular weight (M_n << 10000 g·mol^{-1}) and often poorly defined materials.

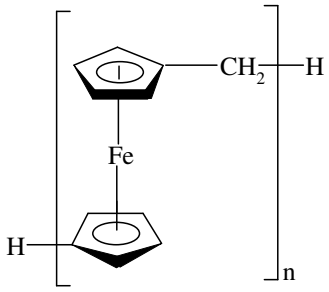

(4)

Subsequently, a set of new strategies was developed for polycondensation to obtain more defined materials. For example, poly(ferrocenylenes) prepared via the condensation reaction of 1,1'-dilithioferrocene were structurally well defined but materials with molecular weights higher than 4000 g·mol^{-1} could not be obtained. Similarly, reaction of equimolar amount of 1,1'-dilithioferrocene and 1,1'-dihaloferrocene in the presence of TMEDA gave well defined polyferrocenylenes. Another method of synthesis involved reaction of 1,1'-dihaloferrocene with Mg, leading to low molecular weight quasicrystalline material with M_n = 4600 g·mol^{-1} (**Scheme 3**). [81]

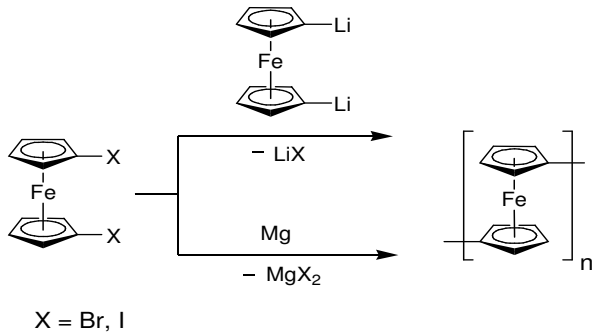

Scheme 3

In summary, up to very recently all methods developed failed to yield polymeric materials containing ferrocene in the main chain with well-defined structure and high molecular weight. Further efforts on the synthesis of polymers containing ferrocene in the skeleton produced a large number of well-defined ferrocene containing block copolymers with high molecular weight. Manners et al. have reported many structurally defined high molecular weight PFS (Polyferrocenyldimethylsilane) containing diblock and multiblock copolymers (see below).[107] Similarly, structurally characterized poly(1,1'-ferrocenylene-p-oligophenylenes) have been synthesized by following a different strategy which involved Pd catalyzed polycondensation of 1,1'-bis(p-bromophenyl)ferrocene with arylboronic acid derivatives using conditions required for Suzuki reactions.[82]

1.5.2 ***Polymers Containing Ferrocene as Side Chains***

For the preparation of polymers with ferrocene units as side chain one of the most appropriate strategy would be the usage of ferrocenes substituted with functional groups that can be easily polymerized as monomers (**Fig. 1.5**). These kind of ferrocene derivatives are polymerized by conventional methods of polymerization.

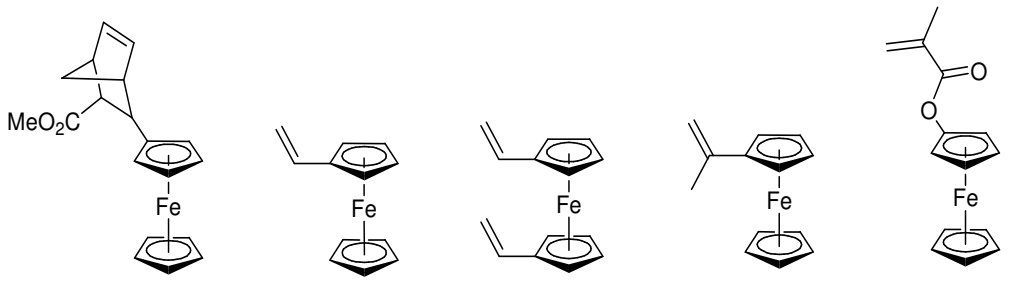

Fig. 1.5 *Polymerizable Ferrocene Derivatives.*

One simple example of such derivatives is vinylferrocene which can be polymerized by radical, cationic as well as Ziegler Natta polymerization technique.[83] Similarly, disubstituted ferrocenes like 1,1'-divinylferrocene[84, 85] is another good example for this purpose. Other monomers include isopropenylferrocene and ferrocenylmethacrylate.[86] Ferrocene containing norbornene derivatives synthesized by Diels-Alder reaction polymerize by ring opening metathesis to give high molecular weight polymers.[87, 88]

Further polyphosphazenes, polysilanes and polysiloxanes with ferrocenyl side groups have been synthesized via the incorporation of this organometallic moiety into the side group structure.[89-91] As a consequence of their electroactive properties, polymers with ferrocenyl side groups have attracted significant interest as electrode mediators and as materials for the construction of electronic devices.[92, 93]

1.5.3 ***Polyferrocenylsilanes***

Another well known class of ferrocene containing polymers is that of polyferrocenylsilanes which contain substituted silane units apart from ferrocene. Initial attempts of synthesis based on polycondensation routes involved reaction of 1,1'-dilithioferrocene and organosilanes. The materials obtained (**Scheme 4**) were of low molecular weight (M_n = 1400-7000 g·mol^{-1}) which is characteristic of condensation processes where exact reaction stoichiometries were virtually impossible as one of the reactants namely dilithioferrocene could not be prepared in pure form (90-95 %). [94, 95]

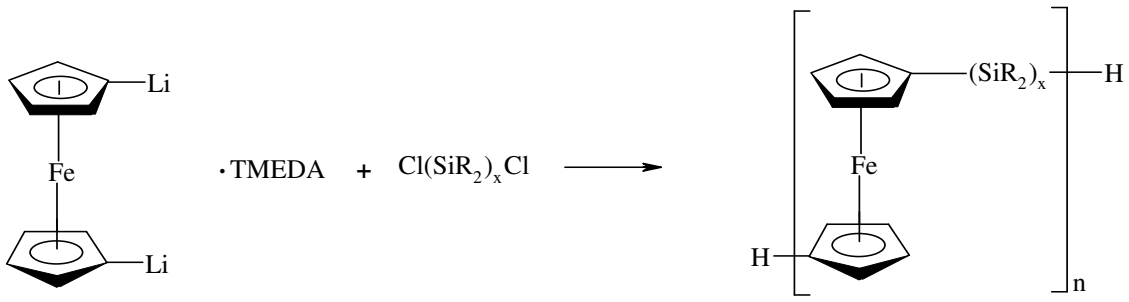

Scheme 4

In 1992, Manners et al. demonstrated that the strained silicon bridged [1]ferrocenophane undergo thermal ROP to afford the corresponding high molecular poly(ferrocenylsilane) ($M_n > 10^5$ g·mol^{-1}). The ferrocenophane monomers as shown (**Scheme 5**) possesses strained ring-tilted structures, in which the planes of the cyclopentadienyl ligands are tilted with respect to one another by 16-21 degrees.[96-98] The relief of strain is believed to provide the driving force for the ROP reactions.[99] Estimates of the strain energy of 1,1-dimethylsilaferrocenophane have been obtained by measuring

the enthalpy of polymerization thermochemically by differential scanning calorimetry (DSC), which is in the range of 70-80 KJ/mol.[100]

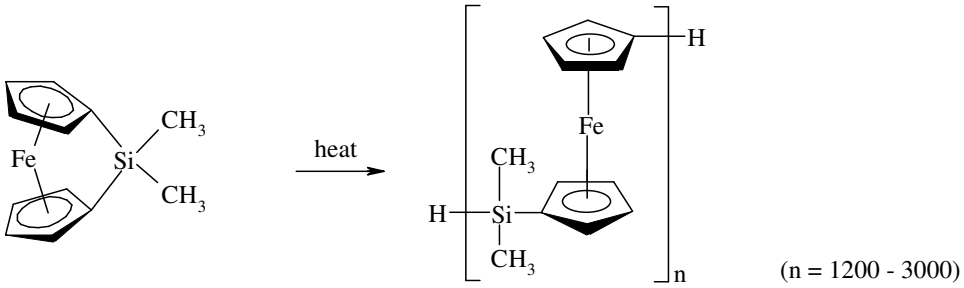

1,1-Dimethylsilaferrocenophane **Polyferrocenyldimethylsilane**

Scheme 5

Since this initial report, the ROP of ferrocenophanes under more convenient and mild conditions have been extensively explored through the use of anionic initiators[101-103] (**Scheme 6**) as well as transition metal catalysts[104, 105] and has allowed the synthesis of well-defined homopolymers with interesting electronic and preceramic properties.[106-108]

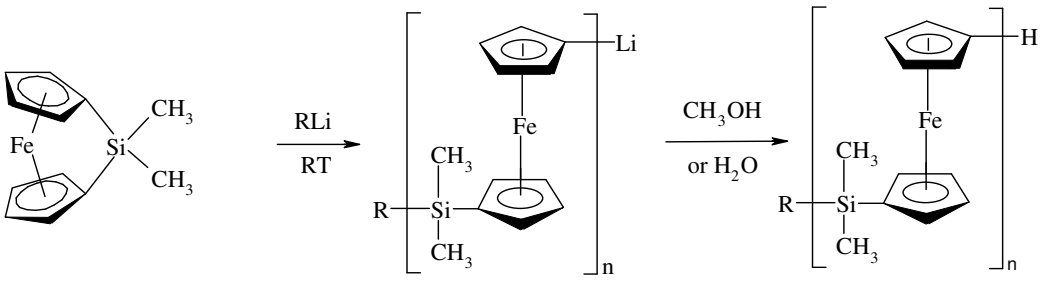

1,1-Dimethylsilaferrocenophane **R = Fc, Ph, n-Bu, sec-Bu** **Polyferrocenyldimethylsilane**

Scheme 6

Living anionic ROP allows the preparation of polyferrocenylsilanes with controlled molecular weights and end-group structures. It also permits access to novel block

copolymers with other monomers such as styrene, methyl methacrylate, hexamethylcyclotrisiloxane etc**.** The mechanism for the anionic polymerization reactions of silicon-bridged ferrocenophanes is believed to involve nucleophilic attack at silicon with the generation of a cyclopentadienyl-based anion, which can subsequently participate in chain propagation. This mechanism is consistent with the products isolated after the addition of end-capping agents such as $SiMe_3Cl$ and also previous studies of the stoichiometric ring-opening reactions with methanol.[109, 110]

Transition metal (Pt^{II}, Pt^0, Rh^I and Pd^{II}) catalyzed ROP of silicon-bridged [1]ferrocenophanes (**Scheme 7**) provides convenient control of the molecular weight and architecture of polyferrocenes to give graft and star copolymers.[111]

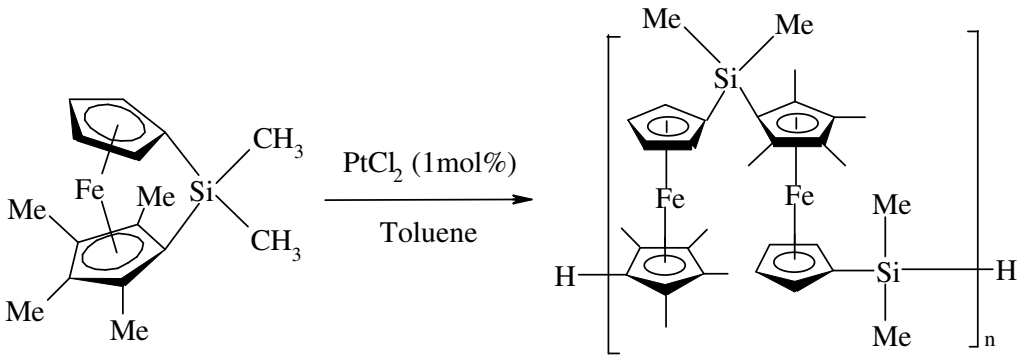

Scheme 7

Furthermore, a variety of p-block elements such as B, Ge, Sn, P, S have been incorporated into [1]ferrocenophane framework and in most cases ROP has led to the corresponding soluble materials.[112-115]

The polyferrocenylsilanes have quite low Tg (Glass Transition Temperature). The ability of the iron atom in ferrocene to act as a nearby freely rotating "molecular ball-bearing" probably plays a key role in generating materials with surprisingly low glass transition temperatures.

1.5.4 ***Pentablock Copolymers containing PFS, PS and PMMA segments***

In principle the synthesis of block copolymers with a number of blocks ca. four or more is quite possible. For instance the synthesis of a linear ABCD tetrablock quaterpolymer having four different chemical blocks can be accomplished by sequential monomer addition. Though this route involves a four-step addition process, it can be made successful if special care is taken during the purification of reagents employed. An alternate method would be the preparation of the two diblocks AB and CD and their subsequent connection using an appropriate coupling agent.

Similarly linear pentablock terpolymers of the ABCBA type have been synthesized by anionic polymerization using a difunctional initiator.[116, 117] The preparation of these polymers with A = PMMA, B = PS, and C = PB (PMMA = polymethyl methacrylate, PS = polystyrene and PB = polybutadiene) started with the formation of the difunctional PB inner center block with two living ends, followed by the addition of S units to form the PS block and finally the synthesis of the terminal blocks. Intermediate products were isolated by sampling before the addition of the next monomer and characterized by SEC.

The synthesis of PEO-*b*-PS-*b*-PI-*b*-PS-*b*-PEO (PEO = polyethyleneoxide and PI = polyisoprene) pentablock terpolymers has been accomplished by the use of a difunctional initiator.[118] Pentablock copolymers of the type PtBuS-*b*-PS-*b*-PB-*b*-PS-*b*-PtBuS [PtBuS = poly(*t*-butylstyrene)] were synthesized by sequential addition of monomers and by coupling preformed living PtBuS-*b*-PS-*b*-PtBuS using Me_2SiCl_2 as the coupling agent.[119] Copolymers prepared in both ways had shown narrow molecular weight distribution and were evaluated as thermoplastic elastomers showing good phase separation and mechanical properties. Synthesis of pentablock copolymers namely, *n*-Bu-PS-*b*-PFS-*b*-PDMS-*b*-PFS-*b*-PS-*n*-Bu [PDMS: poly(dimethoxysilane)] has been carried out by Manners et al. by a coupling process using a three stage strategy so as to prepare a living triblock copolymer which was then coupled with Me_2SiCl_2 to form the pentablock structure (**Scheme 8**). The material was fully characterized and exhibited broad molecular weight distribution with a low molecular weight shoulder suggesting the presence of

uncoupled impurities of triblock copolymer. Similarly, PDMS-*b*-PFS-*b*-PS-*b*-PFS-*b*-PDMS pentablock copolymer prepared by difunctional initiator too was contaminated by triblock copolymer.[107]

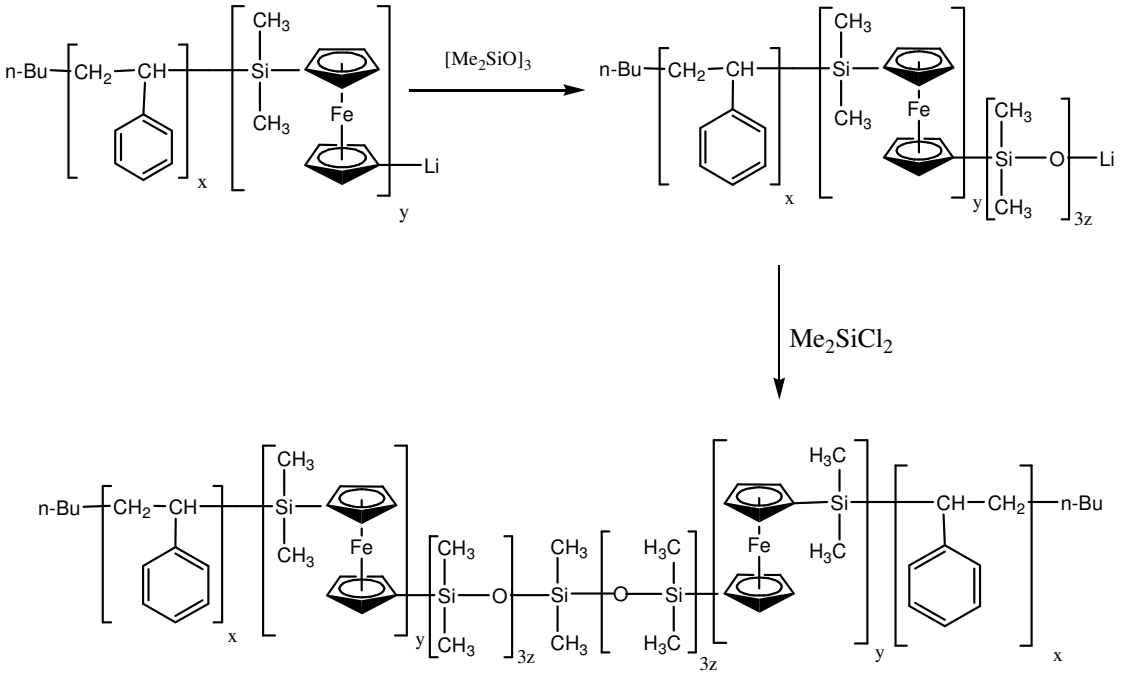

Scheme 8

1.6 Self-Assembly by means of Microphase Separation in Block Copolymers

The spontaneous formation of nanostructured materials via molecular self-assembly has attracted increasing interest throughout the last decade, driven both by its inherent beauty and a wealth of potential technological applications. Incompatible block copolymers are a prominent example of this class of materials as they form a large variety of well-ordered microdomain structures of molecular dimensions.[120-125]

In block copolymers the different blocks are frequently incompatible and demix into A-rich, B-rich and C-rich domains. The tendency of the block copolymers to segregate is referred to as microphase separation that leads to separation of the components in nanoscale domains. As the blocks are covalently linked to each other the domain size cannot grow larger than a typical block length. Due to this molecular size limit, the process is referred to as microphase separation and the A-rich, B-rich, C-rich regions are called microdomains. The microphase morphologies developed by block copolymers depend on a number of microscopic and macroscopic parameters such as overall copolymer chain length, lengths of the individual blocks, distribution of the block lengths, distribution of the overall molecular weights, chain architecture, compatibility of the different blocks, quality of the solvent for the respective blocks, temperature and the method used for sample preparation like film casting or annealing.[126] All these parameters are very important as they can be used to tailor the microphase morphology and thus optimize the properties of materials for a specific purpose.[127]

1.6.1 *Phase Transitions in Block Copolymer Melts*

The diverse spectrum of phase transitions that have been identified or postulated to exist in physical systems are mostly classified as being either first order or second order. Such transitions are referred to as fluctuation-induced transitions.[128, 129] It was first pointed out by Leibler[130] that block copolymer melts belong to the Brazovskii class which undergo transitions from a high-temperature disordered phase to a non-uniform, spatially periodic ordered phase. In general, contacts between unlike monomers will be energetically less favorable than *A-A*, *B-B*, *C-C* contacts, hence the ground state of a block copolymer melt is characterized by microphases of pure A, pure B and pure C in order to reduce these unfavorable contacts. Under various experimental conditions the

microphases are arranged in a spatially periodic array.[131] As the temperature of the block copolymer melt is raised from T = 0, it can no longer possess true long-ranged order because of the sensitivity of one-dimensional structures to thermal fluctuations.[132] However, quasi one-dimensional order still persists and if temperature is further raised without decomposition of the copolymer, the enthalpic barriers maintaining the quasiperiodic structure can be overcome and the sample melts into a compositionally homogeneous disordered phase. This phase transition is referred to as the microphase separation transition (MST). In other words MST occurs when a compositionally homogeneous disordered melt of copolymers transforms to a spatially periodic, compositionally inhomogeneous phase on lowering the temperature.[133] During MST, nucleation processes takes place and the bulk phase transitions have a very weak, fluctuation induced first order character. These order-disorder transitions (ODT) in block copolymers have been studied by SAXS, SANS and rheology.[134] One important conclusion obtained is that the nature of the ODT is a first-order phase transition[135], showing sharp discontinuous changes of various physical quantities such as the principal scattering peak intensity I_m[136, 137], the width of the first-order scattering maximum[138], low frequency rheological properties[139] and birefringence.[140]

1.6.2 ***Flory-Huggins Theory***

Different polymers can be combined into a single material in many ways, which can lead to a wide range of phase behaviors that directly influence the associated physical properties and ultimate applications. Four factors control polymer-polymer phase behaviour: choice of monomers, molecular architecture, composition and degree of polymerization. In this regard the most basic molecular architecture i.e. linear homopolymers and diblock copolymers have been studied most extensively.

Macrophase separation results when thermodynamically incompatible linear homopolymers are mixed. In contrast the covalent bond between blocks in a di/tri/pentablock copolymers leads to microphase segregation. Formation of block copolymers is an alternative method of mixing chemically different polymers. Phase state behavior is governed by a balance between enthalpic (H = U + PV, where U, P and V

represent the system energy, pressure and volume respectively) and entropic (S) factors that together constitute the system (Gibbs) free energy.[141-143]

$$G = H - TS \qquad \textbf{1.6.2a}$$

Flory and Huggins estimated the change in free energy per segment ΔG_m associated with mixing random polymer chains on an incompressible ($\Phi_A + \Phi_B = 1$) lattice as represented by **eq. 1.6.2b**

$$\Delta G_m/k_BT = (\Phi_A/N_A)\ln\Phi_A + (\Phi_B/N_B)\ln\Phi_B + \Phi_A\Phi_B\chi \qquad \textbf{1.6.2b}$$

The first two terms in **eq. 1.6.2b** represent the entropy of mixing (ΔS_m, mix), the last term represents the enthalpy of mixing (ΔH_m, mix) and χ being the Flory-Huggins parameter. With mixing the randomness in the system increases and therefore ΔS_m increases. Further with increasing N (degree of polymerization), ΔS_m decreases because

$$\chi = \frac{1}{k_BT}\left[\epsilon_{AB} - \frac{1}{2}(\epsilon_{AA} + \epsilon_{BB})\right] \qquad \textbf{1.6.2c}$$

large chains can assume fewer mixed configurations. The enthalpy of mixing ΔH_m can increase or decrease ΔG_m depending on the sign of χ. The Flory-Huggins segment - segment interaction parameter is given by **eq. 1.6.2c** as above where ϵ_{ij} represents the contact energy between i and j segments and k_B is the boltzman constant. A negative value of χ results from a favorable energy of mixing i.e. A-B segment - segment interaction produces lower system energy than the sum of A-A and B-B contact.

Further we also have

$$\chi = \frac{\alpha}{T} + \beta \qquad \textbf{1.6.2d}$$

where α and β are the experimentally determined enthalpy and entropy coefficients for a particular composition. In general α and β may depend on Φ, N, T and molecular architecture. The phase diagrams can often be tailored to accommodate experimental constraints such as glass-transition and thermal decomposition temperature. For e.g. in the **eq. 1.6.2d** if α is positive and β is negative, decreasing temperature always increases χ and an upper critical solution temperature results (i.e. two-phase envelope is concave down in the coordinates Φ vs. T). Further if α is negative and β is positive then a lower critical solution temperature (LCST) may result (i.e. two phase envelope is concave up in Φ vs. T). Boltzman pointed out that the connection between mechanics and thermodynamics is most clearly established through the entropy. In the light of this when a system approaches equilibrium at constant E and V there is an increase in randomness which may be measured by the increase in the number of ways of distributing molecules among energy levels. This suggests that the entropy S is proportional to the logarithm of the number ω of distinguishable stationary states available to the system. The basic postulate is **eq. 1.6.2e**

$$S = k \ln\omega \qquad \textbf{1.6.2e}$$

where $k = 1.38 \times 10^{-23}$ J/K and the number ω is the number of the possible quantum states of the whole system with the energy E. On a per molecule basis we have

$$S = R \ln\omega \qquad \textbf{1.6.2f}$$

The thermodynamic weight or partition function (ω) represents the indistinguishable energy (stationary states available to a system or available quantum states to system with total energy E). Now for a two-component system[144, 145] A and B with total energy E we have

$$n_A + n_B = N \qquad \textbf{1.6.2g}$$

and

$$n_A E_A + n_B E_B = E \qquad \textbf{1.6.2h}$$

$$S = \frac{k \ln N!}{n_A! \, n_B!} \qquad \textbf{1.6.2i}$$

Equation **1.6.2i** can be rearranged by using the volume fractions for the individual components ($x_A = n_A/N$, and $x_B = n_B/N$) and the entropy of mixing is given by

$$\Delta S_{mix} = k \, [n_A \ln x_A + n_B \ln x_B] \qquad \textbf{1.6.2j}$$

For ΔS_{mix}/molecule we have,

$$\triangle \, Smix = R \left[\frac{\Phi_A}{N_A} - \ln \Phi_A + \frac{\Phi_B}{N_B} - \ln \Phi_B \right] \qquad \textbf{1.6.2k}$$

wherein Φ_A and Φ_B represent the volume fractions for components A and B respectively and N_A and N_B the degree of polymerization respectively as well.

The product χN represents the degree of incompatibility and in this regard several regimes have been identified namely; weak segregation limit (WSL, $\chi N < 10$), intermediate segregation limit (ISL, $10 < \chi N < 100$), strong segregation limit (SSL, $\chi N > 100$).

1.6.3 ***Strong Segregation Limit Theory***

The first theories for block copolymers were developed for the strong segregation limit (SSL) in the early 1970s.[146-149] In this regime of strong segregation Helfand and co-workers developed a specific self-consistent field theory from a general theory of inhomogeneous polymers that allowed calculation of free energies, composition profiles and chain conformations.[150-152] In this method, the external mean fields acting on a

polymer chain were calculated self-consistently with the composition profile. The theory was simplified by the introduction of the narrow interphase approximation, which assumed that the boundary between A and B domains was narrow compared to the domain width. The interfacial layer thickness was predicted to be $a \cdot \chi^{-1/2}$, where a represented the statistical segment length. Phase boundaries were dependant only on the copolymer composition Φ. Experimental work on strongly segregated block copolymers supported this.[153] This theory does not extend to the weak segregation limit, therefore phase boundaries are terminated at $\chi N = 100$.

1.6.4 ***Weak Segregation Limit Theory***

(i) *Mean Field Theory*

The composition profile of ordered microstructures is approximately sinusoidal near the Order-Disorder Transition (ODT). The phase behavior in this regime, where the blocks are weakly segregated can then be modeled using Landau-Ginzburg theory where the mean field free energy is expanded with reference to the average composition profile. The order parameter for A/B block copolymers may be defined as[154] **eq. 1.6.4a** where $Q_A(r)$ is the local number density of monomer A and f is

$$\Psi(r) = [Q_A(r) - f] \qquad \textbf{1.6.4a}$$

the average composition. The average over the system is denoted by [ ].

(ii) *Composition Fluctuation Theory*

Leibler[154] noted that allowance for composition fluctuations changes the mean field prediction of a second-order phase transition for a symmetric diblock to a first-order transition. Fredrickson and Helfand studied this effect for block copolymers and showed that composition fluctuations incorporated via the method of Brazovski lead to a finite size effect, where the phase diagram depends on chain size i.e. the degree of polymerization. In Landau-Brazovski theory, the density modulation (or composition for block copolymers) is written as **eq. 1.6.4b**

$$\Psi'(r) = \psi(r) + \eta(r) \qquad \textbf{1.6.4b}$$

where $\psi(r)$ is the component possessing the symmetry of the ordered lattice and $\eta(r)$ is the fluctuating component, with a thermodynamic average equal to zero.

1.6.5 *Self -Consistent Field Theory (SCFT)*

Matsen and co-workers have recently unified the strong and weak segregation limit theories for block copolymer melts.[155, 156] This approach involves numerical solution of self-consistent field equations, without approximations such as the narrow interphase approximation. The SCFT reduces the problem of calculating the interactions in an ensemble of polymer chains to that of a single non-interacting polymer in external fields that are obtained self-consistently with the composition profiles. By comparing the free energies for different phases the phase diagram (**Fig. 1.6**) is obtained. This phase diagram is obtained for conformationally symmetric diblocks where the statistical segment lengths of A and B blocks are equal. The SCFT accounts for a stable gyroid phase in the weak segregation regime, between the classical lamellar and hexagonal phases predicted by Leibler.[154]

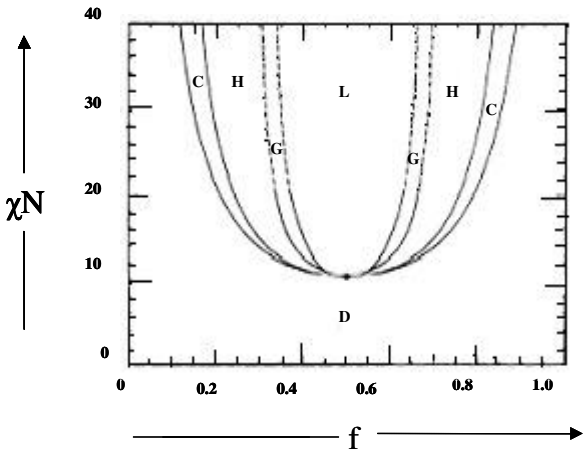

Fig. 1.6 *Phase diagram for a symmetric diblock copolymer, calculated using self-consistent mean field theory. Regions of stability of disordered* **(D)**, *lamellar* **(L)**, *gyroid* **(G)**, *hexagonal* **(H)**, *BCC* **(C)** *and close-packed spherical (CPS) phases are indicated.*[157] *All phase transitions are first order, except for the critical point, which is marked by a dot.*

1.6.6 ***Integral Equation Theories***

David and Schweizer have recently applied liquid state theory to block copolymer melts.[158, 159] In this approach, the polymer molecules are modeled as chains of interaction sites (which usually represent a collection of monomers) using an extension of the liquid state theory used for systems of small molecules or atoms. The off-lattice polymer reference interaction site model (PRISM) theory was applied to block copolymers, using a "Gaussian thread" model for symmetric copolymers. The theory was related to Leibler theory using the 'Reference Molecular Mean Spherical Approximation' (RMMSA) closure within the thread idealization. This closure can be viewed as the integral equation theory realization of mean field theory. Further in the strong segregation limit, the following sequence of phases is observed for PS-*b*-PI diblocks (**Fig. 1.7**) say for instance $\Phi_{PS} < 0.17$; BCC, $0.17 < \Phi_{PS} < 0.28$; hex, $0.28 < \Phi_{PS} < 0.34$; gyroid, $0.34 < \Phi_{PS} < 0.62$; Lam, $0.62 < \Phi_{PS} < 0.66$; gyroid, $0.66 < \Phi_{PS} < 0.77$; hex, $\Phi_{PS} > 0.77$; BCC.[160]

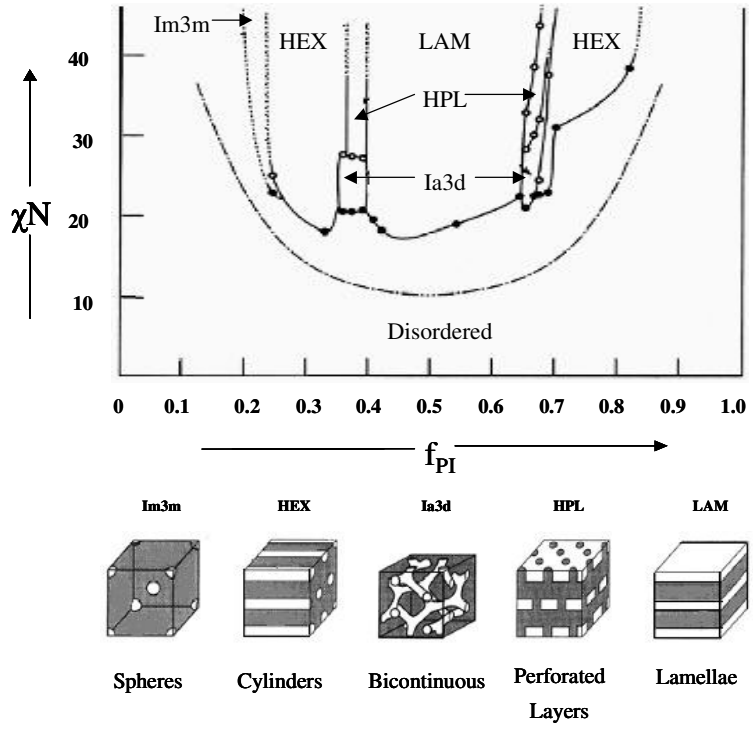

Fig. 1.7 χN *versus* f_{PI} *diagram for PI-PS diblock copolymers. Open and filled circles represent the order-order* **(OOT)** *and order-disorder* **(ODT)** *transitions, respectively.*

1.6.7 *Nanoscale Morphologies generated by Self-Assembly of Diblock Copolymers*

In diblock copolymers two polymer segments are covalently joined to one another. Self-assembly or phase segregation on nm length scales is governed mainly by three parameters viz. total polymer length ***N***, interaction parameter χ and relative block length or volume fraction ***f***. In general four stable morphologies (**Fig. 1.8**) have been observed in a wide variety of diblock copolymers depending upon the block length ***f*** namely short/long: spheres in matrix, ~20%: cylinders, ~33%: gyroid and equal lengths: lamellar.

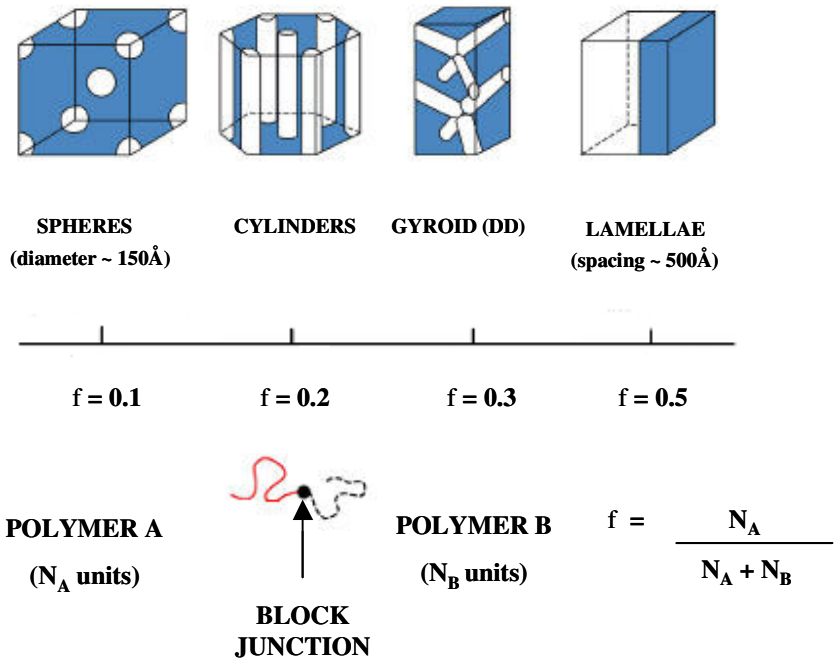

Fig. 1.8 *Some morphologies for linear AB diblock copolymers.*

1.6.8 *Complex Phases in Block Copolymers*

Recently, a number of so-called complex phases, such as the bicontinuous gyroid (**Fig. 1.9**) and perforated layer structures have been identified. The former is an equilibrium structure, whereas the latter seems to be a metastable structure observed during transformation to and from the gyroid structure (a term coined by Seddon).[161] The gyroid phase (*Ia3d* symmetry) was discovered independently by two groups in 1994.[162]

Schulz et al. using SANS, observed this phase on heating a mixture of polystyrene-*b*-poly(2-vinylpyridine) diblocks shear-oriented in the hexagonal phase. The gyroid phase developed epitaxially from the hexagonal phase. Further Hajduk et al. used TEM and SAXS to determine the morphology of a PS-*b*-PI diblock with $\Phi_{PS} = 0.33$ and found the SAXS data to be consistent with an *Ia3d* space group.[163] There have been many misassignments of structures as being ordered bicontinuous double diamond (OBDD, space group *Pn3m*) that is based on a tetrahedral arrangement of channels when in fact they were gyroid that has a *Ia3d* symmetry and is based on a tripod arrangement of channels.

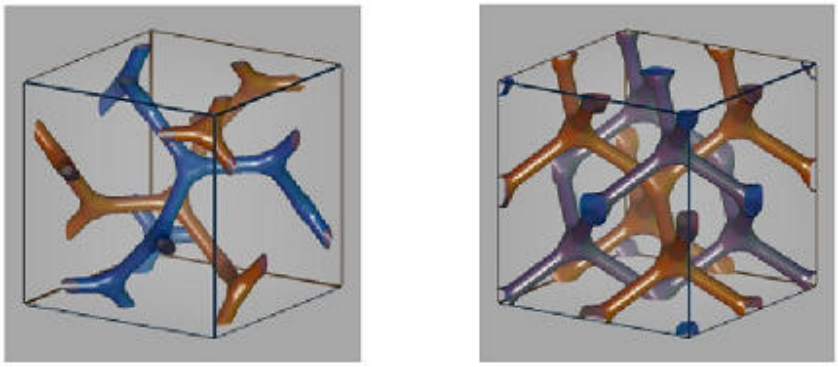

Gyroid **OBDD**

Fig. 1.9 *Structures belonging to space group Ia3d (gyroid) and space group Pn3m ('double diamond').*

Further, Bates and coworkers had largely explored the existence of second class of complex phases namely the modulated and perforated layer structures (**Fig. 1.10**). [164, 165] Hexagonal modulated lamellar (**HML**) and hexagonal perforated layer (**HPL**) structures were observed on heating PEP-*b*-PEE, PE-*b*-PEP and PE-*b*-PEE diblock copolymers, where PEP is poly(ethylene-propylene), PEE is poly(ethyl ethylene) and PE is poly(ethylene).

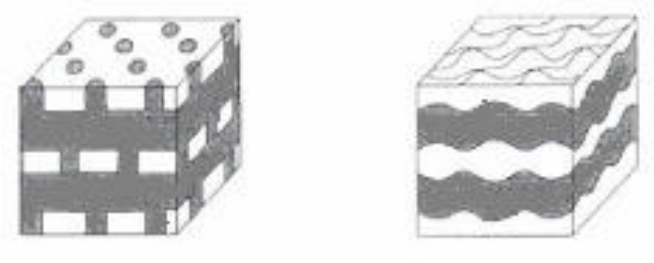

Fig. 1.10 *Representation of the hexagonal-perforated lamellar* (**HPL**) *and the hexagonal-modulated lamellar* (**HML**) phases.

1.6.9 ***Microphase Separation in Multiblock Copolymers such as ABC-Triblock Copolymers, CBAB-Tetrablock Copolymers and CBABC-Pentablock Copolymers etc*.**

The phase behavior of multiblock copolymers is even more rich and complex in contrast to two component diblock and triblock copolymers. An important driving force for the structure formation in these polymers is the relative strength of incompatibilities between the components.[166] A combination of block sequence (ABC, ACB, BAC), composition and block molecular weights provides enormous parameter space for new morphologies (**Fig. 1.11**).

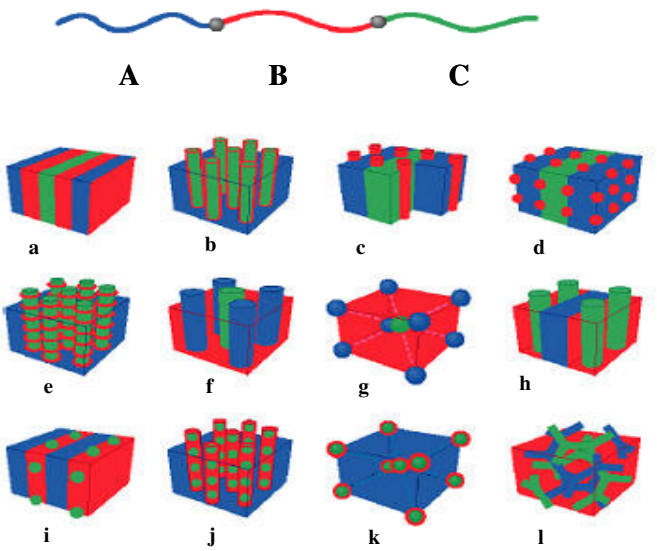

Fig. 1.11 *Some morphologies for linear ABC triblock copolymers.*[171, 167]

One can tailor the properties of each phase with polymer block selection leading to precise control of feature size with block lengths (1-100 nm). Stadler et al. have recently discovered a number of remarkable new morphologies in PS-*b*-PB-*b*-PMMA triblock copolymers and their hydrogenated analogues such as PS-*b*-PEB-*b*-PMMA (**Fig. 1.12**).[168-171] The common features of the polymers exhibiting this complex phase behaviour are that the midblock is the minority component and that the incompatibility between the outer blocks is much weaker than the incompatibility of each of these blocks with respect to the midblock. The morphologies were investigated by TEM using a selective staining agent such as OsO_4 for the PB domains in PS-*b*-PB-*b*-PMMA and RuO_4 for PS-*b*-PEB-*b*-PMMA as it stains both the PS and PB domains.

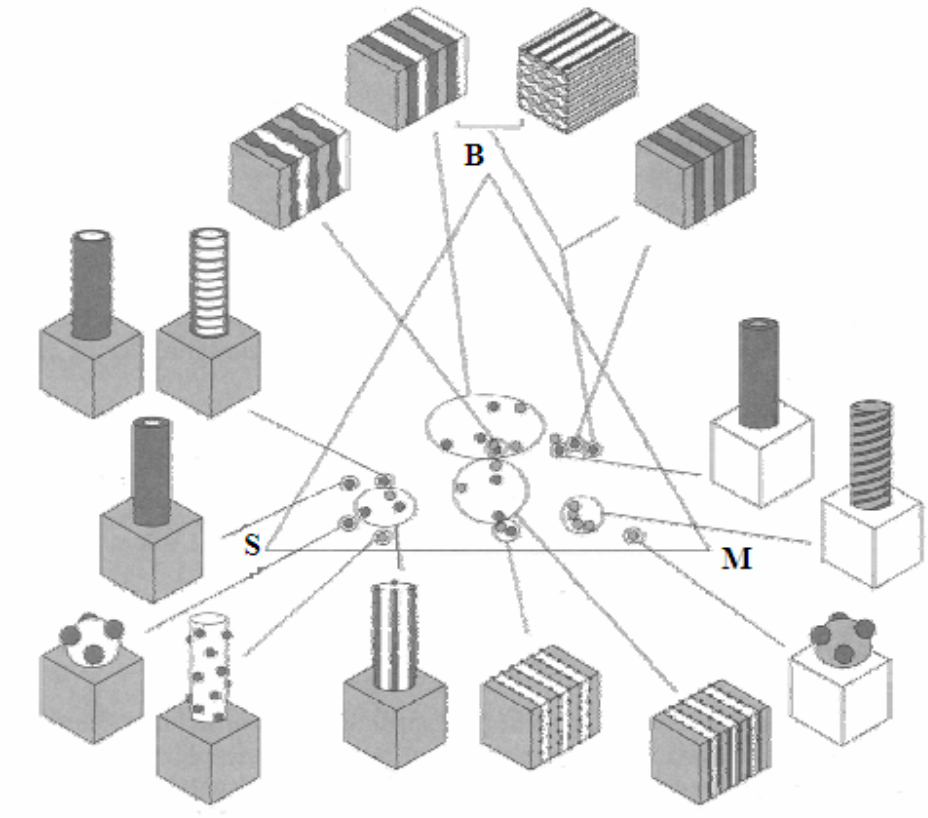

Fig. 1.12 *Microphase separated morphologies of ABC triblock copolymer (*P*olystyrene-b-*P*olybutadiene-b-*P*olymethyl methacrylate).* [172]

1.6.10 ***Microphase Separation and Nanolithography***

Nanoscale chemical patterns written on a substrate can direct the self-assembly of polymer overlayers with remarkable precision. These polymer films, in turn, can be used as templates for nanofabrication. Nanolithography/nanopatterning exploits the microphase separation behavior of block copolymers (**Fig. 1.13**) in the design and fabrication of semiconductors, chips, integrated circuits, microprocessors and memory storage devices.[222, 223]

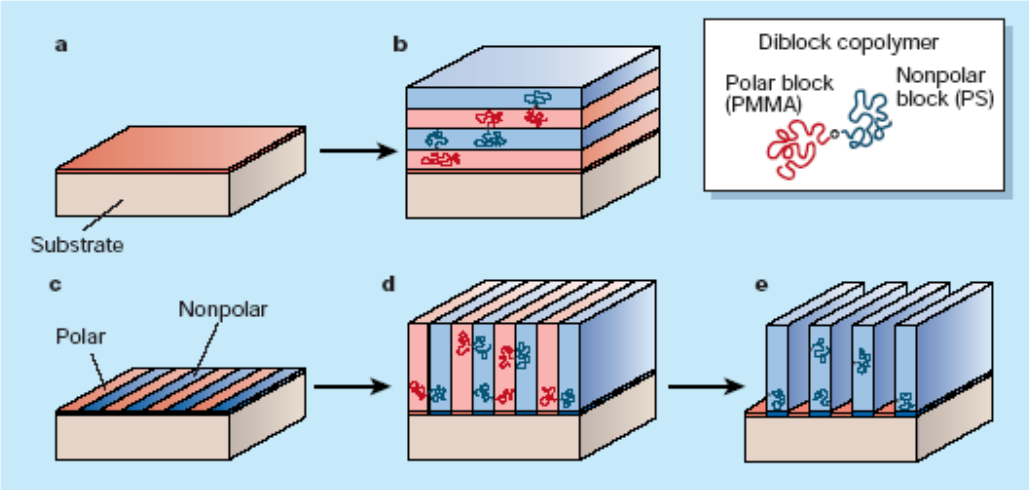

Fig. 1.13 *Self-Assembly of block copolymers on substrates.* PS-*b*-PMMA *(diblock copolymer) - it contains two polymer chains, of PS (blue) and PMMA (red). The polar PMMA block adsorbs to a uniformly polar substrate (a) driving the PS and PMMA lamellae, with a period of about 50 nm, to lie parallel to the substrate (b) if instead, the substrate is patterned with alternating polar and nonpolar stripes (c) with a period that is similar to that of the* PS-*b*-PMMA*, the block copolymer self-assembles epitaxially, with lamellae forming perpendicular to the surface and in precise register with the underlying pattern (d) further chemical modification of the block copolymer film, such as depolymerization of the PMMA block (e) can translate the original chemical pattern on the substrate into a template for patterned functional materials.*

1.7 Conducting Polymers

Conducting polymers are conjugated polymers having an extended delocalized π-electron system through which the electrons can move from one end of the polymer to the other. All conjugated polymers (**Fig. 1.14**) have a σ-bond backbone of overlapping sp^2 hybrid orbitals. The remaining out-of-plane p_z orbitals on the carbon (or nitrogen) atoms overlap with neighboring p_z orbitals to give π-bonds. Polyaniline (PAN) and poly(N-vinylcarbazole) (PVCZ) etc are well known conjugated polymer systems, with the nitrogen p_z orbital assisting the delocalisation of the π-electrons. In polymers such as polyacetylene (PA) and polyaniline (PAN) the delocalization results in a single (degenerate) ground state, whereas in other polymers the alternating single and double bonds lead to electronic structures of varying energy levels. In this regard three classes of conjugated polymers have shown potential applications for example in photovoltaic devices and optoelectronic materials in recent years namely, poly(*p*-phenylenevinylenes)[173, 174], polyanilines[175-178] and polythiophenes.[179-181]

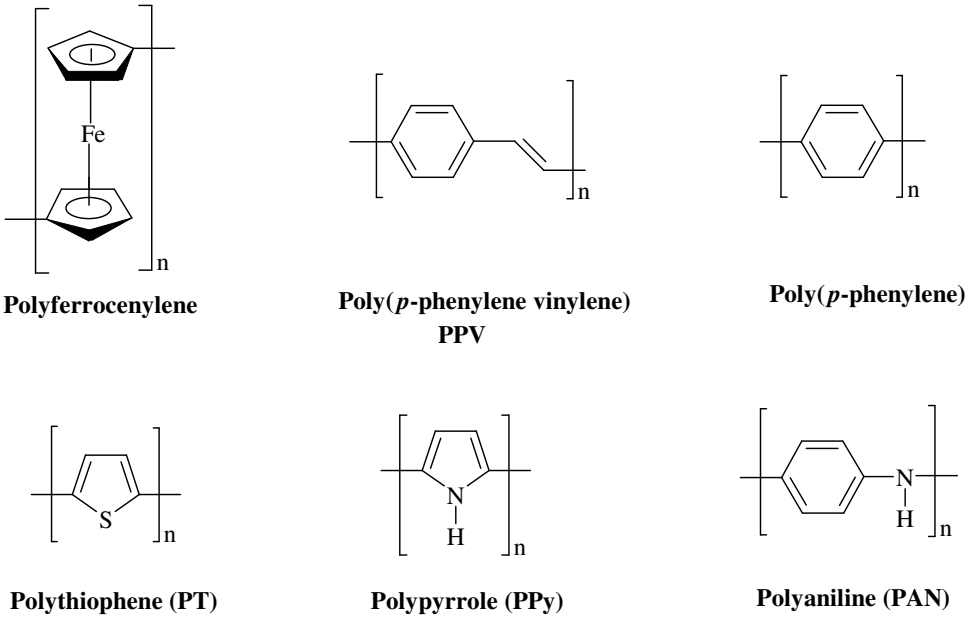

Polyferrocenylene

Poly(*p*-phenylene vinylene) PPV

Poly(*p*-phenylene)

Polythiophene (PT)

Polypyrrole (PPy)

Polyaniline (PAN)

Fig. 1.14 *Typical conjugated polymeric systems having an extended π-electron system.*

In the year 1977 it was shown for the first time by MacDiarmid et al. that chemical doping[182] of these materials resulted in increased electron conductivities over several orders of magnitude. Treatment with halogen was called "doping" by analogy with the doping of semiconductors. The "doped" form of polyacetylene had a conductivity of 10^5 S/m, which was higher than any previously known polymer.[183-185] This discovery captured the thoughts for developing materials with important optoelectronic properties of metals and desirable mechanical properties, with processing advantages of polymers and their low cost. Today conducting plastics are being developed for many uses, such as in corrosion inhibitors, compact capacitors, antistatic coating, electromagnetic shielding of computers and in "*smart*" windows that can vary the amount of light they allow to pass etc. A second generation of electric polymers has also appeared such as in transistors, light-emitting diodes and lasers.

Conjugated polymers exhibit electron-hole conduction similar to conventional semiconductors and this effect is enhanced by chemical doping. A dopant is required to introduce charge carriers in the form of extra electrons or "holes" in the material. A hole is a position, where an electron is missing. When an electron jumps in from a neighbor and fills such a hole, a new hole is created and so on allowing charge to migrate a long distance. Separating the electron-hole pairs produces electrical currents. Both *n*-type (electron donating - e.g. Na, K, Li, Ca, tetrabutylaluminium) and *p*-type (electron accepting - e.g. I_2, PF_6, BF_6, AsF_6) dopants have been utilized to induce an insulator-to-conductor transition in electronic polymers.

$$[CH]_n + 3x/2\ I_2 \rightarrow [CH]_n^{x+} + xI_3^- \qquad \text{Oxidative Doping}$$

$$[CH]_n + xNa \rightarrow [CH]_n^{x-} + xNa^+ \qquad \text{Reductive Doping}$$

The doping procedures involve exposing the polymer films or powders to vapors or solutions of the dopant, or by electrochemical means. The polymer backbone and dopant ions form new three-dimensional structures. The doped polymer is thus a salt. However, it is not the counterions, I_3^- or Na^+, but the charges on the polymer that are the mobile charge carriers. By applying an electric field perpendicular to the film, the counter ions

can be made to diffuse from or into the structure, causing the doping reaction to proceed backwards or forwards. In this way the conductivity can be switched off or on. Different conductivity ranges have been used so as to classify materials such as *conductors* (10^4 to 10^6 S/cm), *semiconductors* (10^2 to 10^{-12} S/cm) and *insulators* (10^{-12} to 10^{-20} S/cm).[186]

1.7.1 Band Theory of Conductivity

The quantum mechanical overlap of p_z orbitals actually produces two orbitals, a bonding (π) orbital and an antibonding (π^*) orbital. The lower energy π orbital produces the valence band and the higher energy π^* orbital forms the conduction band. The difference in the energy between the two levels produces the band gap that determines the optical properties of the material. Most semiconducting polymers appear to have a band gap that lies in the range 1.5-3.0 eV, which makes them ideally suited as optoelectronic devices working in the optical light range. The charge conduction mechanism appears to be more complex for the conducting polymers than for inorganic semiconductors. After the excitation of an electron from the valence band to the conduction band, the resulting electron and hole are bound together and their motion through the material is coupled. These coupled moieties are known as excitons and are responsible for the unusual electronic properties of polymeric systems. One needs to split the exciton so that the holes and electrons can move freely towards opposite electrodes. The use of electron acceptors dopants such as I_2, TCNE (tetracyanoethylene), TCNQ (tetracyanoquinoline) etc provides interfaces along the polymer network wherein the splitting of excitons can take place and hence the probability of electron transfer between the polymeric units gets increased. For instance in polyferrocenylenes after partial oxidation the presence of ferrocene and ferrocenium units splits the exciton and has conductivity (10^{-5} S/cm)[187-189] in comparison to the undoped polyferrocenylene.

1.8 Scope/Motivation of the Work

The increasing interest in functional block copolymers having electrically conducting substructure[190-192] has led to many developments in this field particularly with respect to PFS containing block copolymers.[193-195] Recently the work conducted by Rehahn et al. demonstrated[196] an efficient method for the synthesis of diblock copolymers PFS-*b*-PMMA using FS and MMA monomers wherein PMMA plays the thermoplastic's part with potential further benefit as a photoresist in lithographic processes. The blocks were found to be rather incompatible leading to microphase separation. The phase behaviour in the medium segregation limit yielded three classic micromorphologies namely spheres, cylinders and lamellae.[197] The bicontinuous gyroidic morphology was observed for low molecular weight materials and high annealing temperatures.[198] These bicontinuous phases combined the PMMA's mechanical properties with the benefits of the functional PFS block in an ideal manner. But the main problem and drawback of this bicontinuous phase was the high content of PFS (Φ_{PFS} ~ 0.4), which is very expensive to synthesize both with respect to time and resources. So the important goal of this research work was to lower the volume fraction of PFS block without losing its well-defined micromorphology and to investigate the influence of morphology on the conductivity of these functional materials both in the undoped/doped state.

1.9 Strategy

A strategy that might allow the realization of low volume fraction functional PFS blocks without losing its well-defined micromorphology consisted of the preparation of CBABC type pentablock copolymers, having long thermoplastic A and C blocks together with two short functional B blocks formed by PFS. In combination with polystyrene PS (hard, brittle) forming nonpolar domains and polymethyl methacrylate PMMA (excellent mechanical, thermal and chemical properties) forming polar domains, well defined pentablock copolymers of CBABC type (PMMA-*b*-PFS-*b*-PS-*b*-PFS-*b*-PMMA) had to be synthesized.[199] With the dilution of functional PFS subunits upon their implementation into pentablock copolymers, a variety of fascinating morphologies can be expected.[172]

Chapter 2

Synthesis and Polymerization of [1]Dimethylsilaferrocenophane

2.1 Synthesis of Monomer (FS)

The synthesis of [1]dimethylsilaferrocenophane (FS) is a two-step reaction involving[50] dilithiation of ferrocene followed by cyclization with dichlorodimethylsilane[109] as shown in the **Scheme 9**.[201-204] The first step involves lithiation of ferrocene (**5**) in hexane at room temperature using two equivalents of *n*-BuLi in the presence of tetramethylethylenediamine (TMEDA) to obtain dilithioferrocene (**6**). TMEDA functions as a catalyst by breaking up the less reactive aggregated structures of butyllithium (hexamer) by coordinating to lithium. With the addition of TMEDA in the reaction mixture the ferrocene dissolved completely turning the reaction mixture amber in color.

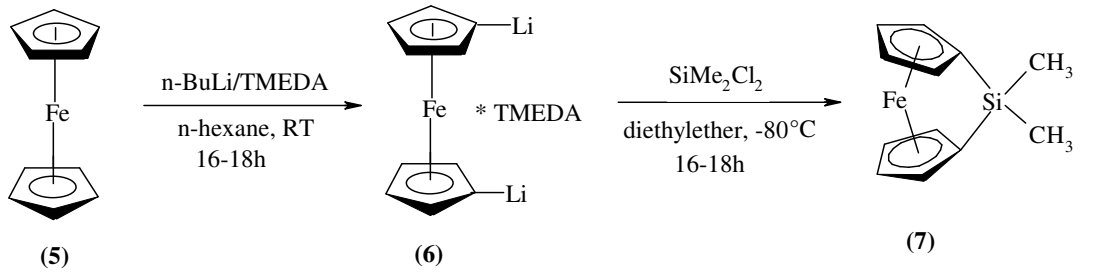

(5) **(6)** **(7)**

[1]Dimethylsilaferrocenophane

Scheme 9

After the addition of *n*-BuLi the change of color of the reaction mixture from amber to red indicated the beginning of lithiation. In about an hour a yellow-orange precipitate of dilithiated ferrocene was observed. Reaction of (**6**) with dichlorodimethylsilane in dry diethylether at -80 ºC yielded the red crystalline [1]dimethylsilaferrocenophane (**7**). A slight excess (ca. 4.5 mol% over the exact stoichiometric amount) of dichlorodimethylsilane was preferred to avoid formation of oligomers. This ensured that both the lithiated sites of ferrocene react with the same molecule of dichlorodimethylsilane leading to cyclization and thereby minimizing oligomerization. However it still contained some oligomers and was not pure enough for living anionic polymerization.

2.2 Purification of Monomer (FS)

In living anionic polymerizations, the high reactivity of anionic centers towards atmospheric moisture, oxygen, carbon dioxide and other contaminants demands highly pure monomeric materials in order to avoid premature living chain termination.[26] If full use of the living character of the anionic systems is desired then all the possible impurities capable of deactivating the initiator and the propagating chain ends must be removed from the polymerization mixture. The monomer purity determines the polydispersity index of the polymer formed and its compositional homogeneity, which in turn is a further crucial parameter for microphase separation and phase behaviour of the domains. Manners et al. had suggested a purification procedure involving three cycles of successive high vacuum sublimation (0.005 mmHg, 40 °C) and recrystallizations from hexanes (-15 °C). However the purification procedure was revisited[196] and various drying agents were tried out (**Fig. 2a**). When fluorenyllithium (pKa = 19), which is only slightly reactive[206] as compared to other organolithium compounds, was used for cleaning the protic impurities present in crude FS monomer, formation of a large amount of oligomer was observed. In the case of triphenylmethyllithium, the formation of triphenylmethane took place, which sublimed along with the FS monomer thereby preventing efficient purification. Further, triphenylmethane reacted with the initiator *n*-BuLi during the FS polymerization. Triethylaluminium and dibutylmagnesium, which are very common drying agents for monomers such as styrene and methacrylates could not be used as they also sublimed with the FS monomer at 40 ºC. Finally, out of $LiAlH_4$ and CaH_2, the latter turned out to be the best reactive drying agent in THF as a solvent. The FS monomer was dissolved in THF and CaH_2 (~1 g) was added to the same. The solution was stirred overnight in the glove box at room temperature.

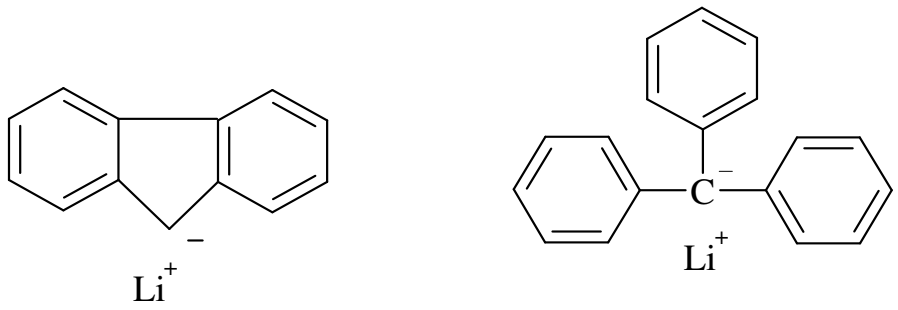

Fluorenyllithium **Triphenylmethyllithium**

$AlEt_3$ **Bu_2Mg** **$LiAlH_4$** **CaH_2**

Fig. 2a *Various drying agents used for FS monomer purification* **(7)**.

Tetrahydrofuran was removed under reduced pressure on a high vacuum line. Finally, the FS monomer was separated from CaH_2 by means of sublimation at 40 ºC. This step of stirring the monomer over CaH_2 in THF was coupled with the Manners et al. purification steps. Thus the crude FS monomer after lithium chloride separation was subjected to the following sequence of purification steps:

(i) Sublimation at 50 ºC under reduced pressure on to a cold probe at 3 ºC.

(ii) Recrystallization from *n*-hexane at -60 ºC.

(iii) Dissolution in 20 mL freshly distilled THF and stirring over CaH_2 (24 h).

(iv) Removal of THF and drying (4 h) under vacuum.

(v) Sublimation at 40 ºC under reduced pressure on to a cold probe at 3 ºC.

(vi) Recrystallization from *n*-hexane at -60 ºC.

(vii) Dissolution in 20 mL freshly distilled THF and stirring over CaH_2 (24 h).

(viii) Removal of THF and drying (4 h) under vacuum.

(ix) Last sublimation at 40 °C under reduced pressure on to a cold probe at 3 °C.

The complete sequence of purification yielded about 60-65% of the pure [1]ferrocenophane that was good enough for anionic polymerization. Further a 20 times expansion of the vertical scale of the ^{1}H-NMR spectrum (**Fig. 2b**) of a solution containing 15 mg of (**7**) in 0.5 mL of C_6D_6 showed no extra signals apart from those for the [1]dimethylsilaferrocenophane and benzene.

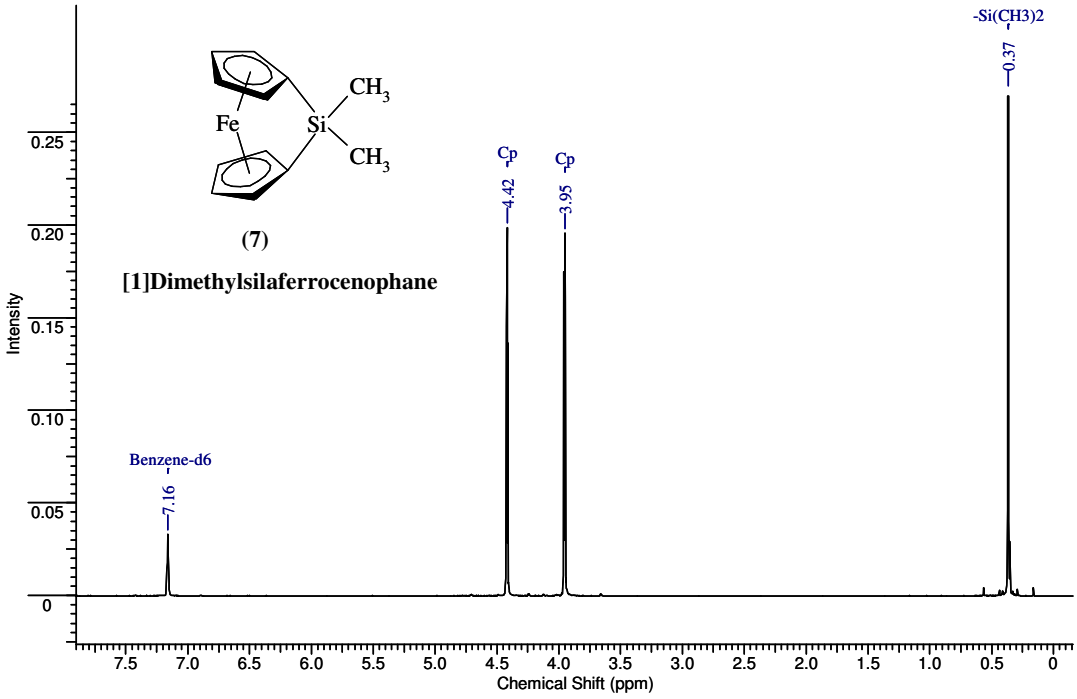

Fig. 2b *500 MHz ^{1}H-NMR spectrum of FS monomer* (**7**).

2.3 Living Anionic Polymerization of [1]Dimethylsilaferrocenophane

2.3.1 *Anionic Ring Opening Polymerization Initiated by n-BuLi*

The polymerization reaction was performed by the addition of *n*-BuLi in a THF solution of [1]dimethylsilaferrocenophane inside the glove box (**Scheme 10**). The color of the solution changed from red to amber in about 10 min indicating the start of polymerization. The PFS polymer obtained after precipitation into *n*-hexane and drying was analyzed by SEC for its molecular weight distribution. An SEC elugram shown in **Fig. 2c** represents a PFS polymer **(8)** having a narrow molecular weight distribution with PDI and M_n of 1.02 and 25,000 g·mol^{-1} respectively.

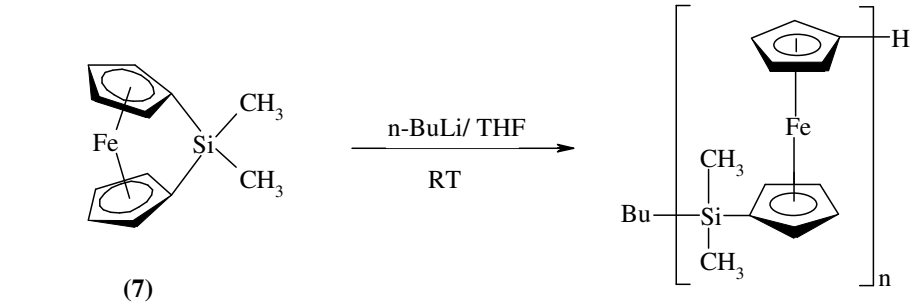

(7)

[1]Dimethylsilaferrocenophane

FS

(8)

Polyferrocenyldimethylsilane

PFS

Scheme 10

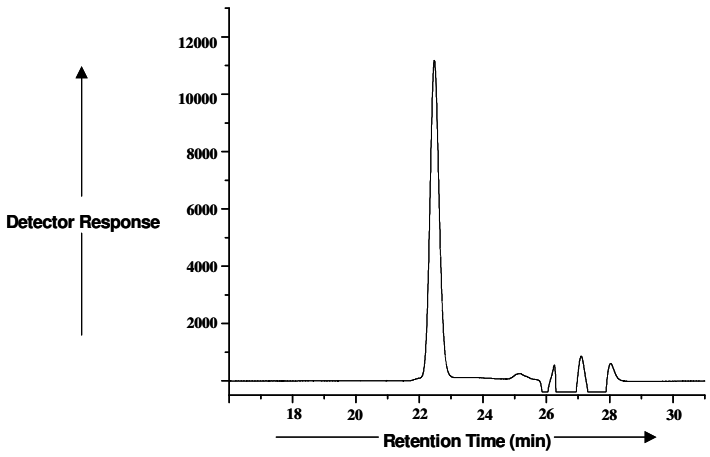

Fig. 2c *A typical SEC trace of polymer PFS* **(8)**.

2.3.2 *Influence of Impurities on FS Polymerization Initiated by n-BuLi*

To demonstrate the influence of impurities on FS polymerization by *n*-BuLi the FS monomers obtained by two different purification procedures were employed. A sample of crude FS was sublimed, recrystallized at -60 ºC and again sublimed after stirring over CaH_2 in THF (**A**). Further another sample was subjected to complete nine-step purification procedure as explained in section **2.2**. Equal amounts of each of them were polymerized by the usual procedure. The experimental data obtained from these two experiments are summarized and compared in **Table 2a**. Comparison of the calculated and observed M_n values showed that in sample (**A**) there were significant amounts of impurities that killed most of the initiator molecules, which resulted in quite high molecular weight of PFS polymer **(8)** in comparison to calculated. While in case of sample (**B**) the complete cycle of purification led to the significant removal of impurities thereby minimizing chain termination and giving a polymer PFS with M_n close to the calculated value.

Table 2a *Polymerization of FS* **(7)** *obtained by two different purification procedures*

Sample*	FS (mg)	Initiator (µL)	Reaction Time (min)	M_n (g/mol) Calculated	M_n (g/mol) Observed	PDI
A	550	20	40	17200	35250	1.12
B	552	20	40	17250	19500	1.04

* Sample **A** was purified by one sublimation, one recrystallization and one stirring over CaH_2 in THF whereas sample **B** was purified by three sublimations, two recrystallizations and two stirrings over CaH_2 in THF (complete series of purification steps).

2.3.3 *Investigation of the 'Living Character' of Polymerization*

The synthesis of a multiblock copolymer like PMMA-*b*-PFS-*b*-PS-*b*-PFS-*b*-PMMA containing two functional PFS blocks is very sensitive to the '*Living Character*' of FS polymerization. The living FS ends initiate the polymerization of the two terminal PMMA blocks. Therefore a good understanding of the living character of FS polymerization is quite important in this context. This is with respect to the pentablock

copolymer syntheses as the presence of a living system allows one to achieve different molecular weights while ensuring all the time a narrow distribution, which on the other hand is an essential requirement for microphase separation of the individual domains. To investigate the '*Livingness*' of FS polymerization with regard to the monomer obtained by series of modified new purification steps, the monomer:initiator ratio was varied from 10:1 to 250:1 in ten different *n*-BuLi initiated polymerization experiments. All these experiments yielded monodisperse PFS homopolymers (PDI = 1.02-1.08) having molecular weights ranging from M_n = 1950-62750 g·mol^{-1} (**Table 2b**). A linear plot of M_n (g·mol^{-1}) vs. mole ratio of monomer:initiator (**Fig. 2d**) clearly suggested the existence of a living system under experimental conditions. The observed molecular weights in **Table 2b** are in close agreement to the calculated values for all the experiments that support the 'living' character of FS polymerization.

Table 2b *Anionic ROP of FS* **(7)** *initiated by 1.6 M n-BuLi in hexanes*

Exp	**M:I**	**Monomer (mg)**	**Initiator (µL)**	**Reaction Time (min)**	**M_n (g·mol^{-1}) Calculated**	**M_n (g·mol^{-1}) Observed**	**PDI**
1.	10:1	213	55	40	2420	1950	1.08
2.	20:1	387	50	40	4838	4200	1.07
3.	40:1	620	40	40	9688	10100	1.05
4.	60:1	697	30	40	14520	15500	1.04
5.	80:1	620	20	40	19375	21500	1.02
6.	100:1	775	20	40	24200	25600	1.03
7.	140:1	542	10	40	33875	35500	1.04
8.	170:1	658	10	40	41125	43000	1.06
9.	200:1	775	10	40	48438	50550	1.07
10.	250:1	968	10	40	60500	62750	1.07

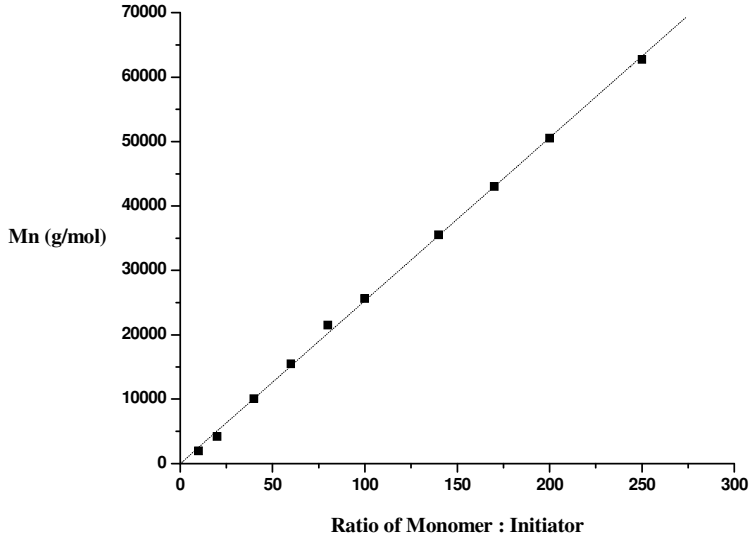

Fig. 2d *A plot of the mole ratio of monomer: initiator vs. M_n (g/mol) for the n-BuLi (1.6 M in hexane) initiated synthesis of PFS* **(8)**.

In separate experiments, addition of another small lot of monomer FS **(7)** to the living polymer system and termination by few drops of methanol yielded PFS polymers **(8)**, which also showed the expected increase in molecular weight characteristic of a living process (**Table 2c**).

Table 2c *Further addition of FS* **(7)** *to the polymerization solution*

Exp	**Monomer (mg)**	**Initiator (µL)**	**Reaction Time (min)**	**Mn ($g \cdot mol^{-1}$) Calculated**	**Mn ($g \cdot mol^{-1}$) Observed**	**PDI**
1.	620	40	40	9688	10100	1.05
2.	Monomer added 200			12800	13200	1.05

Thus all these polymerization experiments clearly show that the FS polymerization is '*living*' in character under the chosen conditions.

Chapter 3

Synthesis and Characterization of **PMMA-*b*-PFS-*b*-PS-*b*-PFS-*b*-PMMA** *Pentablock Copolymers*

The nucleophilicity of the living chain ends estimated on the basis of pKa values determines the order and sequence of the blocks. The pKa for living polystyryl anions is 43 (in DMSO), [66] 39 for polyferrocenyl[209] and 27-28 for polymethyl methacrylate chain ends (pKa of ethyl acetate as a model substance: approx. 27-28).[210] The pKa values clearly explain that with these above mentioned three monomers one has to polymerize styrene (**S**) first followed by [1]dimethylsilaferrocenophane (**FS**) and finally methyl methacrylate (**MMA**) by means of sequential anionic polymerization steps (**Scheme 11**).

This chapter deals with the synthesis and characterization of well-defined pentablock copolymers from styrene as the medium-size central A block, [207] PFS as the small functional B block, and using the 1,1-dimethylsilacyclobutane (DMSB)-mediated 1,1-diphenylethylene (DPE) end-capping technique, PMMA as the long final C block.[199] Lithium naphthalide was selected as a difunctional initiator for styrene polymerization first.[25, 208, 49] The employed preparative strategy should lead to an efficient synthesis of three component pentablock copolymers meeting the criteria of high block efficiency and narrow molecular weight distribution.

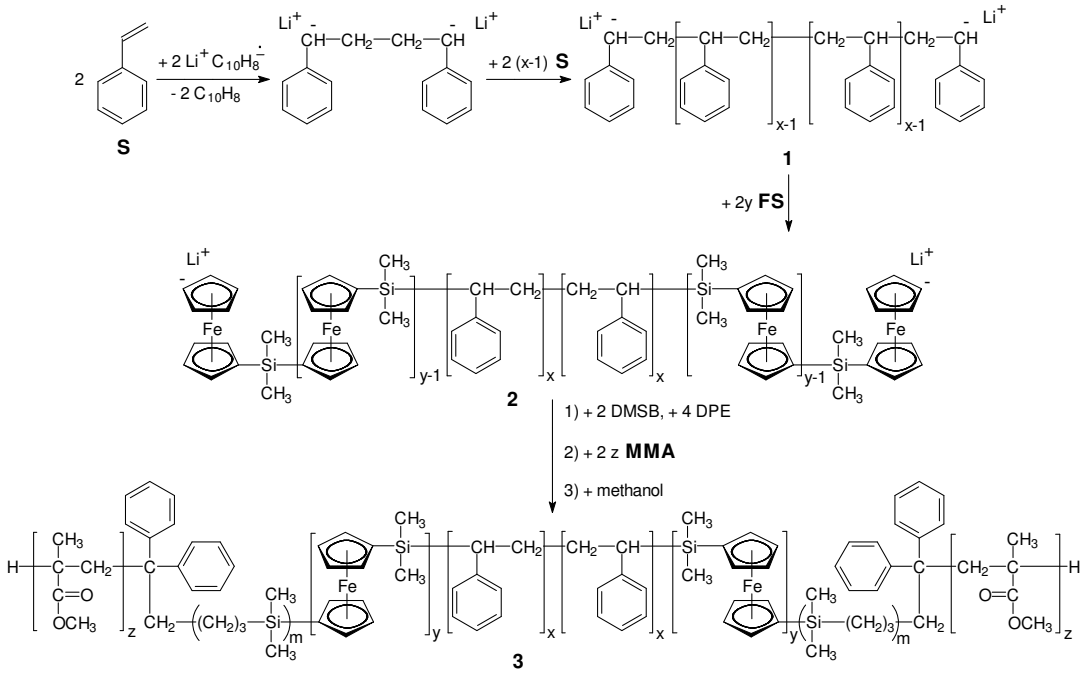

Scheme 11

3.1 Difunctional Initiator 'Lithium Naphthalide'

3.1.1 *Radical Anion*

Naphthalene reacts with alkali metals such as lithium and sodium in THF as a solvent to form stable solutions of the corresponding radical anion (**Fig. 3a**). These solutions when stored at –20 ºC remain active for about 3-4 weeks.

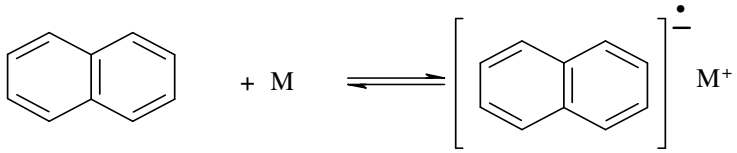

Fig. 3a *Naphthalene radical initiator system,* M= *Li or Na.*

Lithium was chosen over sodium because of its small size and covalent nature of bonding with alkyl groups. With lithium as the counterion one has a good balance between the kinetics of initiation and propagation that is crucial for living anionic polymerization.[206]

3.1.2 *Analysis of the Initiator Solution*

The concentration of the lithium naphthalide initiator solution used for the synthesis of pentablock copolymers was back calculated from the polymerization of styrene at -50 ºC. SEC analysis (**Fig. 3b**) gave M_n = 19,850 g·mol^{-1} and PDI = 1.02, from which the concentration of the lithium naphthalide initiator solution was calculated to be 0.504 M.

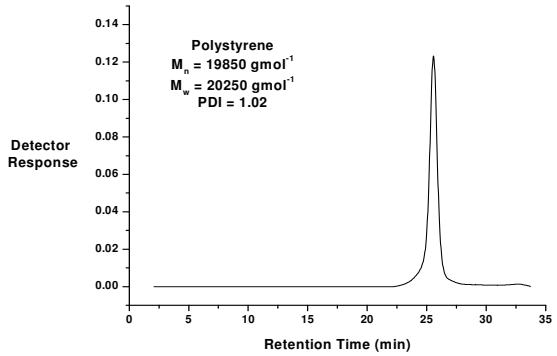

Fig. 3b *SEC chromatogram of polystyrene polymerized by lithium naphthalide initiator.*

3.2 DMSB as "Carbanion Pump" for Efficient End-Capping/Trapping of Living PFS Chain Ends during MMA Polymerization

Attempts to polymerize MMA by the living PFS chain ends failed due to their high nucleophilicity causing predominant attack on the carbonyl group and thereby leading to limited monomer conversion and metal methoxide formation.[211, 116, 196] In order to make a selective attack on the double bond of MMA possible, the living precursor PFS chain ends must therefore be modified in such a way that its nucleophilicity is reduced and the steric requirements are also increased. This secondary reaction involving the nucleophilic attack on the carbonyl group can be limited when a sterically hindered initiator system[45] like diphenylhexyllithium, formed by the reaction of *n*- or *sec*-butyllithium with (one unit of) 1,1-diphenylethylene, is used in a polar solvent (THF) below -70 ºC. MMA polymerization then becomes a living process. This end-capping reaction in THF is quite fast at room temperature and takes place quantitatively as employed by Jérôme et al. in the synthesis of MSBSM pentablock copolymers from butadiene (B), styrene (S) and methyl methacrylate (M) monomers.[212]

With the usage of DPE, the living chain ends prior to MMA polymerization are less reactive (pKa of diphenylmethane: approx. 32) [206] than the PFS chain ends (pKa: 39).[209] The applicability of this method to the synthesis of PFS-*b*-PMMA was examined and it was found that the reaction between PFS living chain ends and DPE was very slow at room temperature in the glove box and even after 2 days only 80 % conversion took place. These observations were supported by the determination of unreacted DPE by GC against decane as internal standard and MALDI TOF mass spectrometry of the terminated reaction product by methanol.[213]

In order to increase the efficiency of the end-capping/trapping reaction with respect to both conversion and time, one needs to activate the living PFS chain ends in relation to the reaction with DPE. In the year 2001, a Japanese research group of Kawakami proposed[216] the concept of a carbanion pump wherein a silacyclobutane having high ring distortional energy[214] was used to convert an oxyanion into a carbanion, which was efficiently trapped by DPE and used to polymerize methyl methacrylate in a controlled manner at -78 ºC (**Fig. 3c**).

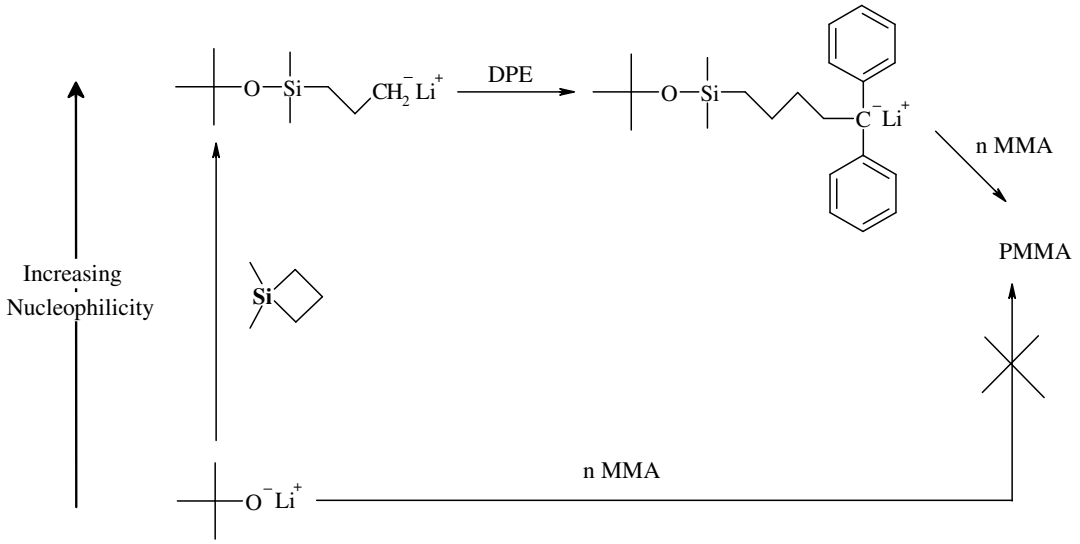

Fig. 3c *Schematic representation of the DMSB based Carbanion Pump.*

The use of DMSB, which besides increasing the nucleophilicity of the PFS chain ends, also shifts the active reaction center from the ferrocene ring to one silicon and three carbon units in sequence. Thus some steric hindrances existing in the reaction of living PFS with DPE earlier are reduced appreciably. A mole ratio of 1:4:2 for Initiator:DPE: DMSB was employed along their addition to the reaction mixture in a sequence wherein DPE was added first followed by DMSB so as to avoid unwanted homopolymerisation of silacyclobutane.[215] DPE reacts slowly with the living PFS chain ends. The actual end-capping starts with the addition of DMSB where the alkyl lithium chain ends formed instantaneously and immediately react with DPE present in excess in the reaction mixture.

3.3 Pentablock Copolymer Synthesis

At first, an appropriate quantity of styrene was added to the solution of lithium naphthalide in tetrahydrofuran at -50 ºC. The color of the reaction mixture turned yellow due to the living polystyryl anions. When the polymerization was complete, the reaction mixture was allowed to come to room temperature. A small test sample of **1** was taken

from the reaction flask and quenched with degassed methanol for subsequent analysis. A solution of FS in THF was then added to the reaction mixture thereby changing the color of the reaction mixture to red and gradually to amber. After complete conversion and withdrawl of a further small sample of **2** for analysis, the living chain termini of the PFS-*b*-PS-*b*-PFS triblock copolymer **2** were end capped by adding a mixture of 1,1-diphenylethylene and 1,1-dimethylsilacyclobutane in sequence.[216, 196] Subsequently, MMA was added at -80 ºC to grow onto the formed bifunctional macroinitiator **2** in a controlled way and the reaction mixture turned yellow immediately. Finally, the whole reaction mixture was deactivated by degassed methanol. The final products **3**, as well as samples **1** and **2** taken during the synthesis, were analyzed using (SEC) Size Exclusion Chromatography (**Fig. 3d**).

One can clearly see from the elution curves of the PS as well as that of the PFS-*b*-PS-*b*-PFS triblock copolymer **2** that they are very narrow and do not show any evidence of a bimodal or trimodal molecular weight distribution. Thus on the basis of the elugrams we can say that there is almost no termination when FS is grafted onto the difunctional polystyrene chains **1**. Only during DPE/DMSB end-capping and subsequent addition of MMA to the bifunctional PFS-*b*-PS-*b*-PFS macroinitiator, approx. one quarter of the living chain ends terminate. The content of terminated species was roughly estimated by graphic separation of the coincident SEC peaks, assuming Gaussian distribution of the length of the individual block species and comparison of the peak areas. Based on this analysis, approx. 20 % of PFS-*b*-PS-*b*-PFS-*b*-PMMA tetrablock copolymer and 5 % of PFS-*b*-PS-*b*-PFS triblock copolymer are formed in addition to 75 % of the desired PMMA-*b*-PFS-*b*-PS-*b*-PFS-*b*-PMMA pentablock system during the final grafting step. This result reflects a higher degree of termination when MMA grows onto living PFS chain termini in a triblock copolymer such as **2** compared with the growth onto pure PFS macroinitiators as described recently.[196] This might be caused by traces of impurities in the solvent or in the FS monomer, which play a more significant role here because of the very low concentration of living centers present during the pentablock copolymer synthesis.

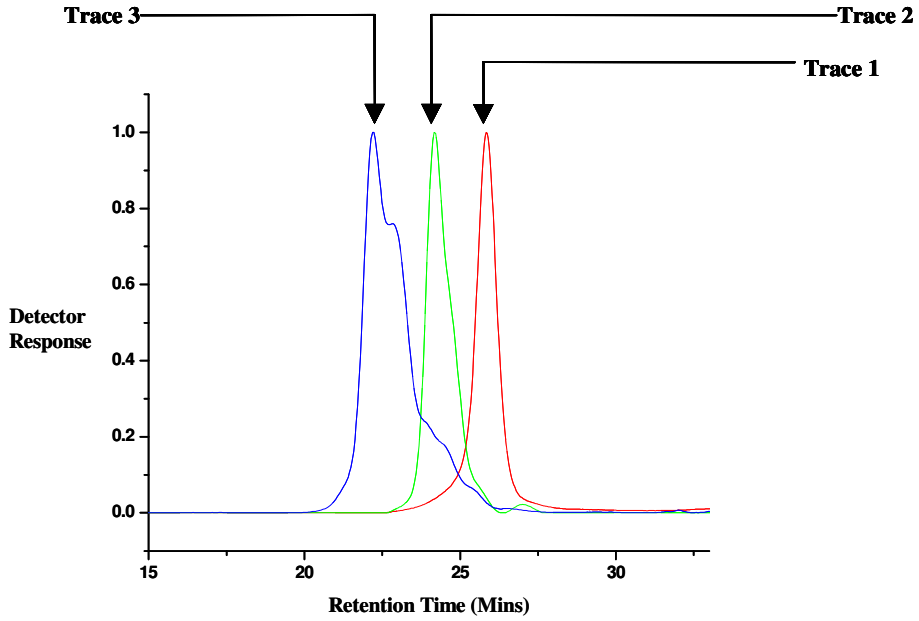

Fig. 3d *Characteristic SEC traces of PS* **1** *(**Trace 1**, **Red**), the PFS-b-PS-b-PFS intermediate* **2** *(**Trace 2**, **Green**), and the final PMMA-b-PFS-b-PS-b-PFS-b-PMMA pentablock copolymer* **3** *(**Trace 3**, **Blue**). Samples are taken during a typical polymerization experiment according to* **Scheme 11**.

Nevertheless, difference in reactivity of the living PFS chain ends associated with the macroinitiator's block copolymer architecture might be responsible as well for the more significant chain termination observed here. Therefore, the influence of the time provided for the DPE/DMSB end-capping on the degree of chain termination was studied. In parallel entries, MMA was added to the reaction mixture after the interval of 15, 30, 45 and 75 min after the addition of DPE and DMSB. Multimodal distributions such as trimodal (**Fig. 3e**) were obtained for 15 and 30 min time periods before the addition of MMA indicating that the end capping was not complete and there may be more than one kind of living species in the system such as *DPE-PFS-*b*-PS-*b*-PFS-DPE*, *DPE-PFS-*b*- PS-*b* -PFS* and *PFS-*b*-PS-*b*-PFS* where * indicates a living chain end.

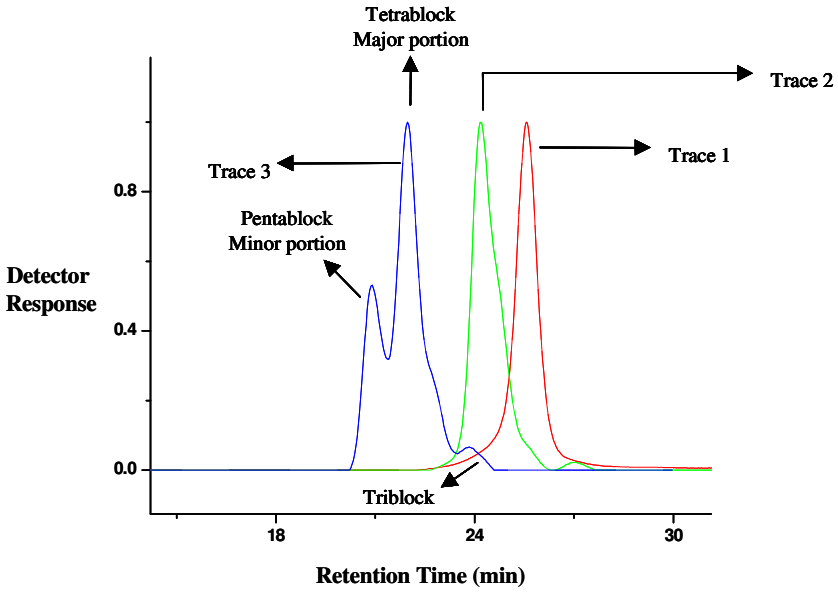

Fig. 3e *Characteristic SEC traces obtained after 30 min time period for end capping reaction leading to a trimodal distribution. (Tetrablock Major, Pentablock Minor and Triblock about ~5%)*

The best results, that is, the smallest portion of terminated chains were obtained for 45 and 75 minute periods for end capping. This is clearly longer than during the synthesis of PFS-*b*-PMMA diblock copolymers where end-capping was already complete after 5 min.[196] This result points towards some influence of the macroinitiators chain architecture on the reactivity of the chain termini, may be through a changed aggregation behavior of the living chain ends. Moreover, the pentablock copolymer architecture makes efficient purification of the products difficult: the removal of tri- and tetrablock copolymer contaminations from pentablock systems is a well-known problem associated with multiblock copolymer syntheses.[217, 218] Nevertheless an efficient procedure (section **3.4**) of repeated precipitation was developed that allowed the removal of all impurities except approximately 15% of the tetrablock species. The latter amount of tetrablock copolymer might also be removable either by multiple repetition of the precipitation procedure or using preparative SEC. But, the material's micro morphologies are not

influenced in an irreproducible way by that minor amount of tetrablock copolymers which has the same polarity as the pentablock. Hence it was decided to continue the investigations with respect to the bulk properties in some more detail.

3.4 Purification of Pentablock Copolymer by Means of Selective Precipitation

Attempts for the purification of the pentablock copolymer by precipitation were made with various solvents. Three solvents namely hexane, cyclohexane and toluene were employed for the experiments. The best results were found for cyclohexane and the pentablock was purified by three cycles of repetitive precipitation in cyclohexane. The crude pentablock was dissolved in THF and to this solution cyclohexane was added dropwise. This addition of cyclohexane changes the polarity of the solvent mixture and

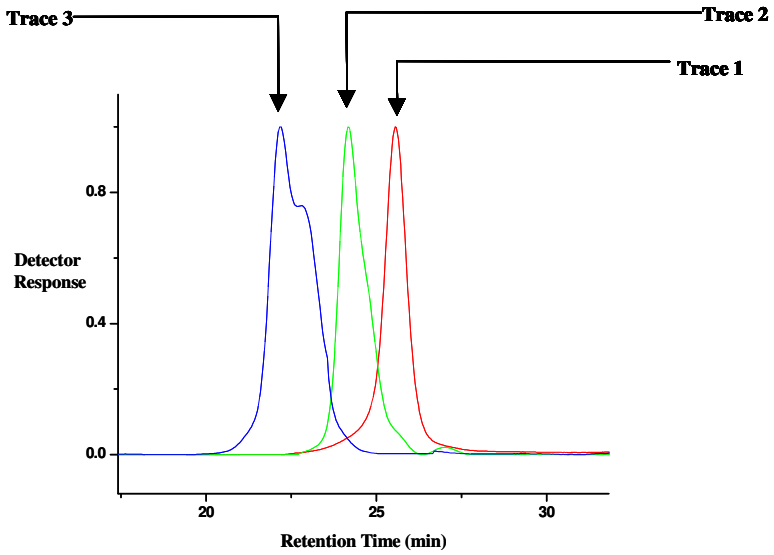

Fig. 3f *Characteristic SEC traces of PS* ***1*** *(**Trace 1**, Red), the PFS-b-PS-b-PFS intermediate* ***2*** *(**Trace 2**, Green), and the PMMA-b-PFS-b-PS-b-PFS-b-PMMA pentablock copolymer* ***3*** *(**Trace 3**, Blue) after threefold precipitation according to the above purification procedure.*

the pentablock precipitates out along with the small quantity of tetrablock copolymer. The triblock remains in the solution and is separated off from the precipitate by means of

a centrifuge (**Fig. 3f**). The procedure can be repeated several times, depending on the required purity of the materials.

3.5 Molecular Characterization of the Pentablock Copolymers

A series of pentablock copolymers were synthesized by the sequential addition of the monomers (quantities mentioned in **Table 1**).

Table 1 *Quantities of monomers (**S**, **FS** and **MMA**) and initiator (**I**) used for the synthesis of pentablock copolymers*

Sample	S (g, mmol)	FS (g, mmol)	MMA (g, mmol)	I (µmol)
A	0.28, 2.688	0.2, 0.8261	0.9, 8.989	25.2
B	0.25, 2.4	0.2, 0.8261	0.8, 7.9904	25.2
C	0.85, 8.16	0.4, 1.6522	1.2, 11.985	50.4
D	0.45, 4.32	0.2, 0.8261	0.65, 6.4919	25.2
E	0.6, 5.76	0.2, 0.8261	0.6, 5.9925	25.2
F	0.7, 6.72	0.2, 0.8261	0.5, 4.9938	25.2
G	0.75, 7.2	0.2, 0.8261	0.35, 3.4958	25.2

After synthesis, a careful molecular characterization of the materials by various spectroscopic and chromatographic techniques was carried out. The molecular weights of the pentablock copolymers as well as of all intermediates were determined through size exclusion chromatography by the evaluation of the SEC elution curves vs. commercially available polystyrene (PS) standards (see *Chapter 7 Experimental*). The experimentally determined values of M_n were found to be in good agreement with the calculated M_ns. The polydispersity indices were clearly below 1.2 in all cases (**Table 2**).

The block lengths in the pentablock copolymers are the values expected from the amounts of monomers and initiators used in the respective entry.

Table 2 *Characterization of the* PMMA-*b*-PFS-*b*-PS-*b*-PFS-*b*-PMMA *pentablock copolymers, synthesized in THF using lithium naphthalide as a difunctional initiator*

Sample	M_n (g/mol) Pentablock	M_w (g/mol) Pentablock	M_n (g/mol) Triblock	M_n (g/mol) PS	*PDI*	ϕ (NMR)			Block Length *N*		
						MMA	FS	S	MMA	FS	S
A	50 000	56 000	19 500	12 000	1.12	**60**	13	27	300	35	104
B	51 000	57 000	20 000	11 000	1.12	**59**	15	26	294	35	100
C	49 000	56 000	29 000	16 500	1.14	**47**	16	37	248	39	150
D	50 000	57 000	27 000	18 000	1.14	**45**	16	39	240	39	160
E	50 000	57 500	30 000	22 000	1.15	**37**	13	50	207	33	208
F	51 000	58 000	34 500	27 000	1.13	**29**	13	58	168	33	249
G	52 000	59 000	36 500	29 000	1.13	**21**	15	64	125	39	285

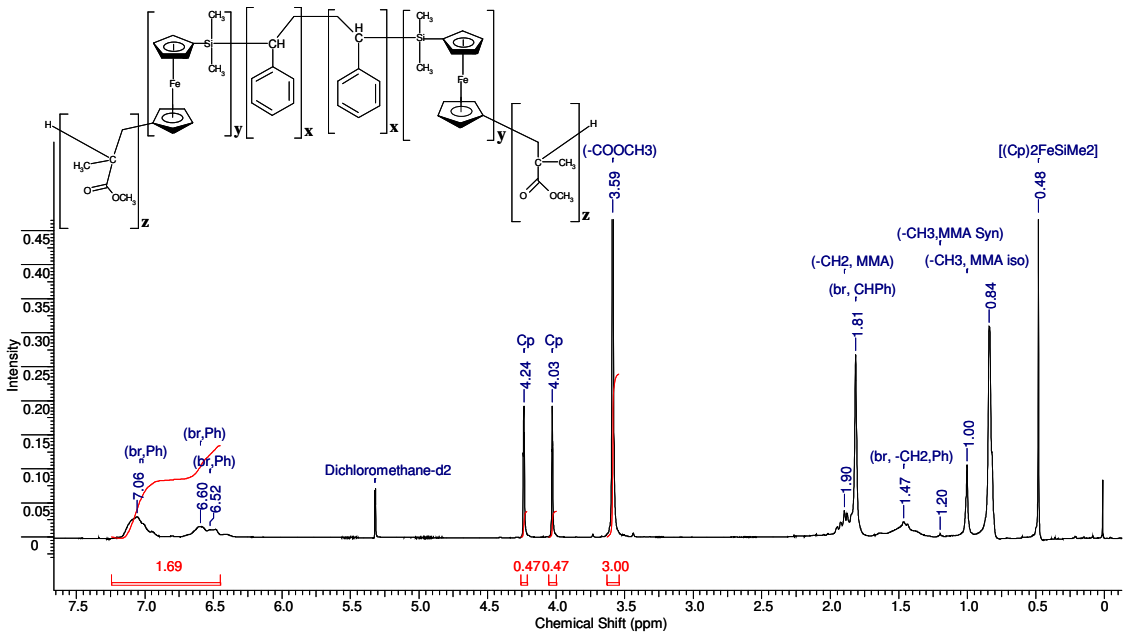

Fig. 3g *^1H NMR spectrum (500MHz) of a* PMMA-*b*-PFS-*b*-PS-*b*-PFS-*b*-PMMA *pentablock copolymer in CD_2Cl_2.*

The pentablock copolymer was further analyzed by NMR spectroscopy. Integration of the characteristic proton resonances (**Fig. 3g**) namely for the eight protons of mono substituted cyclopentadienyl ring (δ = 4.24, 4.03 ppm), the three protons of the methyl ester in MMA (δ = 3.59 ppm) and the five aromatic protons from the benzene ring in styrene appearing as broad signals (δ = 6.5-7.02 ppm) along with the absorption intensities allowed determination of the molar composition of the materials. Broad signals typical for PMMA tacticity[219, 220] were also observed viz. (δ = 1.20 ppm, PMMA Isotactic) and (δ = 1.00 ppm, PMMA Syndiotactic). Furthermore, the degree of polymerization of each block was estimated by combining the overall values of M_n with the ratios of the ^{1}H NMR integrals. The bulk densities taken for the calculation of volume fraction ϕ are 1.26 g.cm^{-3} for PFS[207], 0.906 g.cm^{-3} for PS and 1.15 g.cm^{-3} for PMMA.[221] Finally detailed analysis and peak assignment was also done for the ^{13}C NMR spectrum so as to complete the spectral characterization (**Fig. 3h**).

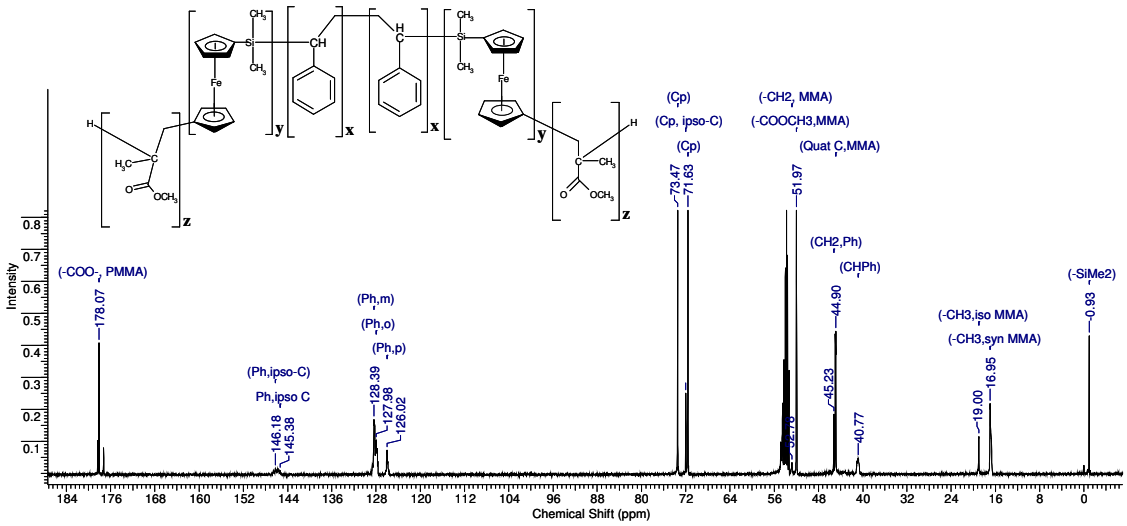

Fig. 3h *^{13}C NMR spectrum (125MHz) of a* PMMA-*b*-PFS-*b*-PS-*b*-PFS-*b*-PMMA *pentablock copolymer in CD_2Cl_2.*

Thus, the strategy for the synthesis of CBABC type pentablock copolymers was effectively realized. The block copolymers were well defined and synthesized in good yield (75%) using lithium naphthalide as a difunctional initiator and DMSB as an accelerator for more efficient DPE end-capping. Molecular characterization of the materials was done by NMR spectroscopy and Size Exclusion Chromatography (SEC) with respect to their narrow molecular weight distributions (PDI< 1.2).

Chapter 4

Self-Assembly of **PMMA-*b*-PFS-*b*-PS-*b*-PFS-*b*-PMMA** *Pentablock Copolymers*

This chapter describes in detail the self-assembly of PMMA-*b*-PFS-*b*-PS-*b*-PFS-*b*-PMMA pentablock copolymers including the sample preparation and characterization by TEM and SAXS. The huge multitude of possible microphases is determined by composition variables, the volume fractions (ϕ_A, ϕ_B, ϕ_C) and the three Flory-Huggins interaction parameters (χ_{AB}, χ_{AC} and χ_{BC}). In general suitable samples were prepared by slow evaporation of a solution of the block copolymers in an appropriate solvent. The solvent has a large influence on the formation of equilibrium morphology [224-229] of interest. The solubility of polymers in low molecular weight solvent is described by means of Hildebrand's solubility parameter, which provides a guide for the solvent selection.

4.1 Determination of Solubility Parameters

The solubility of polymers in different solvents is determined by Hildebrand solubility parameters, which is a fundamental thermodynamic property of polymers and is used extensively for the discussion of the miscibility of polymers in solvent and blends. The process of dissolving an amorphous polymer in a solvent is governed by the free energy of mixing given by

$$\Delta G_m = \Delta H_m - T\Delta S_m \qquad \textbf{4.1a}$$

Where, ΔG_m is the Gibbs free energy change of mixing, ΔH_m is the enthalpy change of mixing, T is the absolute temperature, and ΔS_m is the entropy change of mixing. Hildebrand, Scott and Scatchard[230] proposed that the enthalpy change of mixing (ΔH_m) can be related to the energy of vaporization (ΔE^v) by

$$\Delta H_m = V\,[(\Delta E^v_1/ V_1)^{1/2} - (\Delta E^v_2/ V_2)^{1/2}]^2\,\Phi_1\Phi_2 \qquad \textbf{4.1b}$$

where V is the volume of mixture ($V_1 + V_2$), ΔE^v_i is the energy of vaporization of species i and Φ_i is the volume fraction of species i.

The solubility parameter, δ_i, of a liquid is defined as the square root of the cohesive energy density ($\Delta E^v_i / V_i$) that describes the attraction between molecules of the material

$$\delta_i = (\Delta E^v_i / V_i)^{1/2} \qquad \textbf{4.1c}$$

where V_i is the molar volume of species i. Thus materials with similar cohesive energy density have quite similar intermolecular attractive forces, which explain their miscibility. Equation **4.1b** can be rewritten to give the heat of mixing per unit volume for a binary mixture:

$$\Delta H_m/V = (\delta_1 - \delta_2)^2 \Phi_1\Phi_2 \qquad \textbf{4.1d}$$

For the Gibbs free energy of mixing (ΔG_m) to be favorable i.e. negative, the heat of mixing must be smaller than the entropic term ($T\Delta S_m$). In general $(\delta_1 - \delta_2)^2$ must be small for the components to be miscible. Therefore a good knowledge of the solubility parameter of a polymer is of fundamental significance.

The solubility parameter determination for solvents and other volatile substances is done by calorimetric measurements of the enthalpy of evaporation (ΔH_{vap}). Since polymers are non-volatile and they decompose before the heat of vaporization can be measured, their solubility parameters are determined indirectly by methods such as refractive index[231], intrinsic viscosity[232], turbidimetric titrations[233], gas chromatography[234] and swelling measurements.[235] The solubility parameter of PFS was determined by swelling studies of a crosslinked poly(ferrocenyldimethylsilane)-poly(carbosilane) network in various solvents (**Fig. 4b**).[236]

The solubility parameter range for the poly(ferrocenyldimethylsilane) homopolymer was estimated by swelling studies of the weakly crosslinked gel in fourteen different solvents with δ values ranging from 14.4 to 24.3 $MPa^{1/2}$. The best solvents for poly(ferrocenyldimethylsilane) turned out to be tetrahydrofuran, chloroform and dichloromethane with a solubility parameter of 18.7 $MPa^{1/2}$. Further the solubility parameter for PS and PMMA are 18.2 $MPa^{1/2}$ and 18.6 $MPa^{1/2}$ respectively.[221]

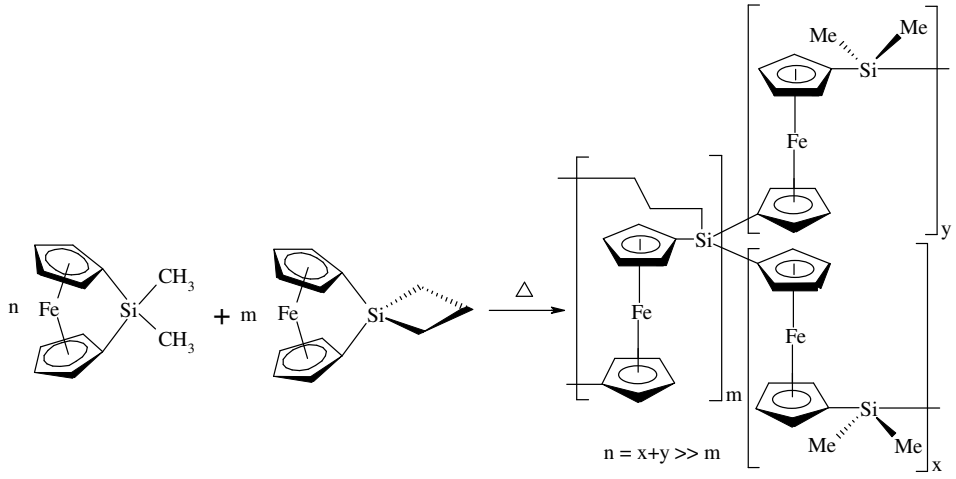

Fig. 4b *Synthesis of a crosslinked poly(ferrocenyldimethylsilane)-poly(carbosilane) network.*[236]

Table 1 *Hildebrand's Solubility Parameters for various solvents*[221]

Solvent	**n-Hexane**	**Cyclohexane**	**Ethyl acetate**	**Toluene**	**THF**	**CH_2Cl_2**	**$CHCl_3$**	**MEK**
Δ MPa$^{1/2}$	14.9	16.8	18.2	18.3	18.5	18.6	18.7	19.3

Table 2 *$(\delta_1 - \delta_2)^2$ for Homopolymer-Solvent Pairs*

Polymer	**n-Hexane**	**Cyclohexane**	**Ethyl acetate**	**Toluene**	**THF**	**CH_2Cl_2**	**$CHCl_3$**	**MEK**
PS	10.89	1.96	0.00	0.01	0.09	0.16	0.25	1.21
PFS	14.44	3.61	0.25	0.16	0.04	0.01	0.00	0.36
PMMA	13.69	3.24	0.16	0.09	0.01	0.00	0.01	0.49

It is quite clear and evident from the above two tables that toluene, THF and dichloromethane are the best solvents for PS, PFS and PMMA blocks in the pentablock copolymer i.e. when no selectivity is observed. Ethyl acetate is good for both PS and PMMA but PFS has a very low solubility in it. Further *n*-hexane, cyclohexane and methyl

ethyl ketone were also ruled out because of large differences in the solubility parameters between them and the blocks of the pentablock copolymer.

4.2 Thermal Characterization of the Pentablock Copolymer

Thermal stability of pentablock copolymer samples was investigated so as to have a fair idea about the appropriate/possible annealing temperatures under vacuum for film preparation. One should avoid working very close to the decomposition temperature while forcing microphase separation in the block copolymer melt. Thermal characterization was therefore required to decide the safe temperature range without causing decomposition.

4.2.1 *Thermogravimetry and Thermal Stability*

Thermogravimetric analysis (TGA) of the pentablock copolymer (**Fig. 4c**) showed

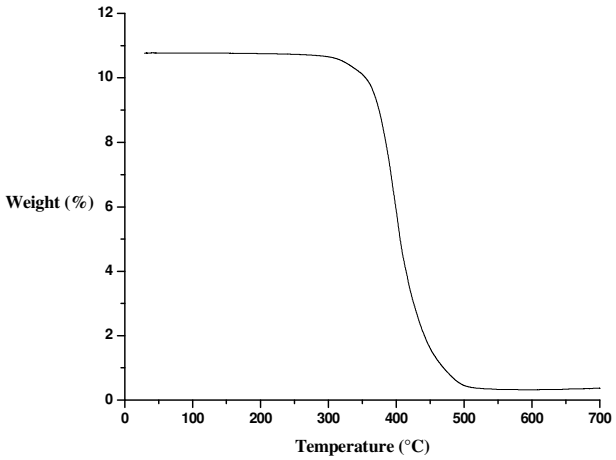

Fig. 4c *TGA trace of pentablock copolymer sample* ***A*** *(heating rate of 10 °C min^{-1}).*

that the decomposition started at around 300 °C. This observation is consistent with the stability of anionically polymerized PMMA[237], which is stable up to approximately 300 °C and PFS wherein decomposition starts only at around 350 °C.[238, 239] PFS homopolymer undergoes Fe-Si-C ceramic formation when heated in the range of 450-500 °C. Polystyrene is also thermally stable upto 400 °C.[145] Thus a narrow temperature range

of weight loss (300-500 °C) accompanied by cross-linking and depolymerization reactions is observed for the pentablock copolymer.

The influence of high temperature on the block copolymer films was also investigated by means of size exclusion chromatography. Samples after annealing at various temperatures for 24 h in vacuum were analyzed for their molecular weight distribution. An overlay of various SEC elugrams (**Fig. 4d**) clearly shows that broadening of the peak shape starts somewhere around 260 °C wherein a shoulder appears to the right of the peak. This can be explained due to the low molecular weight portions formed by depolymerization of PMMA.

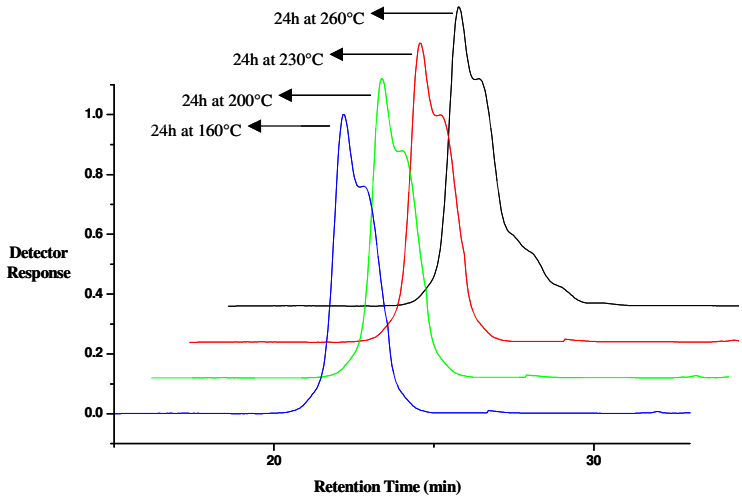

Fig. 4d *Comparison of GPC elugrams from films of pentablock copolymer **D** (from CH_2Cl_2) after annealing in the vacuum at temperatures 160 °C to 260 °C for 24 h. (M_n = 50,000 g·mol^{-1}) [Volume fraction ϕ; MMA: 45, FS: 16, S: 39]*

4.2.2 ***Differential Calorimetry***

It has been reported[203] by Manners et al. that the glass transition temperatures (measured by DSC) of monodisperse PFS increase from 8 °C to 33 °C as the M_n value

increases from 1800 g·mol^{-1} to 22000 g·mol^{-1} and then it remains the same for very high molecular weight ($M_n > 10^5$). In contrast to PFS that is semi-crystalline PMMA is amorphous and depending on the tacticity it has different glass transition temperatures. Anionic polymerization of MMA at –78 °C yields 80 % syndiotactic PMMA having a Tg of 128 °C.[240] Further for PS the Tg ranges from 88 °C to 110 °C depending on the molecular weight.[241]

The thermal transition behavior of the pentablock copolymers was investigated by DSC (**Fig. 4e**). The glass transition for PFS was not observed primarily because of its low volume fraction in the pentablock copolymer (ϕ = 0.13 – 0.16). The two glass transitions for PS and PMMA were at 90 °C and 130 °C respectively which were found to be in a similar range to those of the corresponding homopolymers thereby strongly suggesting that the blocks are incompatible.[211, 242] Thus in the solid state, the formation of microscopic heterogeneities in composition would be expected.

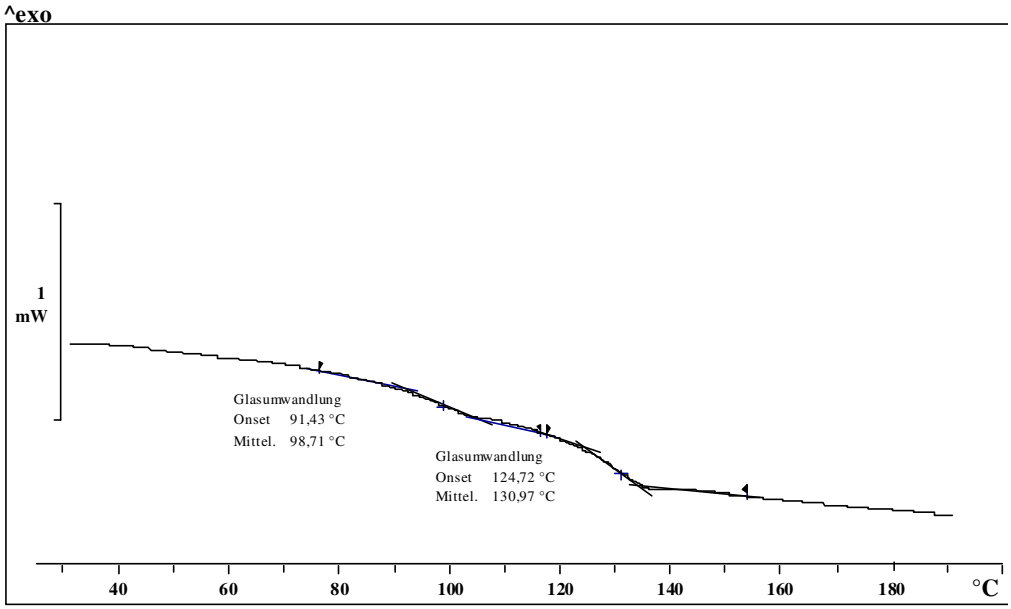

Fig. 4e *DSC trace of pentablock copolymer sample* ***A*** *(heating rate of 10 °C min^{-1}).*

4.3 Phase Behavior of the Pentablock Copolymers

The phase behavior was studied in the bulk block copolymer melt. The pentablock copolymer films were initially cast onto glass plates from solutions (5 % w/v) in dichloromethane, tetrahydrofuran and toluene.[197] Freshly cast films were then stored in the saturated atmosphere of the corresponding solvent for 3-4 weeks so as to induce and drive the formation of thermodynamically stable morphologies. The micromorphologies formed by these materials have a PFS volume fraction of ϕ_{PFS} = 0.13 to 0.16. All the relevant data of the samples under further investigation are listed in **Table 3**.

Table 3 *Molecular weight and volume fraction of the pentablock copolymer samples investigated by TEM and SAXS.*

Sample	M_n (g/mol) Pentablock	M_w (g/mol) Pentablock	*PDI*	ϕ (NMR)			Block Length *N*		
				MMA	FS	S	MMA	FS	S
A	50 000	56 000	1.12	**60**	13	27	300	35	104
B	51 000	57 000	1.12	**59**	15	26	294	35	100
C	49 000	56 000	1.14	**47**	16	37	248	39	150
D	50 000	57 000	1.14	**45**	16	39	240	39	160
E	50 000	57 500	1.15	**37**	13	50	207	33	208
F	51 000	58 000	1.13	**29**	13	58	168	33	249
G	52 000	59 000	1.13	**21**	15	64	125	39	285

When the annealing procedure was carried out at temperatures above 200 °C followed by direct quenching of the films in ice water, apparently biphasic morphologies were observed by TEM, which was further supported by SAXS scattering pattern. They were either lamellar or cylindrical, depending on the PMMA's volume fraction. Under these annealing conditions there is rather high compatibility between PS and PFS[207] and hence low segregation tendency, which results in a homogeneous mixture of these segments (dark grey phase in the TEM pictures). Only PMMA, which is incompatible with both PFS and PS, creates its own phase (white phase in the TEM pictures). Consequently a biphasic morphology is formed which assumes a lamellar structure when both ϕ_{PMMA} and ϕ_{PS+PFS} are between 0.4 and 0.6 and is in full agreement with expected results. As an example (**Fig. 4f**) shows the TEM picture of a film of sample **B** treated in this way. Similar pictures were obtained for samples **A, C** and **D** under analogous conditions.

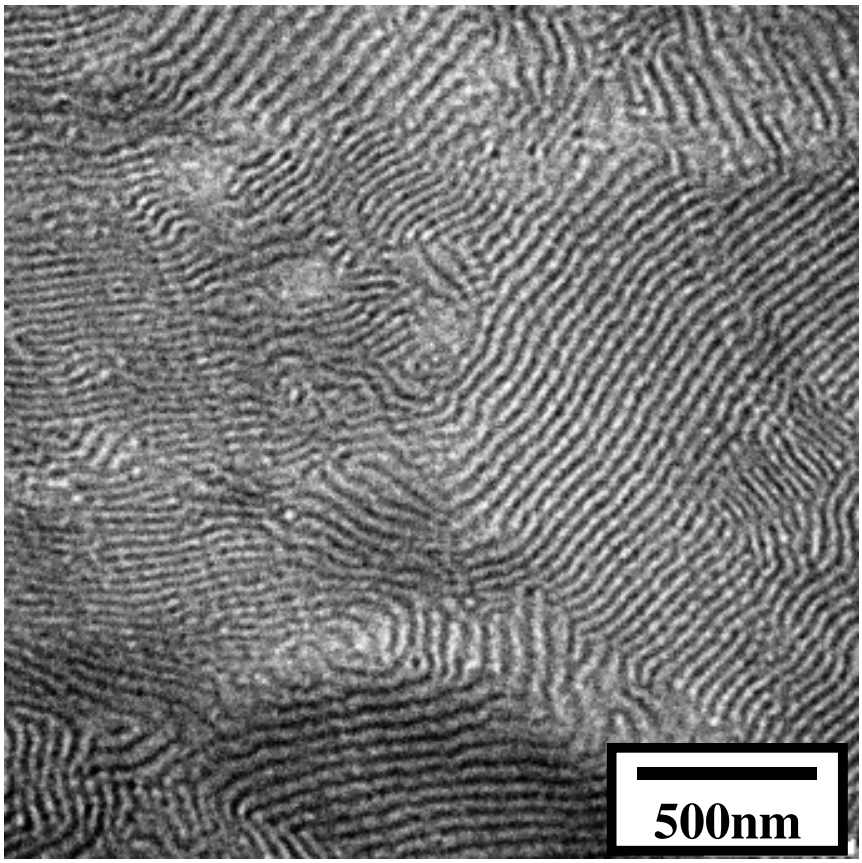

Fig. 4f *Bright field transmission electron micrographs for sample **B*** (**LAMELLAR Morphology**). *Black regions represent the blend domains of PS and PFS while the PMMA phases appear in white. Samples were prepared from CH_2Cl_2 and annealed for 24 h at 200 °C.*

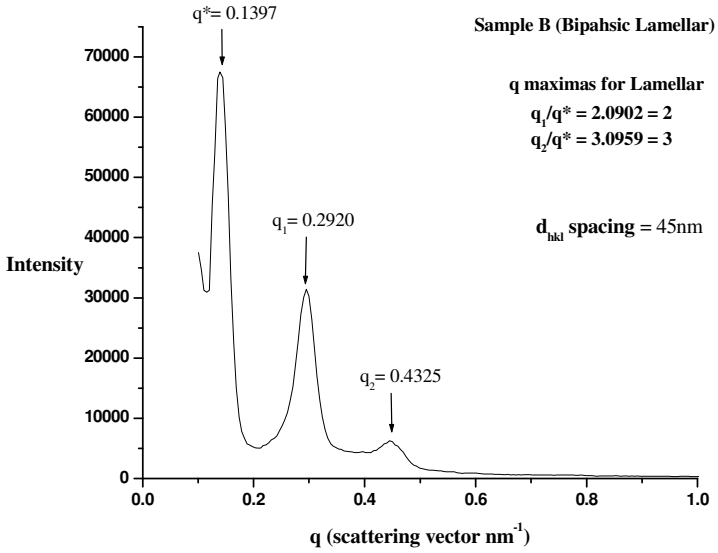

Fig. 4g *SAXS-pattern of sample **B** annealed at 200 °C for 24 h. (Scattering vector q = 4π/λ sinθ; with λ= 0.1542 nm and 2θ the scattering angle)*

The SAXS scattering profile (**Fig. 4g**) shows three strong peaks, which agree with a lamellar structure with q_n/q_1 ratios which equal 1.0, 2.0 and 3.0. Similar SAXS patterns were observed for samples **A**, **C** and **D** under analogous conditions. The d-spacing for the lamellar repeating unit is calculated as 45 nm from both the first peak and from a plot of d_{n00} versus 1/n (**Fig. 4h**). [243] (Refer *Chapter 7: Analysis of the X-ray data*)

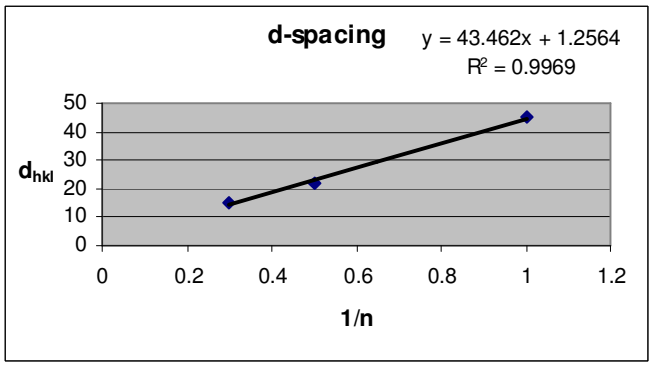

Fig. 4h *A plot of d_{hkl} vs. 1/n for the SAXS scattering profile of sample **B** (d-spacing = slope of the plot).*

On the other hand, when $\phi_{PMMA} < 0.4$, the PMMA segments form cylinders in a continuous homogeneous blend matrix of PS and PFS (**Fig. 4i**).

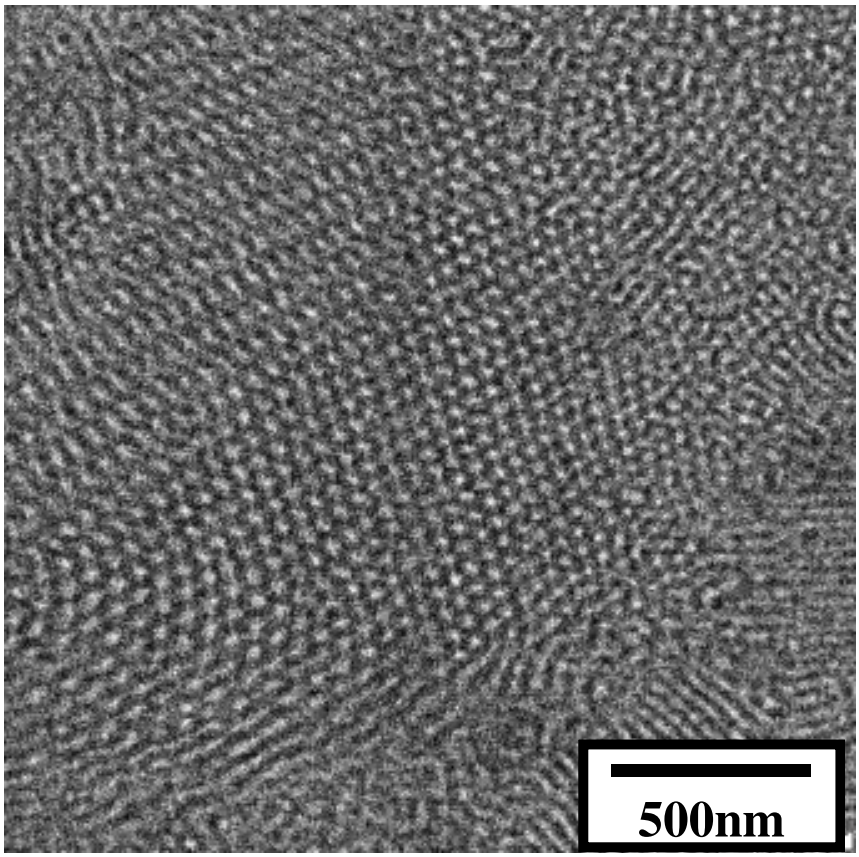

Fig. 4i *Bright field transmission electron micrograph for sample **E*** (**CYLINDER Morphology**). *Black regions represent the blend domains of PS and PFS while the PMMA phases appear in white. Samples were prepared from CH_2Cl_2 and annealed for 24 h at 200 °C.*

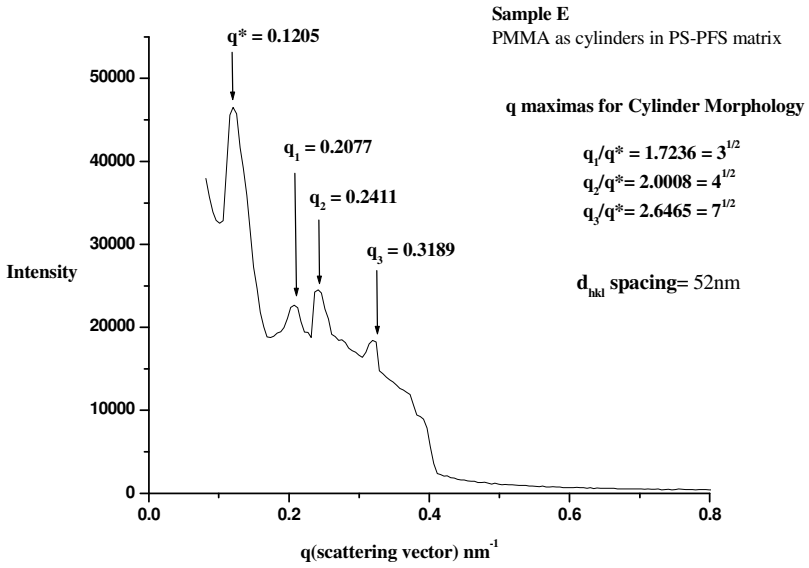

Fig. 4j *SAXS-pattern of sample **E** annealed at 200 °C for 24 h. (Scattering vector q = 4π/λ sinθ; with λ= 0.1542 nm and 2θ the scattering angle)*

The SAXS scattering profile (**Fig. 4j**) shows four discernible peaks in the q dependence of the scattered intensity, centered at q/q* ratios of 1: √3: √4: √7, where q* is the principal peak position. This is consistent with the allowed reflections for cylinder orientation of microdomains.[244] The d-spacing is 52 nm as calculated from the first reflection peak. Thus there is a close agreement between the TEM micrographs and the SAXS profiles.

A completely different picture was found when annealing was carried out at slightly lower temperatures. This lowering of temperature is equivalent to a higher value of the Flory-Huggins interaction parameter 'χ'. This is related to the temperature given by the following equation,

$$\chi = \frac{1}{k_B T}\left[\epsilon_{AB} - \frac{1}{2}(\epsilon_{AA} + \epsilon_{BB})\right] \qquad \textbf{4.3a}$$

From **eq. 4.3a** it is clear that decreasing the temperature increases the interaction parameter as χ is inversely related to temperature T. Hence phase separation of PFS and PS was also expected at lower temperature condition.[207] The best TEM pictures were obtained for samples annealed at 180 °C and then immediately quenched in ice water. Stepwise cooling to 100 °C did not improve the microphase separation significantly.

Thus in the samples prepared, three distinct morphologies could be identified by TEM. On one hand, a spheres-in-spheres ("ball in the box"; *sis*) morphology[245, 246] was observed for samples **A** and **B** (**Fig. 4k**): Larger spheres or ellipsoids are formed by the PS (grey) wherein, next to the surface, small PFS spheres are integrated. The latter appear as black dots in the TEM picture. The PMMA majority component, on the other hand represents the continuous (white) matrix.

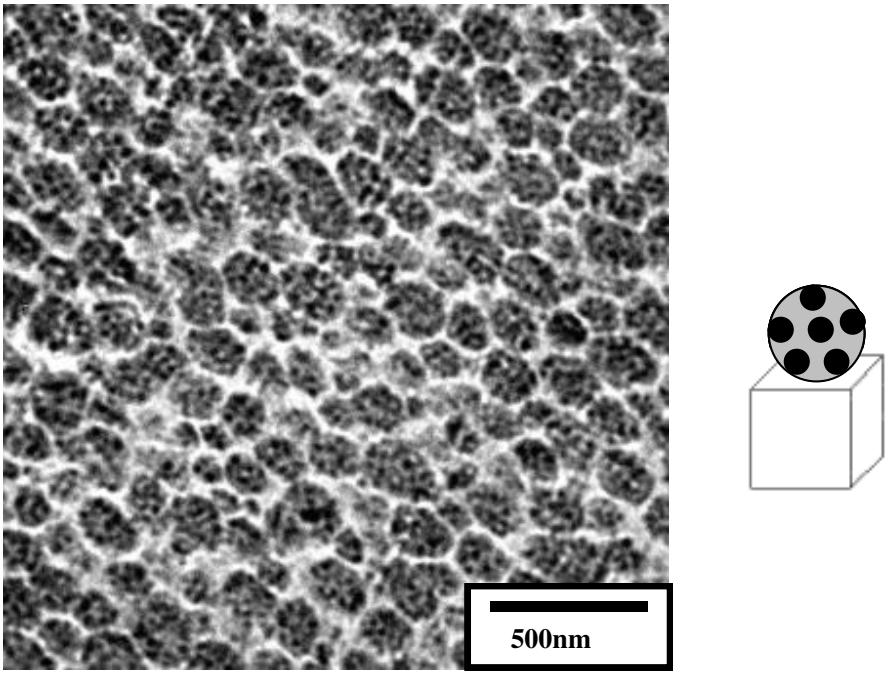

Fig. 4k *Bright field transmission electron micrograph of sample **A** (spheres-in-spheres morphology); the film was cast from dichloromethane solution and annealed for 1 day at 180°C. Grey, black and white regions in the picture as well as in the schematic drawing represent the domains of PS, PFS and PMMA, respectively.*

The *sis* morphology was found whenever ϕ_{PMMA} was approximately 0.60 while ϕ_{PS} was ≈ 0.25 and ϕ_{PFS} ≈ 0.15 (samples **A** and **B**). It is the favored morphology here because of the lower interfacial tension, γ_{AB}, between the rather compatible PS and PFS phases in comparison to the interfacial tensions γ_{AC} and γ_{BC} of these two phases with that of PMMA.

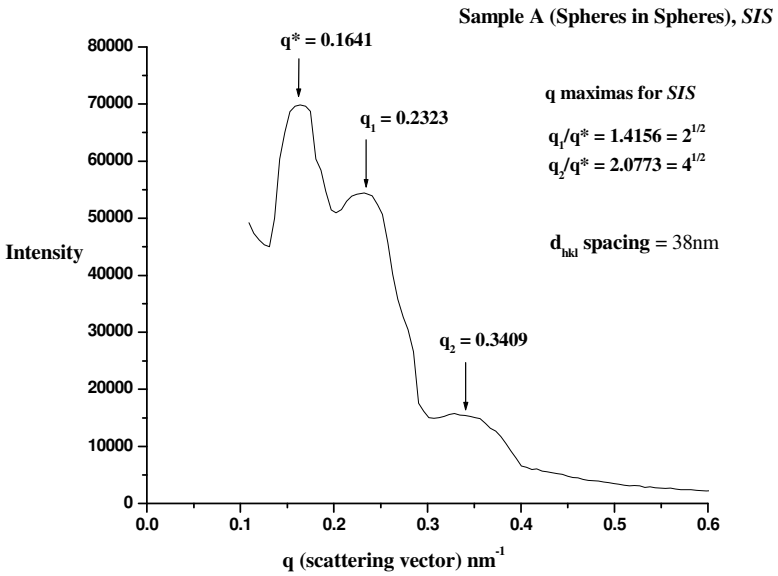

Fig. 4l *SAXS-pattern of sample **A** annealed at 180 °C for 24 h. (Scattering vector q = 4π/λ sinθ; with λ= 0.1542 nm and 2θ the scattering angle)*

In the SAXS intensity pattern (**Fig. 4l**) of sample **A** besides the primary peak which occurs at the scattering vector ($q^* = 0.1641$ nm^{-1}), maxima at higher q-values are located at $q_1 = 0.2323$ nm$^{-1} \approx \sqrt{2}q^*$ and at $q_2 = 0.3409$ nm$^{-1} \approx \sqrt{4}q^*$ as it would be expected for a body centered cubic lattice (bcc) or a simple cubic (sc) lattice. A similar scattering pattern was also observed for sample **B** under analogous conditions. The broad maximum at q ≈ 0.3409 relates to the structure factor of the spherical domains. Using Bragg's law the d_{hkl} spacing (distance between the two inner spheres) of 38 nm is obtained from the first peak, which relates well with the TEM in **Fig. 4k**.

When the PS volume fraction is increased at the expense of PMMA then PMMA and PS form a lamellar morphology. At their interphase small PFS spheres are observed, which seem to be integrated mainly into the PS lamellae, again because of the interfacial tension (**Fig. 4m**). [243, 166, 247, 248] This morphology was found for samples **C**, **D** and **E**. Here, the volume fractions of the majority components, that is, PMMA and PS, are quite similar (ϕ_{PMMA}, $\phi_{PS} \approx 0.4$), leading to the lamellar arrangement. The minority component, PFS, forms its own microphase at the boundaries of the lamellar phase and appears as droplets because of its low volume fraction ($\phi_{PFS} < 0.2$). In some TEM pictures, moreover, the PFS spheres seem to merge into cylinders. This observation might be attributed to an incomplete phase separation between PS and PFS in these samples, leading to a some what higher volume fraction of the "PS-dilute" PFS domains and thus to the cylinder shape.

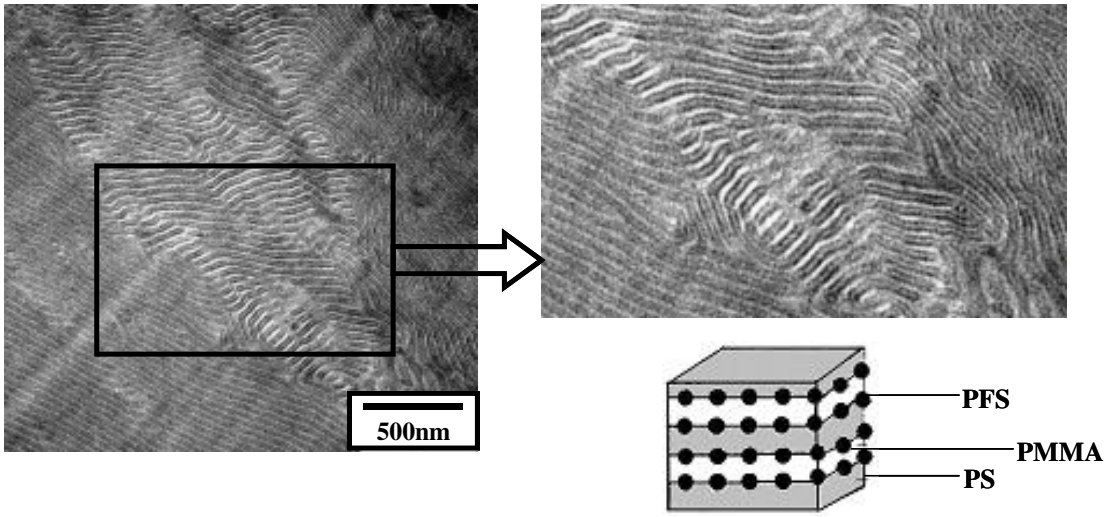

Fig. 4m *Bright field transmission electron micrograph of sample **C** (lamellar morphology of PS and PMMA with PFS droplets at the interphase); right side: zoomed section of the picture shown left; thin films were cast from dichloromethane and annealed for 24 h at 180 °C. Grey, black and white regions in the picture as well as in the schematic drawing represent the domains of PS, PFS and PMMA, respectively.*

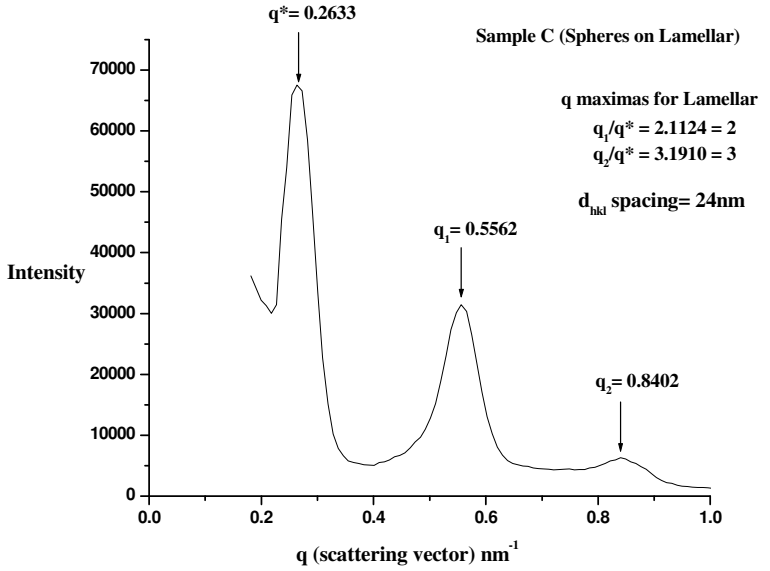

Fig. 4n *SAXS-pattern of sample* ***C*** *annealed at 180 °C for 24 h. (Scattering vector q = 4π/λ sinθ; with λ= 0.1542 nm and 2θ the scattering angle) {SOL: Spheres on Lamellar interphase}*

The SAXS scattering profile (**Fig. 4n**) shows three strong peaks, which agree with a lamellar structure[243] with q_n/q_1 ratios, which equal 1.0, 2.0 and 3.0. The d-spacing for the lamellar repeating unit is calculated as 24 nm from both the first peak and from a plot of d_{n00} versus 1/n (**Fig. 4o**). However the scattering pattern does not reveal any information about the presence of spheres on the lamellar interface. Similar SAXS patterns were also observed for samples **D** and **E** under analogous conditions.

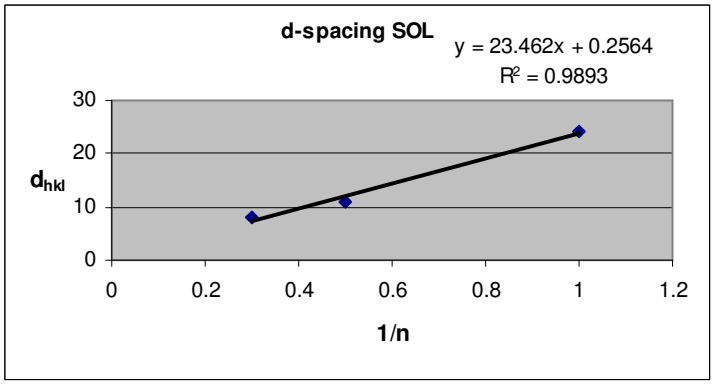

Fig. 4o *A plot of d_{hkl} vs. 1/n for sample* ***C*** *(d-spacing = slope of the plot).*

Further for samples **F** and **G**, where PS is the majority constituent ($\phi_{PS} \approx 0.6$) and where the volume fraction of PMMA is only $\phi_{PMMA} = 0.2 - 0.3$ ($\phi_{PFS} \approx 0.15$), the TEM micrographs allow assumption of the occurrence of a spheres-on-spheres (***SOS***) morphology.[246] Here, the PS represents the continuous phase and PMMA is the material that forms the larger spheres while PFS gives the small droplets sitting on the surface of the PMMA spheres (**Fig. 4p**).

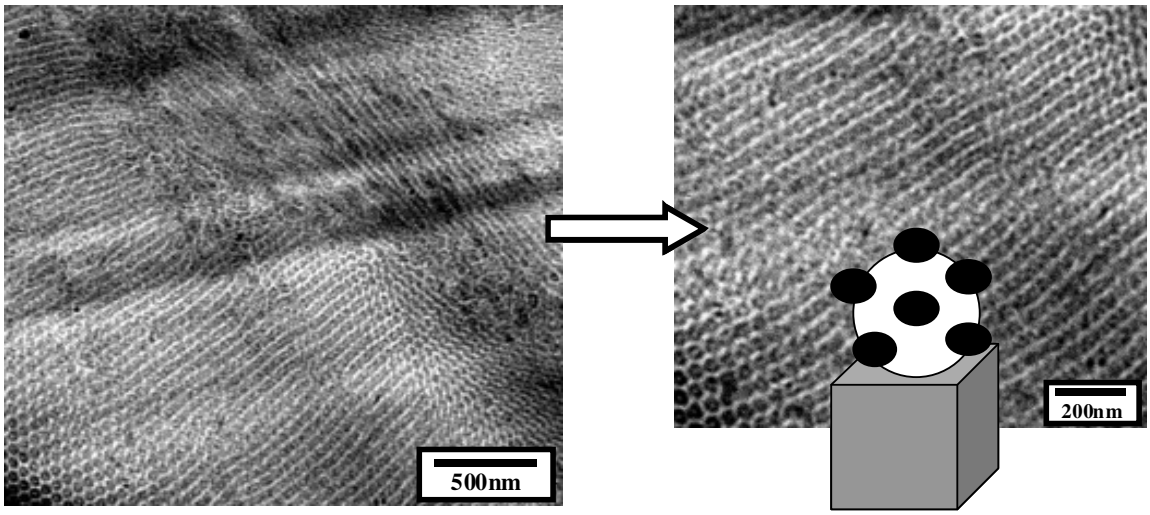

Fig. 4p *Bright field transmission electron micrograph of sample **F** (spheres-on-spheres morphology, **SOS**); right side: zoomed section of the picture shown left; the film was cast from dichloromethane solution and annealed for 1 day at 180 °C. Grey, black and white regions in the picture as well as in the schematic drawing represent the domains of PS, PFS and PMMA, respectively.*

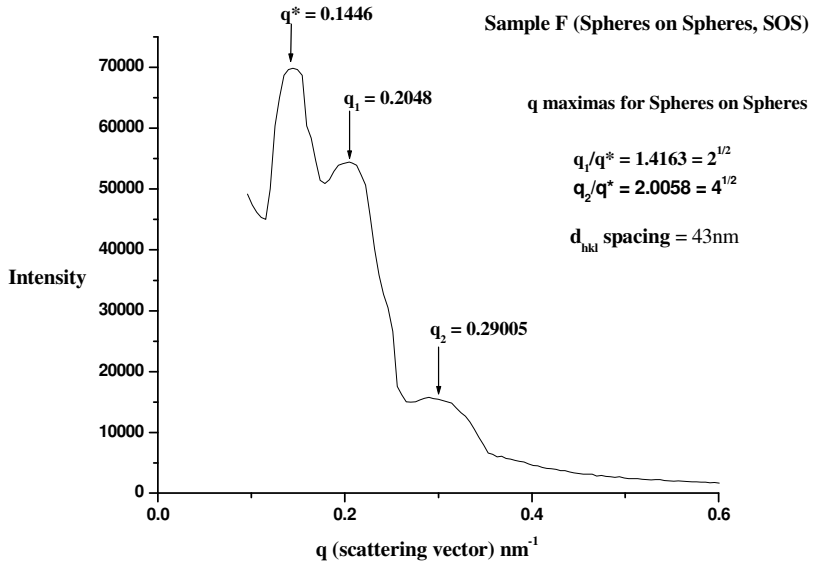

Fig. 4q *SAXS-pattern of sample **F** annealed at 180 °C for 24 h. (Scattering vector q= 4π/λ sinθ; with λ= 0.1542 nm and 2θ the scattering angle)*

In the SAXS intensity pattern (**Fig. 4q**) of sample **F**, besides the primary peak which occurs at the scattering vector ($q^* = 0.1446$ nm^{-1}) maxima at higher q-values are located at $q_1 = 0.2048$ nm$^{-1} \approx \sqrt{2}q^*$ and $q_2 = 0.2901$ nm$^{-1} \approx \sqrt{4}q^*$ as it would be expected for a body centered cubic lattice (bcc) or a simple cubic (sc) lattice. The broad maximum at $q \approx 0.2901$ relates to the structure factor of the spherical domains. A similar scattering profile was observed for sample **G** as well under the same experimental conditions. Using Bragg's law the d_{hkl} spacing (distance between the two inner spheres) of 43 nm is obtained from the first peak and this relates well with the TEM picture in (**Fig. 4p**).

Next with high molecular weight samples (~ 70000 g·mol^{-1}, **Table 4**) a spheres on cylinder (s_oc) morphology[169] is observed for sample **H** (**Fig. 4r**) and a spheres on spheres (sos) morphology[245] for sample **I** (**Fig. 4u**) with the same method of sample preparation and annealing conditions for both of them.

Table 4 *Characterization data for high molecular weight pentablock copolymer samples investigated by TEM and SAXS*

Sample	M_n (g/mol) Pentablock	M_w (g/mol) Pentablock	*PDI*	ϕ (NMR)		
				MMA	FS	S
H	72000	81000	1.13	**65**	13	22
I	75000	84500	1.13	**57**	13	30

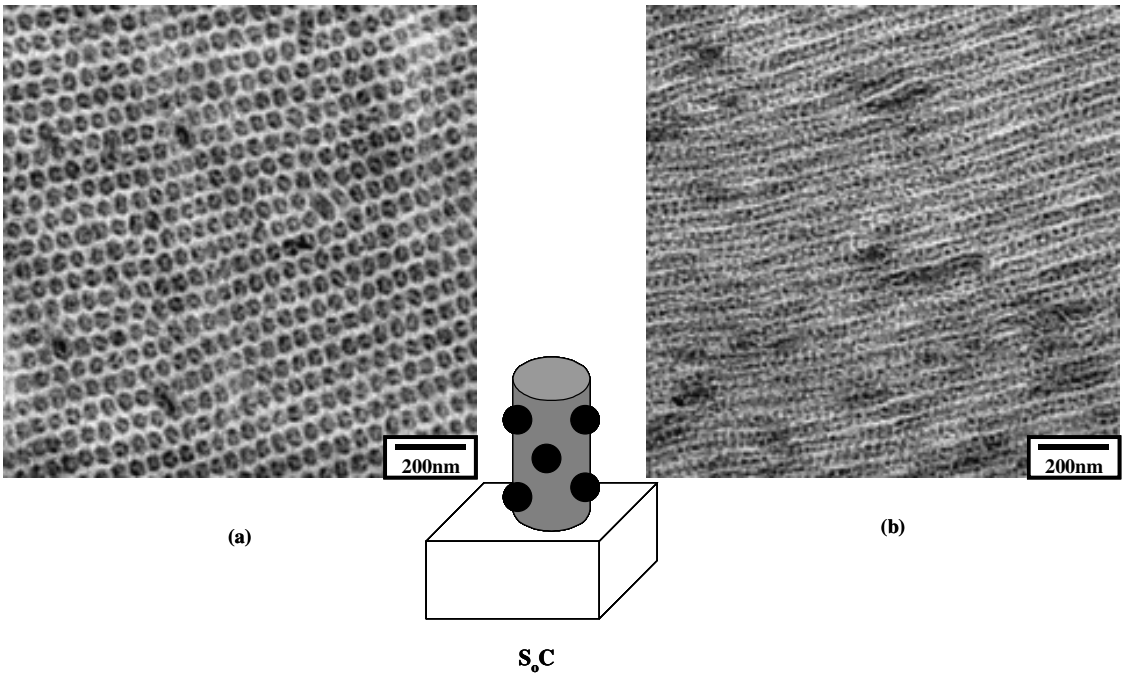

Fig. 4r *Bright field transmission electron micrograph of sample **H** (**spheres on cylinder morphology, S_OC**)* **(a)** *PS cylinders perpendicular to the plane of paper (sample cut perpendicular to the cylinder axis) and* **(b)** *PS cylinders parallel to the plane of paper (sample cut parallel to the cylinder axis). The film was cast from dichloromethane solution and annealed for 24 h at 180 °C. Grey, black and white regions in the picture as well as in the schematic drawing represent the domains of PS, PFS and PMMA, respectively.*

In sample **H**, PFS being the minority component forms small spheres on the PS cylinders in a matrix of PMMA. This is consistent with the cylinder morphologies observed by Breiner et al.[169] with different arrangement of the central block in SBM and SEBM ABC terblockcoplymers as a function of the composition within the range $\phi A + \phi B = 0.26$-0.41. The different possible structures are represented below (**Fig. 4s**).

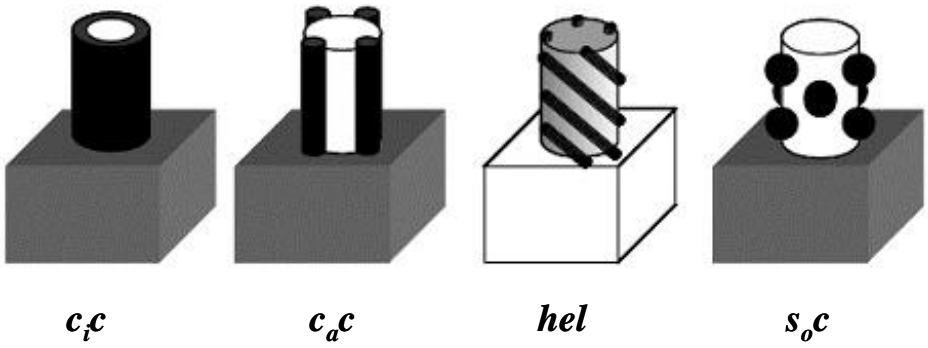

Fig. 4s *Cylinder structures in SBM triblock copolymers as observed by Breiner et al.*[169] *Grey, black and white regions in the schematic drawing represent the domains of PS, PB and PMMA, respectively.*

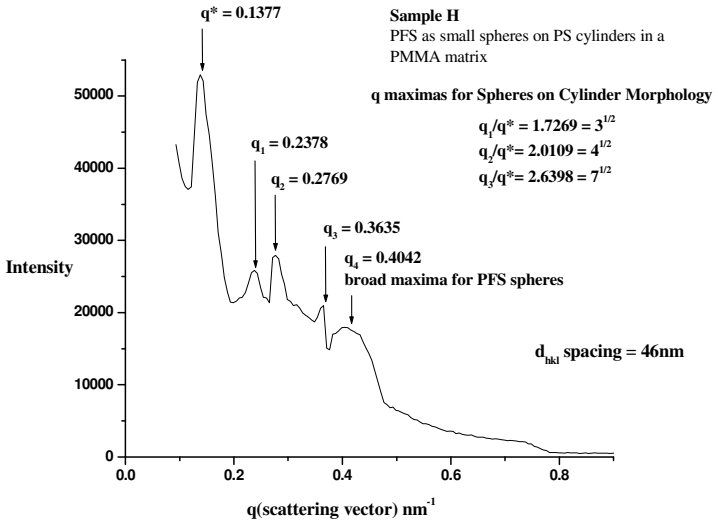

Fig. 4t *SAXS-pattern of sample **H** annealed at 180 °C for 24 h. (Scattering vector $q = 4\pi/\lambda \sin\theta$; with $\lambda = 0.1542$ nm and 2θ the scattering angle).*

Another evidence of this morphology is obtained from the SAXS scattering pattern (**Fig. 4t**). Besides the four discernible peaks in the q dependence of the scattered intensity, centered at q/q* ratios of 1: √3: √4: √7, where q* is the principal peak position, there is a broad maximum observed at q = 0.4042 nm^{-1} which relates to the structure factor of spherical domains formed by PFS as the minority component.[245] This also holds good with the principle of X-ray scattering wherein the scattering angle is inversely related to the domain size.[249] The d-spacing is 46 nm as calculated from the first reflection peak.

Finally in sample **I** which has the same PFS volume fraction of ϕ = 0.13 as sample **F**, but nearly opposite volume fractions for MMA (ϕ = 0.57) and S (ϕ = 0.30) a similar spheres on spheres (sos) morphology is observed with PFS forming small spheres over large spheres of PS in a matrix of PMMA (**Fig. 4u**).

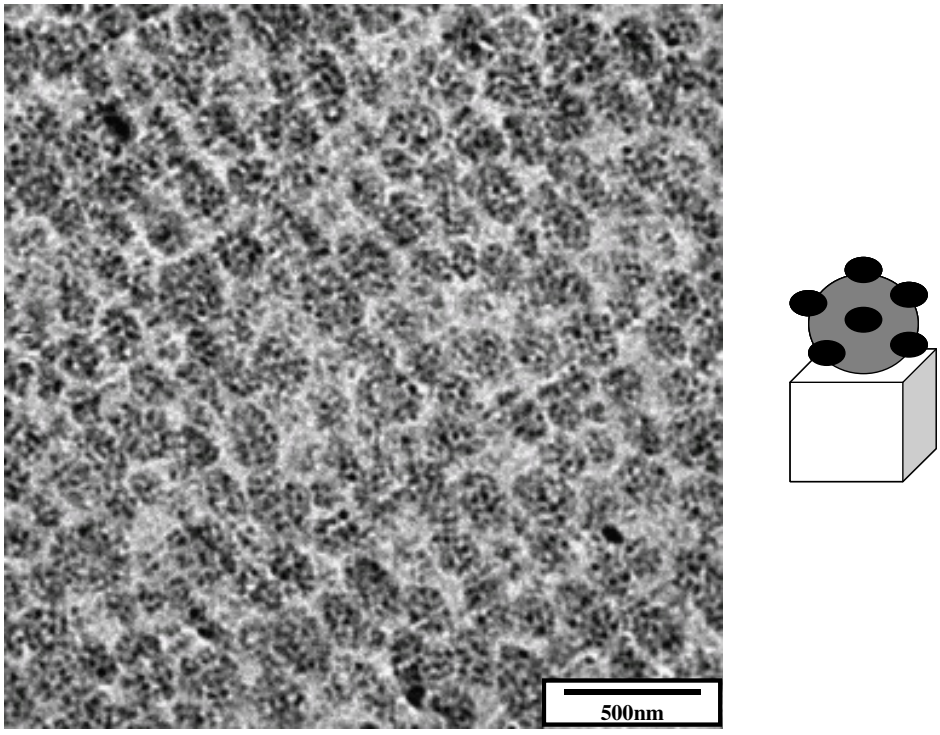

Fig. 4u *Bright field transmission electron micrograph of sample **I** (spheres-on-spheres morphology, **SOS**). The film was cast from dichloromethane solution and annealed for 24 h at 180 °C. Grey, black and white regions in the picture as well as in the schematic drawing represent the domains of PS, PFS and PMMA, respectively.*

The X-ray scattering profile (**Fig. 4v**) was found to be very similar to the one obtained for sample **F** with a broad maximum at q = 0.3219 nm^{-1} which is related to the spherical domains[245] of PFS.

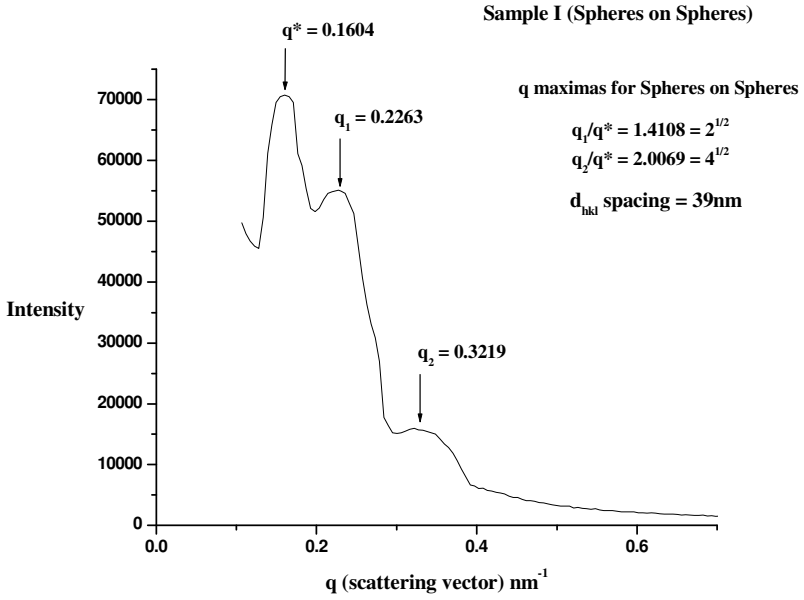

Fig. 4v *SAXS-pattern of sample **I** annealed at 180 °C for 24 h. (Scattering vector q = $4\pi/\lambda \sin\theta$; with λ= 0.1542 nm and 2θ the scattering angle)*

4.4 Phase Behavior of the Pentablock Copolymer Blends with PS, PFS and PMMA Homopolymers

Investigation of the stability range of the ordered bicontinuous phase between the cylindrical and lamellar regions is the main motivation for most of the work on blends of diblock copolymers with a homopolymer being chemically identical to one of the blocks.[250, 198] For e.g. Winey et al. investigated polystyrene-*b*-polyisoprene (SI) and polystyrene-*b*-polybutadiene (SB) diblock copolymers which were blended with the corresponding homopolymers. The stability window of the bicontinuous morphology was found to be comparable to that of the diblock copolymers with a corresponding overall composition. The advantage of blend preparation is in the number of samples with different compositions that can be easily prepared by the simple addition of a

homopolymer to a given block copolymer rather than the tedious alternative of synthesizing additional block copolymers with different volume fractions.

When a block copolymer is blended with the constituent homopolymers there can be two different situations depending on its length. There is a favorable mixing between a block copolymer and a homopolymer when the homopolymer is shorter than the corresponding block of the block copolymer. This corresponds to the '*wet brush*' situation[251-253] (**Fig. 4w**) wherein the microphase separation is preserved. On the other hand if the homopolymer has a larger degree of polymerization than the corresponding block, the mixing is not favorable and macrophase separation occurs. This corresponds to the dry brush situation wherein the free chains cannot diffuse into the domains of shorter chains grafted to a surface, since the loss of conformational entropy is more than the gain in translational or mixing entropy.[254, 255]

Table 5 *Molecular characterization of the blends from pentablock copolymers with PS, PFS and PMMA homopolymers*

Sample*	M_n (g/mol) Pentablock	M_w (g/mol) Pentablock	M_n (g/mol) Homopolymer	*PDI*	ϕ			ϕ *(Blend)*		
					MMA	FS	S	**MMA**	FS	S
B + ***20% hPS***	50 000	56 000	10 000	1.12	**59**	15	26	**50**	11	39
B + ***5% hPFS***	50 000	56 000	8 000	1.12	**59**	15	26	**56**	19	25
G + ***35% hPMMA***	52 000	59 000	15 000	1.13	**21**	15	64	**42**	11	47

**The amount of homopolymer in the blend samples is expressed in terms of (vol %)*

The blend samples were prepared by dissolving the pentablock copolymer (**Samples B and G**) together with the homopolymers namely PS, PFS and PMMA (**Table 5**) in dichloromethane (5% w/v) followed by stirring for 1 day in order to ensure complete dissolution and homogeneous mixing. Films were prepared in the usual manner by slow solvent evaporation to dryness from Petri dishes (4 cm in diameter) over a period of 3-4 weeks. The films were annealed for 24 h in vacuum at 180 °C followed by quenching in ice water. Thin sections of the order of 50 nm were cut by means of ultramicrotome at room temperature.[199]

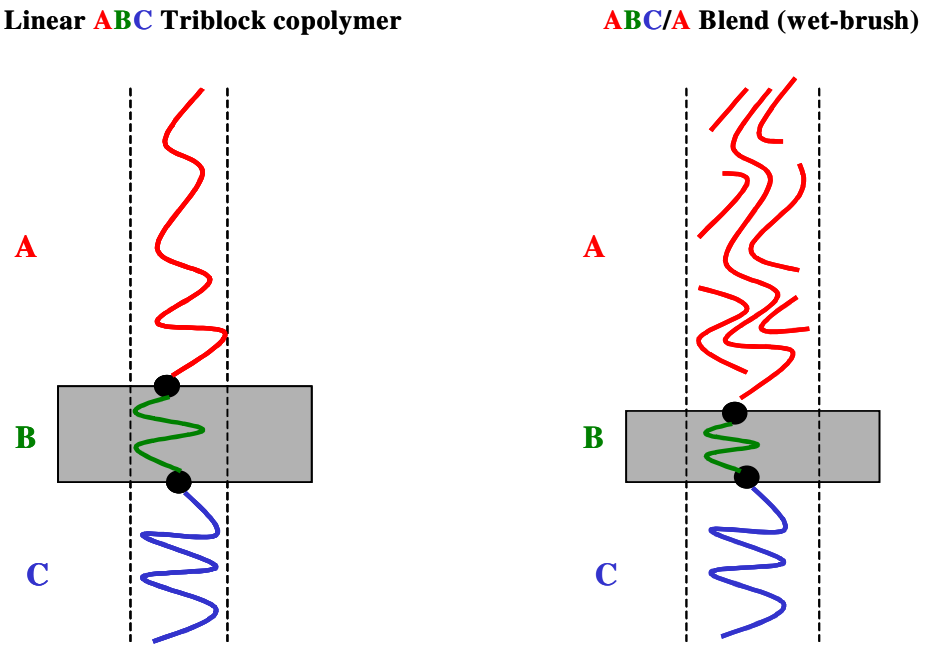

Fig. 4w *Schematic representation of the favorable mixing of a homopolymer having low molecular weight in comparison to the corresponding block on the configuration of the block copolymer chain ends. The addition of homopolymer A causes the swelling of block A chains and contraction of the B-block chains, leading to an increase in the conformational entropy.*

The blended samples did not provide any insight into some complex morphologies such as the bicontinuous gyroid phases. When the pentablock copolymer was blended with PS and PMMA a spheres on lamellar interface pattern was observed very similar to the pure pentablock copolymers (see **Fig. 4m**). However when PFS was blended with block copolymer **B**, a c_ic (cylinder in cylinder) morphological pattern (**Fig. 4x**) seems to be formed quite similar to one observed by Manners et al. in PFS-*b*-PDMS.[256]

The minority component PFS (ϕ = 0.19) is forming cylinders inside bigger cylinders of PS (ϕ = 0.25) in a matrix formed by the majority component PMMA (ϕ = 0.56).

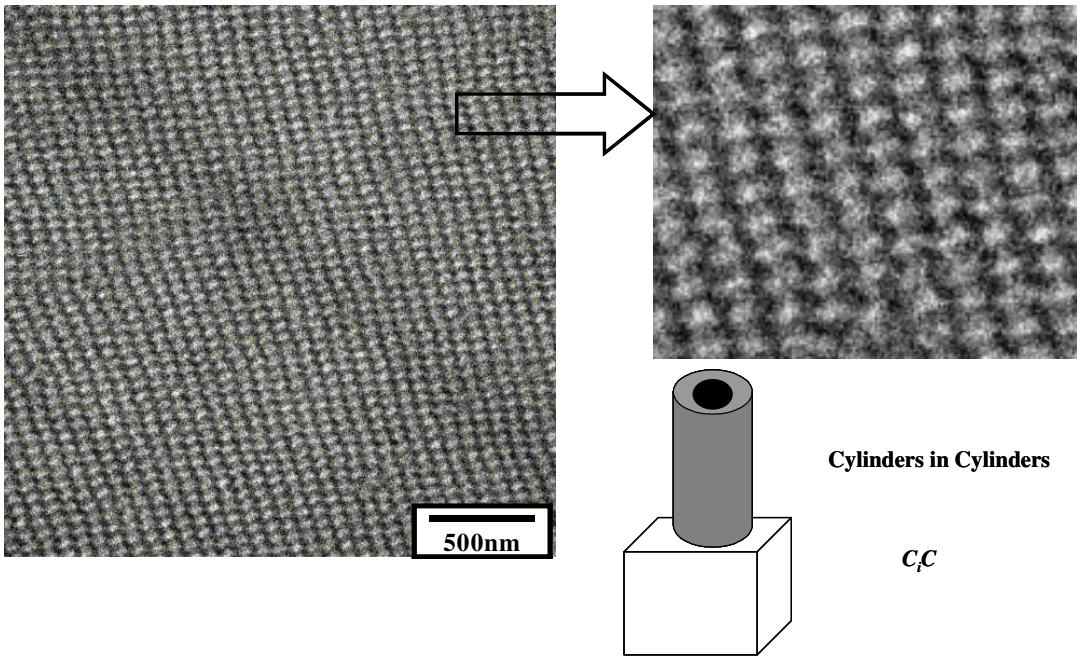

Fig. 4x *Bright field transmission electron micrograph of sample* ***B + 5 % PFS*** *(Cylinders-in-Cylinders morphology,* ***C_iC****). The film was cast from dichloromethane solution and annealed for 24 h at 180 °C. Grey, black and white regions in the picture as well as in the schematic drawing represent the domains of PS, PFS and PMMA, respectively.*

The SAXS pattern of the film cast from dichloromethane and annealed at 180 °C for 24 h shows broad peaks with relative positions of $3^{1/2}$, $4^{1/2}$ and $7^{1/2}$ (**Fig. 4y**). This is consistent with a cylindrical arrangement of the PFS and PS domains. The d_{hkl} spacing was found to be 47 nm.

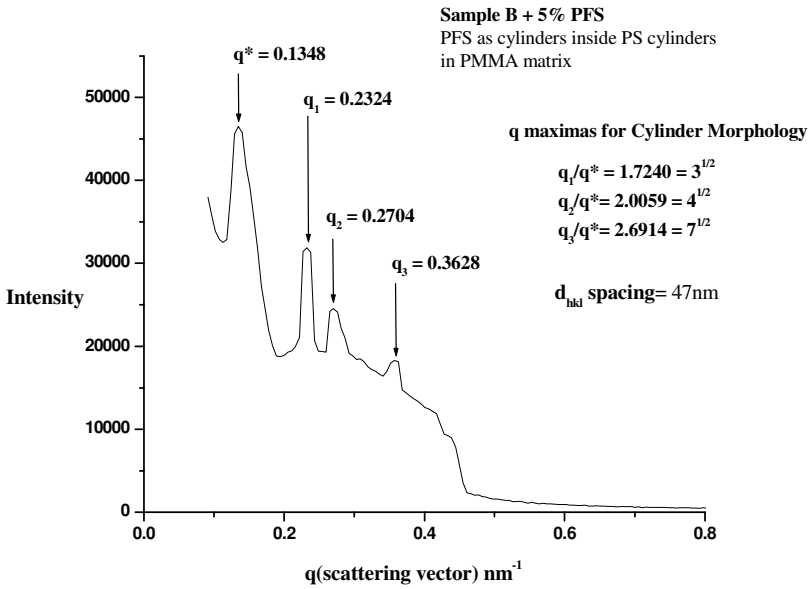

Fig. 4y *SAXS-pattern of blend sample* ***B + 5% PFS*** *annealed at 180* °C *for 24 h. (Scattering vector* $q = 4\pi/\lambda \sin\theta$*; with* $\lambda = 0.1542$ *nm and* 2θ *the scattering angle)*

4.5 Conclusion

The pentablock copolymers form ordered microstructures. Annealing under various conditions followed by analysis with TEM and SAXS revealed good phase separation showing different micromorphologies such as lamellar, cylinders, spheres-on/in-spheres and spheres-on/in-lamellae. The figure below (**Fig. 4z**) summarizes all the observed morphologies with respect to volume fraction of each component as discussed in this chapter.

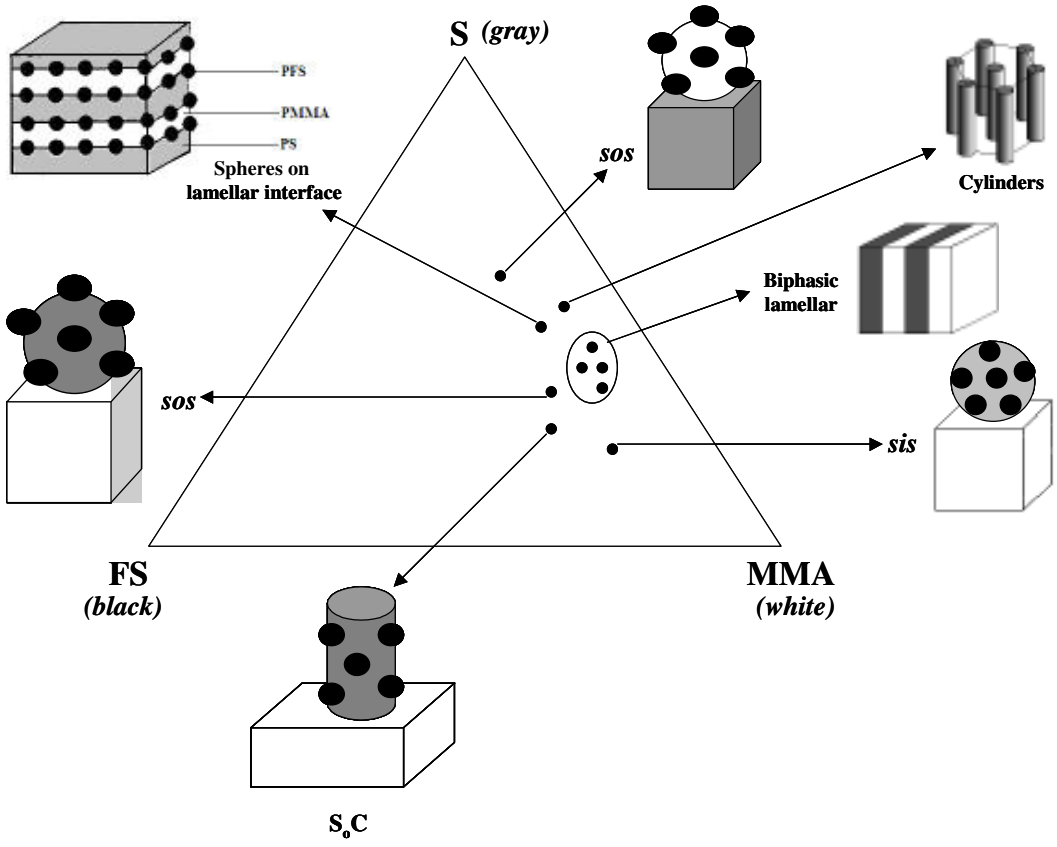

Fig. 4z *Pictorial representation of different morphologies as observed in pentablock copolymers PMMA-b-PFS-b-PS-b-PFS-b-PMMA.*

Chapter 5

Semiconducting Properties of Block Copolymers from PFS, PS and PMMA Segments

As to date with respect to ferrocene containing polymers most of the conductivity studies have been done on doped polyferrocenylenes and its derivatives that are π-electron delocalized systems.[187, 189] Conductivity studies on block copolymers containing PFS have not been done so far. This chapter deals with the doping of homo and block copolymers such as AB, BAB, ABC, CBABC types containing PFS, PS and PMMA segments by oxidants such as iodine and tetracyanoethylene. The influence of "diluting" the functional PFS subunits upon their implementation into various types of block copolymers on the conductivity both in the undoped and doped state was investigated by Dielectric Relaxation Spectroscopy (DRS). The observed conductivities were mainly due to the oxidized PFS block domains.

5.1 Principle of Dielectric Relaxation Spectroscopy (DRS)

Dielectric properties relate to the ability of a material to polarize under the influence of an electromagnetic field. The technique for measuring dielectric properties is known as *Dielectric Spectroscopy*. It has many advantages over other physicochemical measurements such as the following:

(i) Sample preparation is relatively simple.

(ii) Varieties of sample size and shapes can be measured.

(iii) Measurement conditions can be varied under a wide range of temperatures, humidities, pressures etc.

(iv) The technique is extremely broadband (mHz – GHz) thus enabling the investigation of diverse process over wide ranges of time and scale.

5.1.1 ***Measurement Principle***

Dielectric measurements are based on the application of an electrical perturbation (i.e. voltage or current) to a sample of material, and the measurement of a response (i.e. the amplitude and the phase shift of the resultant signal). The ratio of the current to the voltage gives the impedance '**Z**' and the ratio of voltage to current gives the admittance '**Y**'. From the impedance or admittance, a number of parameters can be derived which reflect the dielectric properties of the sample, e.g. permittivity (ε), susceptibility (χ) and conductivity (σ).

5.1.2 ***Measurement Techniques***

There are two approaches to the measurement of dielectric properties namely,

(i) *Frequency Domain Spectroscopy*: The electrical perturbation is a sinusoidal voltage (or frequency spanning many decades) and the response is a sinusoidal current.

(ii) *Time Domain Spectroscopy*: The electrical perturbation is a step voltage and the response is a reflected voltage from the sample/sample holder interface.

5.1.3 ***Polarization Mechanisms***

The main polarization mechanisms that occur in a material under the influence of an electromagnetic field are as follows:

(i) *Orientation Polarization*: This results from the alignment of permanent dipoles (e.g. water) in the direction of an electric field.

(ii) *Electronic and Atomic Polarization*: This is due to the shift of positive and negative charges in the atoms of materials.

(iii) *Maxwell-Wagner Polarization*: This results from the build-up of charges at the interfaces of heterogeneous systems. It is observed when more than one material component is present or when segregation occurs in a material containing incompatible chemical sequences.

(iv) *Charge Migration Polarization*: This is due to the ionic migration, or hopping of charge carriers (e.g. electrons, holes) between localized sites.

Polarization is measured in terms of the permittivity (ε). This permittivity is determined by performing several isothermal scans as a function of frequency. An alternating current (V_{rms} = 0.005 to 1.1 volts) external electric field is applied across the test material in a capacitor plate configuration. The applied alternating electric field interacts with the electric dipole moments of the material under test. The polarization (P) of the material is related to the applied electric field (E) by the equation **5.1.3a**

$$P = \chi E \qquad \textbf{5.1.3a}$$

where χ is the susceptibility. Further the susceptibility is related to the permittivity (ε) by the relation expressed by **5.1.3b**

$$\chi = (\varepsilon\text{-}1)/4\pi \qquad \textbf{5.1.3b}$$

This global polarization consists of four different mechanisms (electronic, atomic, orientation or dipolar and ionic polarization). Each dielectric mechanism has a characteristic relaxation frequency. As the frequency becomes larger, the slower mechanisms drop off. At low frequencies ionic conduction is the most prevalent mechanism. Dielectric relaxation is the result of a movement of dipoles or electric charges due to a changing electric field in the frequency range of 10^2 –10^{10} Hz. This mechanism is a relatively slow process when compared with electronic transitions or molecular vibrations that have frequencies above 10^{12} Hz. In this regard, only when sufficient time is allowed after the application of an electric field for the orientation to attain equilibrium, the maximum polarization corresponding to the highest observable dielectric constant will be realized in a material.[257]

5.2 Doping of Homo and Block Copolymers

The homo and block copolymers were oxidatively doped with iodine and tetracyanoethylene (TCNE) by the addition of the polymer solutions in CH_2Cl_2 into the corresponding solution of oxidant in CH_2Cl_2 (**Fig. 5a**). An excess of the oxidant was added in each case and removed by sublimation. Mass balance estimates calculated from the elemental analysis were used to determine the composition and degree of doping.[258]

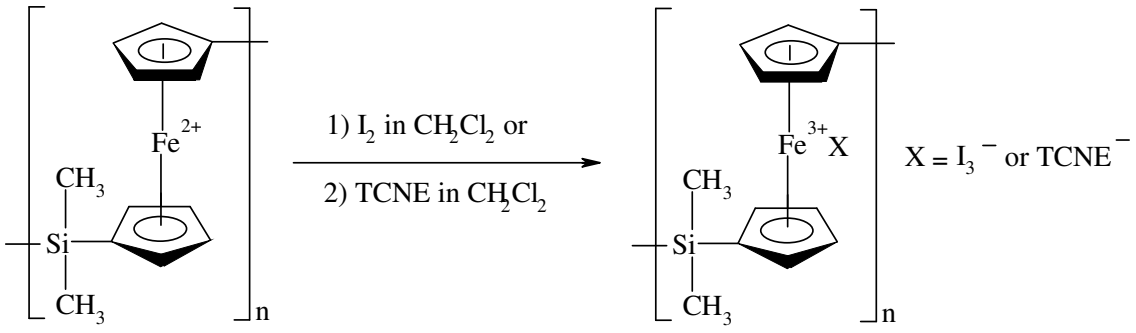

Fig. 5a *Oxidative doping of homo and block copolymers containing PFS as one of the blocks by oxidants such as iodine and tetracyanoethylene.*

5.3 Mechanism of Conductivity in PFS containing Polymers

The electrical properties of a material are determined by its electronic structure. The nature of conductivity in doped polymers is quite different from that in metals. In a metal there is a high density of electronic states containing electrons with relatively low binding energy, and 'free electrons' move easily from atom to atom under an applied electric field. The phenomenon of conductivity in metals is explained on the basis of a simple free-electron molecular orbital model, which provides the elements to describe quantitatively a conductor, semiconductor or insulator built up of a linear chain of atoms.

In materials such as PFS, the role of the dopant is either to remove or add electrons to the polymer. During oxidative doping with iodine an electron is abstracted leading to the formation of I_3^- ions. This removal of an electron locally from one iron atom leads to the formation of a cation called '***polaron***'. The polaron is localized, partly because of coulomb attraction to its counterion [I_3^-] and partly due to a local change in the equilibrium geometry of the cation relative to the neutral molecule. Since the counterion to the positive charge is not very mobile, a high concentration of counterions is required so that the polaron can move in a field of close counterions. This explains why so much doping is necessary. The conductivity in PFS doped polymers seems to arise from hopping mechanism of polarons.

5.4 Conductivity measurements by DRS

The polymers employed for conductivity measurements are designated as ${}^{a}X_{b}$ where the superscript 'a' is the number average molecular weight (M_n, g·mol^{-1}) and 'b' is the degree of polymerization (N).

The influence of the doping/oxidation extent on the conductivity was investigated for the homopolymer ${}^{24000}PFS_{100}$. The homopolymer was treated with varying amounts of the oxidant iodine (**Table 5a**). It was found that the conductivity increased with increasing extent of doping but reached a limiting value of 10^{-7} S/cm for 80-85% oxidation (**Fig. 5b**).

Table 5a *Quantities of* $^{24000}PFS_{100}$ *homopolymer and iodine employed along with the observed conductivities as determined by DRS.*

Polymer (moles)	Iodine (moles)	% Oxidation/doping	Conductivity (S/cm)
1	5	20	~10^{-10}
1	10	42	~10^{-9}
1	15	58	~10^{-8}
1	20	80	~10^{-7}
1	25	82	~10^{-7}
1	30	83	~10^{-7}

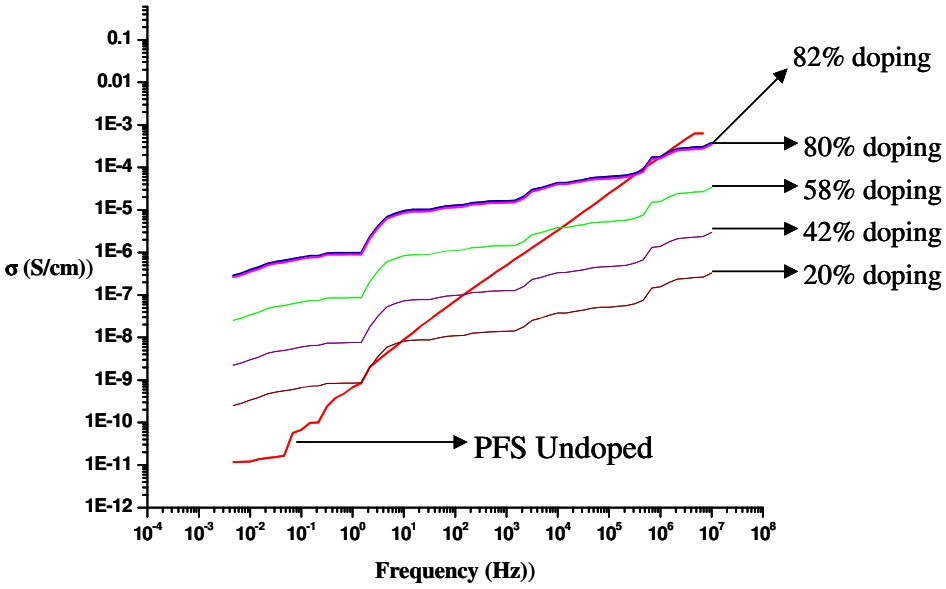

Fig. 5b *Conductivity vs. frequency plots for* $^{24000}PFS_{100}$ *doped samples with varying degrees of oxidation by iodine. (*10^{-3} *to* 10^{0} *Hz represents the static conductivity region).*

As evident from (**Fig. 5b**) in the frequency range of 10^{-2} to 10^{0} Hz the conductivity is more or less independent of the applied frequency. This is the region of interest regarding the conducting properties of doped polymers, representing the ***'Static Conductivity'*** range. Beyond this i.e. 10^{1} to 10^{8} Hz the conductivity increases linearly with the frequency of perturbation called the ***'Dynamic Conductivity'*** range. At low frequencies the slow ionic polarization mechanisms contribute to the susceptibility and permittivity of the material, which in turn are related to the conductivity. With increase in frequency of the applied sinusoidal potential the slower mechanisms subside and only the faster ones such as electronic and atomic contribute to the total rise in conductivity of the material. A similar behavior was observed for the samples doped by TCNE (95% oxidation) with a conductivity of 10^{-7} S/cm.

5.4.1 *DRS Measurements of $^{24000}PFS_{100}$*

The conductivity values for the PFS homopolymer samples (**Table 5b**) and (**Fig. 5c**) show that the film of the original material is almost on the border of semiconductors and insulators. However on oxidation both with iodine and TCNE there is a 10^{4} fold increase in conductivity. In contrast to this the polyferrocenylenes have a conductivity of 10^{-5} S/cm when doped with iodine and TCNE.[187] This high conductivity is attributed to the extended conjugation, which is absent in polyferrocenylsilanes.

Table 5b *Conductivity values of PFS homopolymer as determined by DRS*

Polymer	**Conductivity 'σ' (S/cm)**		
	Undoped	***Iodine Doped (82%)***	***TCNE Doped (95%)***
$^{24000}PFS_{100}$	~10^{-11}	~10^{-7}	~10^{-7}

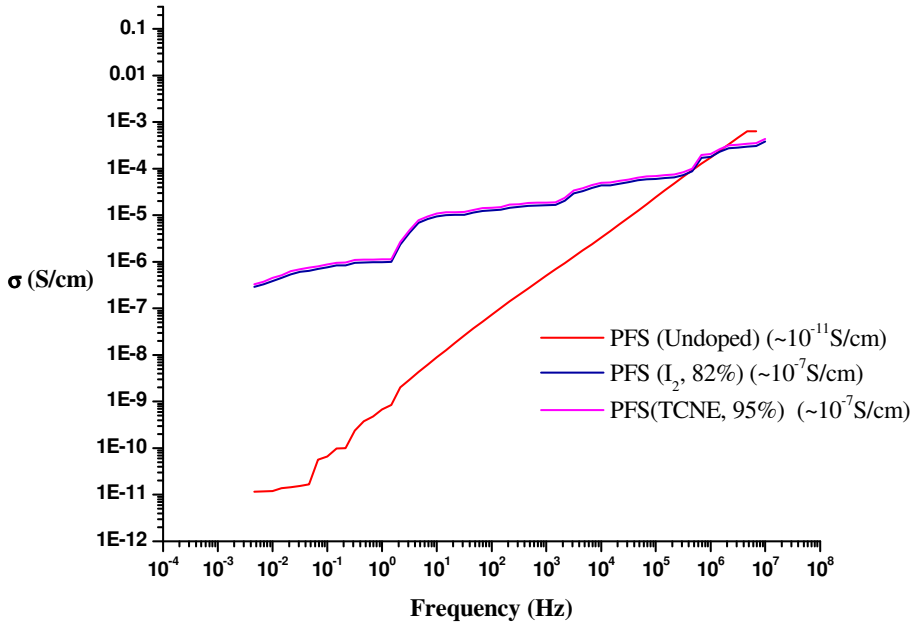

Fig. 5c *Conductivity vs. frequency plots for PFS doped samples.*

5.4.2 *DRS Measurements of Diblock Copolymer AB type, $^{35000}PFS_{102}$-b-$PMMA_{103}$*

In case of block copolymers the influence of morphology on conductivity was also studied. A non-annealed film of the sample was compared with an annealed sample at 180 °C having a lamellar orientation of the domains formed by PFS and PMMA. The conductivity of both the samples was very low in the range of an insulator (~10^{-14} S/cm). With doping the conductivity increased and reached up to the order of ~10^{-9} S/cm. (**Table 5c**) and (**Fig. 5d**)

Table 5c *Conductivity values of PFS-b-PMMA diblock copolymer as determined by DRS*

Polymer	**Conductivity 'σ' (S/cm)**			
	Undoped*	***Undoped, Lamellar***	***I_2 Doped (80%)***	***TCNE Doped (93%)***
PFS-*b*-PMMA	~10^{-14}	~10^{-14}	~10^{-9}	~10^{-9}

* *non-annealed*

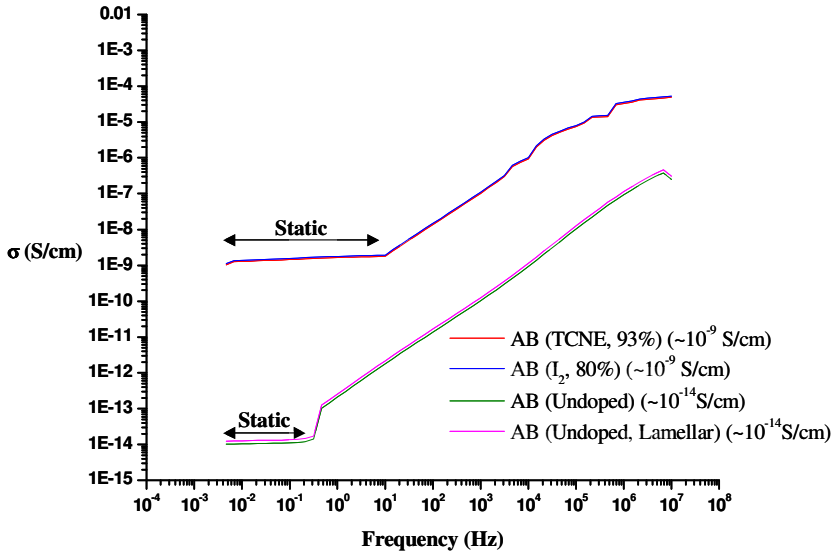

Fig. 5d *Conductivity vs. frequency plots for PFS-b-PMMA samples.*

5.4.3 *DRS Measurements of Triblock Copolymer BAB type, $^{35000}PFS_{50}$-b-PS_{101}-b-PFS_{52}*

A similar influence of morphology on the conductivity of the triblock copolymer film was investigated here. A non-annealed film of the sample without any microphase separation was compared with an annealed sample at 200 °C having a lamellar morphology of the PFS and PS domains. The conductivity of both the samples was again very low in the range of an insulator (~10^{-14} S/cm). With doping the conductivity increased and reached up to the order of ~10^{-9} S/cm. (**Table 5d**) and (**Fig. 5e**). The low conductivity seems to result from the dilution of the charge carriers (oxidized PFS units) by the domains of PS.

Table 5d *Conductivity values of PFS-b-PS-b-PFS triblock copolymer as determined by DRS*

Polymer	Conductivity 'σ' (S/cm)			
	Undoped*	***Undoped, Lamellar***	***I_2 (83%)***	***TCNE (95%)***
PFS-*b*-PS-*b*-PFS	~10^{-14}	~10^{-14}	~10^{-10}	~10^{-9}

* *non-annealed*

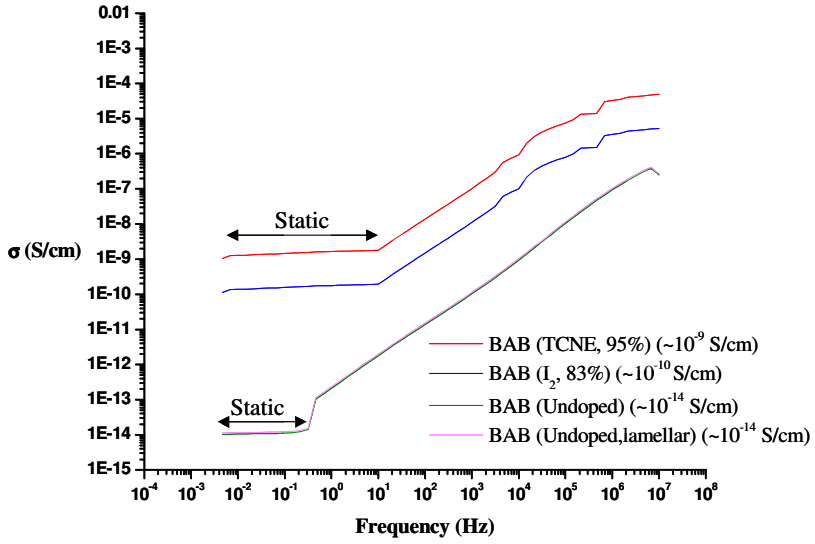

Fig. 5e *Conductivity vs. frequency plots for PFS-b-PS-b-PFS samples.*

5.4.4 *DRS Measurements of Triblock Copolymer ABC type, $^{45000}PS_{103}$-b-PFS_{101}-b-$PMMA_{99}$*

Morphology vs. conductivity relation was investigated by comparing the DRS curves of a non-annealed triblock copolymer film with an annealed sample at 200 °C for 24 h, having a biphasic lamellar orientation of the domains. The conductivity of both the samples was again very low in the range of an insulator (~10^{-15} S/cm). With doping the conductivity increased and reached up to the order of ~10^{-9} S/cm. (**Table 5e**) and (**Fig. 5f**). The low conductivity again suggests dilution of the charge carriers (oxidized PFS units) by the domains of PS and PMMA which are both non-conducting.

Table 5e *Conductivity values of PS-b-PFS-b-PMMA triblock copolymer as determined by DRS*

Polymer	Conductivity 'σ' (S/cm)			
	Undoped*	***Undoped, Lamellar***	***I_2 (81%)***	***TCNE (91%)***
PS-*b*-PFS-*b*-PMMA	~10^{-15}	~10^{-15}	~10^{-10}	~10^{-10}

* *non-annealed*

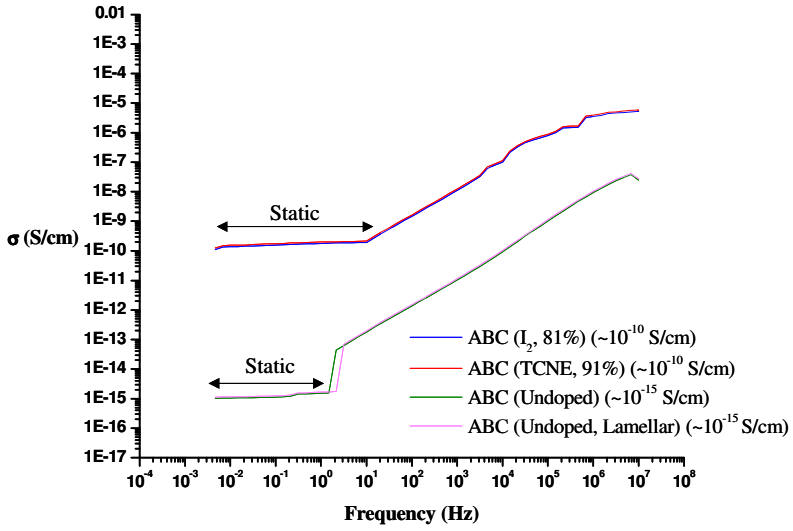

Fig. 5f *Conductivity vs. frequency plots for PS-b-PFS-b-PMMA samples.*

5.4.5 *DRS Measurements of Pentablock Copolymer CBABC type, $^{45000}PMMA_{51}$-b-PFS_{48}-b-PS_{99}-b-PFS_{53}-b-$PMMA_{49}$*

Two block copolymer sample films, with one annealed at 180 °C for 24 h and the other non-annealed were used for DRS measurements. The annealed sample had a biphasic lamellar morphology and showed same conductivity as the non-annealed sample without any microphase separation i.e. ~10^{-15} S/cm. With doping the conductivity increased and reached up to the order of ~10^{-10} S/cm (**Table 5f**) and (**Fig. 5g**).

Table 5f *Conductivity values of PMMA-b-PFS-b-PS-b-PFS-b-PMMA pentablock copolymer as determined by DRS*

Polymer	**Conductivity 'σ' (S/cm)**			
	Undoped*	***Undoped, Lamellar***	***I_2 (80%)***	***TCNE (95%)***
PMMA-*b*-PFS-*b*-PS-*b*-PFS-*b*-PMMA	~10^{-15}	~10^{-15}	~10^{-10}	~10^{-10}

* *non-annealed*

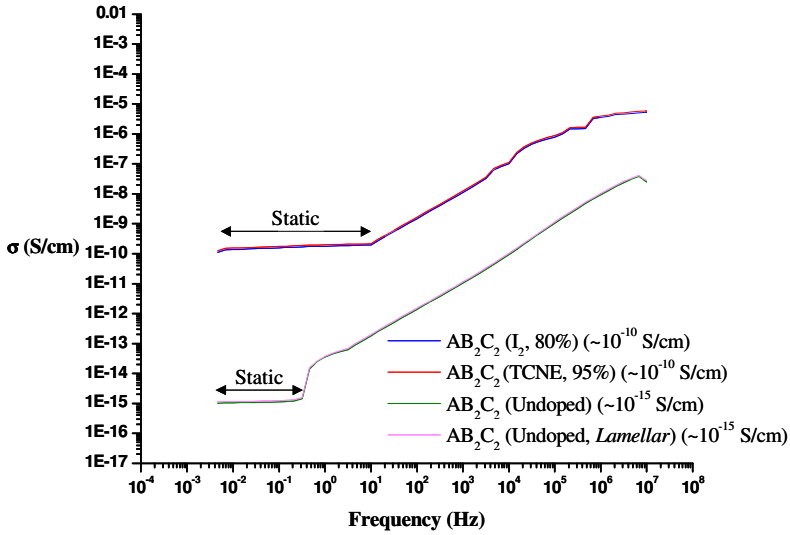

Fig. 5g *Conductivity vs. frequency plots for PMMA-b-PFS-b-PS-b-PFS-b-PMMA samples.*

5.5 Conclusion

Conductivity measurements on original and oxidatively doped samples of PFS containing homo and block copolymers were carried out by *Dielectric Relaxation Spectroscopy* (DRS). The influence of morphology on conducting properties of block copolymers was also investigated. The maximum observed conductivity for the doped PFS sample (10^{-7} S/cm) decreased on dilution by domains of PS and PMMA in the block copolymers with various architectures such as AB (10^{-9} S/cm), BAB (10^{-10} S/cm), ABC (10^{-10} S/cm) and CBABC (10^{-10} S/cm) types. A plausible explanation for this behavior could be the poor extended delocalization/conjugation of charge carriers due to the segregation of blocks in the copolymers. The translating charge carriers get trapped at the interfaces of these heterogeneous systems containing incompatible chemical sequences.

Chapter 6

Abstract and Zusammenfassung

6.1 Abstract

It was the goal of the present work to synthesize a series of well-defined pentablock copolymers of styrene (**S**), [1]dimethylsilaferrocenophane (**FS**) and methyl methacrylate (**MMA**) by sequential addition of monomers. Lithium naphthalide was used as difunctional initiator and a 1,1-dimethylsilacyclobutane (DMSB) mediated 1,1-diphenylethylene (DPE) end-capping technique was applied to ensure high block efficiency. The PMMA-*b*-PFS-*b*-PS-*b*-PFS-*b*-PMMA systems have molecular weights of M_n = 50,000 g·mol^{-1}, polydispersity indices of PDI ≤ 1.12 and PFS volume fractions of around $\phi_{PFS} \approx 0.15$.

First, the difunctional middle block of PS was formed, followed by triblock PFS-*b*-PS-*b*-PFS, which then – after appropriate end-capping – was employed as a macroinitiator to polymerize MMA, leading to the final pentablock copolymer. The block copolymers were characterized by SEC & NMR. Under optimum reaction conditions – i.e. when chain termination during DPE/DMSB end-capping is minimized – the pentablock copolymer was obtained in approximately 75 % purity: the crude product contained – in addition to the pentablock – some tetrablock (20%) and triblock (5%) copolymers. This raw material, however, could be purified by selective precipitation procedures which addressed the differences in polarity of the constituents. By that method, almost quantitative removal of the triblock was possible whereas a small amount of the tetrablock remained in the pentablock fraction. Fortunately the presence of such small amounts of tetrablock copolymers did not influence the pentablock copolymer micromorphologies in an irreproducible way. Thus, profound investigations were possible to analyze the bulk properties of the materials.

The pentablock copolymers were examined with the help of TEM and SAXS for their microphase behavior. The self-assembly was studied starting from dichloromethane, tetrahydrofuran and toluene solutions, after taking into consideration the solubility parameters. The formation of thermodynamically stable micromorphologies was forced by storing the solvent cast films in the saturated atmosphere of the corresponding solvent for 3-4 weeks followed by annealing at elevated temperatures 180 °C – 220 °C. Prior to this, it was ensured by TGA and DSC analysis that the pentablock copolymers are of

sufficient thermal stability for this treatment. Annealing under various conditions followed by TEM analysis revealed good phase separation and the formation of highly ordered microstructures, such as spheres-on/in-spheres, spheres on lamellar interface, biphasic lamellar, cylinders and spheres on cylinders micromorphologies. These morphologies were further verified and supported by SAXS scattering profiles. Conductivity measurements on original and doped samples (I_2 and TCNE) of PFS containing homo and block copolymers with/without microphase separation were carried out by dielectric spectroscopy (DRS). The maximum conductivity observed for the doped PFS sample (10^{-7} S/cm) decreased to 10^{-10} S/cm on dilution by domains of PS and PMMA in the block copolymers of various architectures.

6.2 Zusammenfassung

Ziel der vorliegenden Arbeit war die Synthese einer Serie wohldefinierter Pentablockcopolymerer aus Styrol (S), [1]Dimethylsilaferrocenophan (FS) und Methylmethacrylat (MMA) durch sequentielle anionische Polymerisation. Als bifunktioneller Initiator wurde Lithiumnaphthalid verwendet. Um hohe Blockausbeuten zu gewährleisten, wurden Endcapping-Reaktionen mit 1,1-Diphenylethylen (DPE) in Anwesenheit von 1,1-Dimethylsilacyclobutan (DMSB) durchgeführt. Die zahlenmittleren Molekulargewichte (M_n) der so erhaltenen PMMA-*b*-PFS-*b*-PS-*b*-PFS-*b*-PMMA-Pentablockcopolymeren betrugen etwa 50.000 g/mol. Die Polydispersitäts-Indices (PDI) lagen unterhalb von 1,12, der Volumenbruch des PFS (ϕ_{PFS}) um 0,15.

Im Zuge der Synthese wurde zuerst der Polystyrolblock als mittlerer Block hergestellt, woraus dann die PFS-*b*-PS-*b*-PFS Dreiblockcopolymere gebildet wurden. Nach geeigneter Endcapping-Reaktion dienten diese dann als bifunktionelle Makroinitiatoren für das MMA. So wurden schließlich die gewünschten Pentablockcopolymeren erhalten. Die Blockcopolymeren wurden mit Größenausschlusschromatographie (SEC) und Kernresonanzspekroskopie (NMR) charakterisiert. Bei optimalem Reaktionsverlauf, d.h. bei minimalem Abbruch während der DPE/DMSB-Endcappingreaktion, konnte das Pentablockcopolymere aus der Synthese in einer Reinheit von etwa 75 % erhalten werden.

Das so erhaltene Rohprodukt enthielt weiterhin ca. 20 % Tetrablock- und ca. 5 % Triblock-Copolymeres. Im Anschluß an die Synthese gelang durch fraktionierte Fällung eine Aufreinigung. Dabei wurden die unterschiedlichen Polaritäten der Blöcke genutzt. So war die vollständige Abtrennung der Dreiblockcopolymeren möglich, während eine kleine Menge des Tetrablocks mit vertretbarem Aufwand nicht aus dem Pentablockcopolymeren zu entfernen war. Die Anwesenheit dieser geringen Mengen an Tetrablock-Copolymerer hatte jedoch keinen unreproduzierbaren Einfluss auf die Mikrophasenmorphologie des Pentablockcopolymeren. Deshalb konnten hiermit detaillierte Untersuchungen zu den Eigenschaften im Festkörper durchgeführt werden.

Das Mikrophasen-Separationsverhalten der Pentablockcopolymeren wurde mit Hilfe der Transmissionselektronenmikroskopie (TEM) und der Röntgenkleinwinkelstreuung

(SAXS) untersucht. Konkret wurde die Selbstorganisation in Filmen studiert, die aus Polymerlösungen in Dichlormethan, Tetrahydrofuran und Toluol gebildet wurden. Die Auswahl dieser Lösungsmittel war unter Berücksichtigung der Löslichkeitsparameter erfolgt. Um thermodynamisch stabile Mikrophasenmorphologien zu erhalten, wurden die gegossenen Filme unter gesättigter Atmosphäre des entsprechenden Lösungsmittels drei bis vier Wochen gelagert und anschließend bei 180 °C – 220 °C getempert. Zuvor war die thermische Stabilität der Proben mittels TGA und DSC sichergestellt worden. Die unter verschiedenen Bedingungen getemperten Copolymere zeigen im Transmissionselektronenmikroskop gut separierte Phasen und unterschiedlich geordnete Mikrostrukturen wie beispielsweise Kugeln in/auf Kugeln, Kugeln in lamellaren Grenzflächen, zweiphasige Lamellen, Zylinder und Kugeln auf Zylindern. Diese Mikrostrukturen wurden zusätzlich mit Hilfe von Röntgenkleinwinkelstreukurven verifiziert. Leitfähigkeitsmessungen an unveränderten sowie an oxidativ dotierten (mit I_2 und TCNE) PFS-haltigen Homo- und Blockcopolymeren, die sowohl phasenseparіert als auch einphasig vorlagen, wurden mit Hilfe der dielektrischen Spektroskopie (DRS) durchgeführt. Hierbei zeigte sich, dass die höchste beobachtete Leitfähigkeit von 10^{-7} S/cm bei einem dotierten Homo-PFS bei Verdünnung durch PMMA- und PS-Domänen in Blockcopolymeren bis auf 10^{-10} S/cm abnahm.

Chapter 7

Experimental

7.1 Reagents and Chemicals

7.1.1 ***Solvents***

(a) *Tetrahydrofuran*: THF (Technical Grade) was dried by refluxing over sodium under N_2 atmosphere in the presence of benzophenone until a bright deep purple color was obtained. It was distilled and stored over red 1,1-diphenylhexyl lithium (DPHLi) in the high vacuum line reservoir generated in situ by the reaction of DPE and *n*-BuLi. The permanent red color indicated the purity. It was distilled fresh from the high vacuum line on the day of use.

(b) *n-Hexane*: Hexane (Technical Grade) was stirred over sodium and benzophenone for 18 h and distilled from a blue colored solution. This was then stored over red DPHLi in the high vacuum line reservoir and distilled freshly from the vacuum line before use.

(c) *Diethyl ether*: Technical grade diethyl ether was purified by distillation from deep purple sodium benzophenone.

(d) *Cyclohexane*: Cyclohexane (Technical Grade) was dried by stirring overnight on sodium with little amount of benzophenone till the solution turned blue and later on distilled from the blue solution. This was then stored over red DPHLi in a schlenk flask (500 mL) and distilled prior to use.

(e) *Methanol*: Methanol (HPLC Grade) used for termination reaction was dried by refluxing over magnesium turnings in an atmosphere of N_2, distilled and carefully degassed by repeated freeze-pump-thaw cycles. The precipitation of the block copolymers was done in technical grade methanol and used as received.

(f) *Dichloromethane*: Methylene chloride (HPLC grade) was used as such in film preparation for TEM, SAXS and DRS.

7.1.2 ***Monomers, Initiators and other Reagents***

(a) *Styrene*: Styrene (Aldrich 99%) was dried overnight by stirring over calcium hydride and distilled into a 50 mL vacuum line ampoule. This ampoule was stored in the glove box refrigerator at –20 °C and distilled one more time just prior to use.

(b) *Methyl Methacrylate (MMA)*: MMA (Aldrich 99%) was first dried by stirring over CaH_2. After distillation it was titrated further with a small amount of triethylaluminium (Aldrich, 1.0 M solution in hexane) until a slight yellowish green color appeared and then stored in the glove-box refrigerator at –20 °C. Just prior to use it was condensed in vacuo and kept in liquid nitrogen in order to avoid autopolymerization.

(c) *n*-Butyl lithium: *n*-BuLi (Aldrich, 2.5 M solution in hexane) was used as received.

(d) *sec*-Butyl lithium: *sec*-BuLi (Aldrich, 1.4 M solution in cyclohexane) was taken as received.

(e) *Preparation of the Difunctional Initiator Lithium Naphthalide*: Naphthalene (3.2 g, 25.3 mmol) was dissolved in freshly distilled and degassed THF (15 mL). To this solution lithium metal granules (175 mg, 25.3 mmol) were added and the solution was stirred at room temperature in the glove box. In 5-10 min the solution turned pale yellow and then deep green, indicating the formation of lithium naphthalide.[259] After stirring for further 2 h the solution was stored in the glove box fridge at -20 ºC.

The concentration of the lithium naphthalide initiator solution used for the synthesis of pentablock copolymers was back calculated from the model polymerization of styrene at -50 ºC: a solution containing 100 µL of green colored lithium naphthalide in 20 mL of THF was cooled to -50 ºC in the polymerization reactor. To this styrene (1 g, 9.6 mmol) was added quickly with stirring upon which the solution turned yellow immediately. After stirring for 35 min the living polystyrene was terminated by addition of few drops of CH_3OH and isolated by precipitation in CH_3OH (100 mL). SEC analysis gave M_n = 19,850 $g.mol^{-1}$ and PDI = 1.02, from which the concentration of the lithium naphthalide initiator solution was calculated to be 0.504 M.

(f) *Dichlorodimethylsilane ($SiMe_2Cl_2$)*: Dichlorodimethylsilane (Aldrich, 99 %) was distilled and carefully degassed in order to remove dissolved HCl.

(g) *Ferrocene*: Ferrocene (Aldrich, 98%) was purified by recrystallization from hexane.

(h) *TMEDA*: *N,N,N´,N´*-Tetramethylethylenediamine (TMEDA) (Aldrich, 99.5 %) was distilled over CaH_2 (Fluka, ≥ 95 %).

(i) *DPE*: For the purification of 1,1-diphenylethylene (DPE) (Acros, 99 %), a small amount of *n*-BuLi was added until a deep red color appeared and distilled via a short-path distillation apparatus under high vacuum. The DPE purified and degassed in this manner was divided into small portions in 2 mL screw cap vials and stored in the glove-box refrigerator until used.

(j) *DMSB*: 1,1-Dimethylsilacyclobutane (DMSB) (Fluka) was stirred over CaH_2, degassed, distilled and stored in the glove box. It was freshly distilled on the day of use.

(k) *Drying of N,N,N',N'-Tetramethylethylenediamine (TMEDA)*

TMEDA (99.5%) was further dried by stirring over CaH_2 for 18 h in a vacuum line schlenk ampoule. It was freshly distilled under vacuum at the time of usage.

(l) *Drying of Dimethyldichlorosilane (DMDCS)*

Dimethyldichlorosilane was dried over CaH_2 in a vacuum line ampoule for 24 h and distilled fresh before use.

7.2 Synthesis of [1]Dimethylsilaferrocenophane (FS)

7.2.1 *Synthesis of 1, 1'- Dilithioferrocene*

(a) *Purification of Ferrocene by Recrystallization*

Ferrocene (~30 g) was dissolved in 1L of *n*-hexane and stirred for 2 h to obtain a saturated solution at room temperature. The flask was then cooled down to -4 ºC overnight and shining orange crystals were obtained which were separated by filtration under vacuum.

(b) *Reaction Procedure*

Recrystallized and dried ferrocene (13 g, 70 mmol) was placed in a 500 mL schlenk flask and capped with a turn over rubber flange stopper. After three cycles of evacuating and purging with nitrogen the flask was filled with *n*-hexane (250 mL, freshly distilled) via a double tipped needle. The contents of the flask were stirred for 30 min till most of the ferrocene dissolved. To this 22.6 mL of TMEDA (freshly distilled taken in a disposable plastic syringe in the glove box) was slowly added through the rubber septum with constant stirring. Then *n*-BuLi (62 mL, 2 M solution in hexanes) was added dropwise by syringes filled in the glove box. After 1 h a yellow-orange precipitate of dilithiated ferrocene was observed. The mixture was allowed to stir overnight at room temperature. The reaction work up involved the filtration of the reaction suspension by means of a transfer needle into a set up consisting of a septum-capped sintered glass crucible connected to a 500 mL schlenk flask. The product collected on the crucible (13.5 g, 98% yield) was further dried under vacuum for about 3 h and stored in the glove box fridge at -20 ºC in a single neck 100 mL flask. Due to the extreme air sensitivity no analytical or spectroscopic data could be obtained for 1,1'-dilithioferrocene.

7.2.2 *[1]Dimethylsilaferrocenophane*

In the glove box a 1L 3-necked, round bottom flask with an appropriate stirring bar was filled with the 1,1'-dilithioferrocene (10 g, 51 mmol). The middle neck was capped with a turn over flange stopper, while the other two necks were plugged with stopcocks. The whole arrangement was then transferred outside the glove box. Freshly distilled diethylether (450 mL) was added by using a double tipped needle. The whole set

up was connected to nitrogen gas (purity > 99%) and slowly lowered into an isopropanol-liquid N_2 bath at -80 ºC. Dimethyldichlorosilane (5.0 mL) was added dropwise by means of a syringe over a period of 15-20 mins. The reaction set up was covered with an aluminium foil and allowed to stir overnight. The reaction work up involved the replacement of the flange stopper by a moderately greased glass one under nitrogen flow. A 1L schlenk flask immersed in liquid N_2 was connected to the set up and was used as a cooling trap to remove the diethylether from the reaction contents under vacuum. The complete removal of ether yielded the red to orange colored (due to LiCl) product, which was further dried under high vacuum for 7- 8 h. The LiCl was removed by dissolving the crude reaction product in freshly distilled *n*-hexane (50 mL) and filtered through a sintered glass crucible under N_2 atmosphere. The evaporation of hexane under reduced pressure yielded a deep red colored material. This crude product was then sublimed at room temperature onto a cold probe (3 ºC). Thus 7.5 g (yield: 85 %) of red crystalline [1]dimethylsilaferrocenophane was obtained which contained some oligomers and therefore was not pure enough for living anionic polymerization. Further purifications to obtain a product of "high purity" suitable for living anionic polymerization consisted of alternating high vacuum sublimations (three times, 0.005 mm Hg, 40 ºC) and recrystallizations from *n*-hexane (two times, -60 ºC) coupled with two stirrings over CaH_2 in dry THF for 24 h. This yielded about 4.5 – 5.0 g of the pure [1]dimethylsilaferrocenophane.

^{1}H-NMR (500 MHz, C_6D_6): 0.37 (s, 6H, C***H*****$_3$**), 3.95(t, $J_{H\text{-}H}$ = 1.6 Hz, 4H, cyclopentadienyl-***H***), 4.42 (t, $J_{H\text{-}H}$ = 1.6 Hz, 4H, cyclopentadienyl-***H***) ppm.

7.3 Polymerization

7.3.1 *Synthesis of Polyferrocenyldimethylsilane*

The reaction was performed inside the glove box. A solution of **FS** (760 mg, 3 mmol) was prepared in 15 mL of freshly distilled THF. The polymerization reaction was initiated by the addition of *n*-BuLi (30 µL, 1.6 M in hexanes). The color of the solution changed from red to amber in a period of 10 min indicating the start of polymerization. The reaction was terminated by the addition of a few drops of degassed methanol after 40

min. The homopolymer product was isolated in ~98% yield by precipitation into *n*-hexane and was dried under high vacuum for 10 h.

^{1}H-NMR (500 MHz, CD_2Cl_2): 0.47 (s, 6H, C***H*₃***), 4.02 (m, 4H, cyclopentadienyl-***H***), 4.52 (m, 4H, cyclopentadienyl-***H***) ppm.

^{13}C-NMR (125 MHz, CD_2Cl_2): −0.96 ppm [(η-C_5H_4)$_2$FeSi***Me*₂***]$_y$, 71.67 (***C***, Cp), 72.00 (*ipso*-***C***, Cp), 73.52 (***C***, Cp) ppm.

7.3.2 *Synthesis of PFS-b-PMMA*

The monomer FS (1.5 g, 6.19 mmol) was polymerized[196] in 20 mL of THF by addition of *n*-BuLi (38 µL, 0.06 mmol, 1.6 M in hexane) to give a living PFS precursor with M_n = 25000 g·mol^{-1} and PDI = 1.04. After complete conversion of the monomer (30 min), DPE (32 µL, 0.24 mmol) was added immediately followed by DMSB (16 µL, 0.12 mmol) in a ratio of 1:4:2 for [*n*-BuLi]/[DPE]/[DMSB]. A change in color from amber to deep red within 5 min indicated a fast carbanion trapping reaction. This ampoule was then connected to the polymerization reactor and slowly the whole set up was lowered into a liquid nitrogen/2-propanol bath at -78° C. For the introduction of the second block, MMA (0.61g, 18 mmol) was rapidly introduced from a syringe into the reactor through a Teflon-coated silicon septum under vigorous stirring. The deep red color of the living end-capped PFS precursor disappeared immediately, indicating a fast initiation of the MMA block polymerization. The polymerization was finally terminated after stirring the solution for 75 min at -78° C by adding degassed methanol. After precipitating in methanol and drying under vacuum, 2.0 g (95%) of crude PFS-*b*-PMMA was isolated. The crude polymer contained about 5-10% of PFS homopolymer, the pure diblock copolymer was selectively precipitated from PFS: the crude product was dissolved in THF (20 mL) and after complete dissolution, *n*-hexane (200 mL) was added dropwise until the pure diblock copolymer started to precipitate. The precipitate was isolated by means of an ultracentrifuge for 7 min at 4000 revolutions/min. This procedure allowed almost complete quantitative separation of the pure diblock copolymer from the PFS homopolymer. SEC (RI detection, PS calibrants): M_n = 35000 g·mol^{-1}; PDI = 1.08

^{1}H-NMR (500 MHz, CD_2Cl_2): 0.47 (s, 6H, C***H*****$_3$**, PFS), 0.7-1.02 (m, 3H, C***H*****$_3$**, PMMA), 1.7-1.9 (m, 3H, C***H*****$_2$** and C***H***, PMMA), 3.58 (s, 3H, OC***H*****$_3$**, PMMA), 4.02 (m, 4H, cyclopentadienyl-***H***), 4.24 (m, 4H, cyclopentadienyl-***H***) ppm.

^{13}C-NMR (125 MHz, CD_2Cl_2): −0.91 ppm [(η-C_5H_4)$_2$FeSi***Me*****$_2$**]$_y$, 16.97 (-***C***H_3, PMMA syndiotactic), 19.05 (-***C***H_3, PMMA isotactic), 44.93 (***Quat C***, PMMA), 51.95 (-COO***C***H_3, PMMA), 52.82 (***C***H_2-, PMMA), 71.68 (***C***, Cp), 72.05 (*ipso*-***C***, Cp), 73.51 (***C***, Cp), 178.12 (-***C***OO-, PMMA) ppm.

7.3.3 ***Synthesis of PFS-*b*-PS-*b*-PFS***

Freshly double distilled styrene (0.28 g, 2.688 mmol) was instantaneously injected into a green solution of lithium naphthalide in 20 mL of THF (0.0252 mmol, 50 µL, 0.504 M) at -50 ºC. The solution became yellow immediately and styrene was allowed to polymerize at the same temperature. After 35 min the reaction mixture was allowed to warm up to the room temperature. Silaferrocenophane (0.2 g, 0.8261 mmol) dissolved in 10 mL of THF, was added to the reaction flask with stirring. The resulting red solution gradually changed to amber over 20 min. The polymerization was finally terminated after stirring the solution for 45 min at room temperature by adding few drops of degassed methanol. The polymer was isolated by precipitation into methanol, filtered and dried under high vacuum for 3-4 h. Thus 0.43 g (90 %) of the orange-yellow powdery triblock copolymer was obtained. SEC (RI detection, PS calibrants): M_n = 20000 g·mol^{-1}; PDI = 1.07

^{1}H-NMR (500 MHz, CD_2Cl_2): 0.48 (s, 6H, C***H*****$_3$**, PFS), 1.52 (br, C***H*****$_2$**), 1.82 (br, C***H***Ph), 4.02 (m, 4H, Cyclopentadienyl-***H***), 4.24 (m, 4H, Cyclopentadienyl-***H***), 7.10, 6.70 (br, C_6***H*****$_5$**) ppm.

^{13}C-NMR (125 MHz, CD_2Cl_2): −0.95 ppm [(η-C_5H_4)$_2$FeSi***Me*****$_2$**]$_y$, 40.78 (-***C***H, Ph), 45.26 (-***C***H_2, Ph), 71.64 (***C***, Cp), 72.04 (*ipso*-***C***, Cp), 73.49 (***C***, Cp), 126.06 (*p*-***C***, Ph), 127.95 (*o*-***C***, Ph), 128.36 (*m*-***C***, Ph), 146.1-145.2 (*ipso*-***C***, Ph) ppm.

7.3.4 *Synthesis of PS-b-PFS-b-PMMA*

The triblock copolymer was synthesized by the sequential addition of the monomers namely styrene, silaferrocenophane and methyl methacrylate. Styrene (0.75 g, 7.2 mmol) was polymerized in 15 mL of cyclohexane by addition of *sec*-BuLi (50 µL, 0.07 mmol, 1.4 M in hexane) for 90 min at 40 °C which yielded a yellow colored solution of living PS precursor with M_n = 10000 g·mol^{-1} and PDI = 1.02. The reactor contents were allowed to come to the room temperature. A solution of FS (1.75 g, 7.22 mmol) in 20 mL THF was rapidly added by means of a syringe. The color of the solution immediately changed from yellow to red, which indicated the initiation of the second PFS block. After complete consumption of the monomer in 30 min the color changed from red to amber. DPE (37 µL, 0.28 mmol) was added immediately followed by DMSB (19 µL, 0.14 mmol) in a ratio of 1:4:2 for [*n*-BuLi]/[DPE]/[DMSB]. A change in color from amber to deep red within 5 min indicated a fast carbanion trapping reaction. This ampoule was then connected to the polymerization reactor and slowly the whole set up was lowered into a liquid nitrogen/2-propanol bath at –78 °C. For the second block, MMA (0.7 g, 21 mmol) was rapidly introduced from a syringe into the reactor through a Teflon-coated silicon septum under vigorous stirring. The deep red color of the living end-capped PFS precursor disappeared immediately and the polymerization was finally terminated after stirring the solution for 75 min at –78 °C by adding degassed methanol. After precipitating in methanol and drying under vacuum, 3.0 g (94%) of crude PS-*b*-PFS-*b*-PMMA was isolated.

As this material still contained about 10-15 % of PS-*b*-PFS diblock copolymer, the pure triblock copolymer was selectively precipitated by dissolving the crude product (0.8 g) in THF (10 mL). After complete dissolution, cyclohexane (100 mL) was added dropwise until the pure triblock copolymer started to precipitate. The precipitate was isolated by means of an ultracentrifuge for 10 min at a speed of 4000 revolutions/min. This procedure allowed almost quantitative separation of the pure triblock copolymer from the PS-*b*-PFS diblock copolymer. SEC (RI detection, PS calibrants): M_n = 45000 g·mol^{-1}; PDI = 1.09

^{1}H-NMR (500 MHz, CD_2Cl_2): 0.48 (s, 6H, C***H*****$_3$**, PFS), 1.00 (br, -C***H*****$_3$**, PMMA syndiotactic), 1.20 (br, -C***H*****$_3$**, PMMA isotactic), 1.47 (br, C***H*****$_2$**Ph), 1.81 (br, C***H***Ph), 1.90 (br, -C***H*****$_2$** of PMMA), 3.59 (s, 3H, COOC***H*****$_3$**), 4.02 (m, 4H, cyclopentadienyl-***H***), 4.24 (m, 4H, cyclopentadienyl-***H***), 7.01, 6.60, 6.52 (br, 5**H**, Ph) ppm.

^{13}C-NMR (125 MHz, CD_2Cl_2): −0.91 ppm $[(\eta\text{-}C_5H_4)_2FeSi\boldsymbol{Me_2}]_y$, 17.12 (-***C***$H_3$, PMMA syndiotactic), 19.09 (-***C***H_3, PMMA isotactic), 40.75 (-***C***H, Ph), 44.92 (***Quat C***, PMMA), 45.21 (-***C***H_2, Ph), 51.95 (-COO***C***H_3, PMMA), 52.77 (***C***H_2-, PMMA), 71.61 (***C***, Cp), 72.04 (*ipso*-***C***, Cp), 73.45 (***C***, Cp), 126.05 (*p*-***C***, Ph), 127.95 (*o*-***C***, Ph), 128.37 (*m*-***C***, Ph), 146.0-145.2 (*ipso*-***C***, Ph), 178.06 (-***C***OO-, PMMA) ppm.

7.3.5 ***Synthesis of PMMA-*b*-PFS-*b*-PS-*b*-PFS-*b*-PMMA***

The synthesis of the pentablock copolymer PMMA-*b*-PFS-*b*-PS-*b*-PFS-*b*-PMMA was carried out by sequential monomer addition.[199] Freshly double distilled styrene was instantaneously injected into a green solution of lithium naphthalide in 20 mL of THF (0.0252 mmol, 50 µL, 0.504 M) at -50 ºC. The solution was polymerized at the same temperature. After 35 min then the reaction mixture was allowed to warm up to the room temperature. Silaferrocenophane, dissolved in 10 mL of THF, was added to the reaction flask with stirring. After 45 min the living polymer was trapped by means of dimethylsilacyclobutane-mediated end-capping with 1,1-diphenylethylene so as to yield the living macroinitiator. A molar ratio of 1:4:2 for initiator:DPE:DMSB, respectively, was employed for the trapping reaction in all the block polymerizations. DPE (0.101 mmol, 18 µL) and DMSB (0.05 mmol, 6µL) were added in succession immediately. The solution changed its color from amber to red in 10-15 min and was allowed to stir for 30 min during which the color deepened further. Next, the reaction flask was cooled to -80 ºC and methyl methacrylate was added. MMA block polymerization was carried out for 75 min after which the living copolymer was terminated by addition of few drops of methanol. The block copolymer was then isolated by precipitation in methanol (150 mL) and dried under high vacuum (4 h). Thus an orange-yellow powdery pentablock copolymer was isolated in 90-95 % yield.

The pentablock was purified by three cycles of repetitive precipitation in cyclohexane. About 0.7 g of the crude pentablock was dissolved in 10 mL of THF and to this solution cyclohexane was added drop wise, initially fast but later slowly. After addition of 150 mL (total amount 190 mL) the solution turned turbid and the first grains of precipitate appeared. After addition of all the cyclohexane, the precipitate was separated off by means of an ultracentrifuge for 10 min at a speed of 4000 rpm. By this method, around 0.66 g of the pentablock (containing some tetrablock) copolymer was obtained, and the triblock copolymer was efficiently removed. The procedure can be repeated several times, depending on the required purity of the materials.

^{1}H-NMR (500 MHz, CD_2Cl_2): 0.48 (s, 6H, C***H*****$_3$**, PFS), 1.02(br, -C***H*****$_3$**, PMMA syndiotactic), 1.20 (br, -C***H*****$_3$**, PMMA isotactic), 1.47 (br, C***H*****$_2$**Ph), 1.81 (br, C***H***Ph), 1.90 (br, -C***H*****$_2$** of PMMA), 3.59 (s, 3H, COOC***H*****$_3$**), 4.02 (m, 4H, cyclopentadienyl-***H***), 4.24 (m, 4H, cyclopentadienyl-***H***), 7.01, 6.60, 6.52 (br, 5**H**, Ph) ppm.

^{13}C-NMR (125 MHz, CD_2Cl_2): −0.93 ppm [(η-C_5H_4)$_2$FeSi***Me*****$_2$**]$_y$, 16.95 (-***C***H_3, PMMA syndiotactic), 19.00 (-***C***H_3, PMMA isotactic), 40.77 (-***C***H, Ph), 44.90 (***Quat C***, PMMA), 45.23 (-***C***H_2, Ph), 51.97 (-COO***C***H_3, PMMA), 52.78 (***C***H_2-, PMMA), 71.63 (***C***, Cp), 72.00 (*ipso*-***C***, Cp), 73.47 (***C***, Cp), 126.02 (*p*-***C***, Ph), 127.98 (*o*-***C***, Ph), 128.39 (*m*-***C***, Ph), 146.0-145.0 (*ipso*-***C***, Ph), 178.07 (-***C***OO-, PMMA) ppm.

7.4 Film Preparation for TEM and SAXS

In order to get the required samples, polymer films were initially casted onto glass plates from solutions (5 % w/v) in dichloromethane, tetrahydrofuran and toluene. The formation of thermodynamically stable morphologies was forced by storing the freshly cast films in the saturated atmosphere of the corresponding solvent for 4-6 weeks depending upon the rate of evaporation of the corresponding solvent. The films were then stored for 2 days under vacuum at room temperature. Subsequently, they were annealed for 24 h at elevated temperatures (160, 180, 200, 220 and 230 °C) under vacuum, followed by sudden quenching in ice water or by cooling down slowly (10 °C · h^{-1}) to 100 °C and then quenching in ice water. The annealing temperatures were selected above

the glass transition temperature of each of the three blocks so as to ensure that there is sufficient molecular chain mobility and viscosity required for microphase separation. Quenching in ice water was done to prevent the recrystallization of the PFS block, which can adversely affect the morphology as PFS being semi-crystalline in nature. Finally the films were cut into slices of approx. 50 nm thick using an ultramicrotome. The slices were placed on a copper grid and examined with Transmission Electron Microscopy. The SAXS measurements were done on films with 1cm in diameter and ~1mm in thickness.

7.5 Instrumentation

7.5.1 *Nuclear Magnetic Resonance Spectroscopy (NMR)*

NMR spectra were recorded at room temperature on a Bruker ARX-500 spectrometer at 500 MHz (^{1}H) and 125 MHz (^{13}C). The NMR sample solutions in CD_2Cl_2 (Deutero-GmBH, Kastellaun) and C_6D_6 (Aldrich) were prepared by dissolving an appropriate quantity of the polymer in the respective deuterated solvent.

7.5.2 *Size Exclusion Chromatography (SEC)*

Molecular weights were determined by SEC using a Waters Associates Liquid Chromatograph equipped with a 515 HPLC pump, U6K injector , PSS ultrastyragel columns with pore sizes of 10^3; 10^5; 10^6 Å, a Waters 410 differential refractometer and a Waters 486 UV-detector. A flow rate of 1.0 mL/min was used. Samples were dissolved in THF (HPLC Grade) containing toluene as a flow rate marker. Calculation of the molecular weights was carried out with respect to twelve monodisperse PS standards [elution volume (mL)/M_w ($g \cdot mol^{-1}$): 16.39/2.57 * 10^6, 17.74/1.04 * 10^6, 18.48/6.59 * 10^5, 20.30/2.46 * 10^5, 21.69/1.28 * 10^5, 23.18/6.75 * 10^4, 24.85/3.25 * 10^4, 26.12/1.81 * 10^4, 28.78/4.29 * 10^3, 30.49/1.62 * 10^3, 33.01/3.76 * 10^2, 34.30/1.02 * 10^2]. The software Win-GPC, Version 6.1 was used for the data analysis. (The PS standards and the software were purchased from PSS Polymer Standards Service GmbH, Mainz, Germany). The polymer samples were prepared by dissolving 2 mg in a HPLC autosampler vial containing 2 mL of THF. This yielded a solution of 0.1 % w/v or 1000 ppm sufficient for analysis by the differential refractometer and UV-detector.

7.5.3 *Thermogravimetric Analysis (TGA)*

With the help of thermogravimetry the thermal stability of the pentablock copolymers was examined. The measurements were carried out under N_2-atmosphere in the temperature range from 25 °C to 700 °C in a TGA-50 equipment (Shimadzu) with a heating rate of 10 K/min.

7.5.4 *Differential Scanning Calorimetry (DSC)*

The DSC measurements were accomplished on a DSC822e (Mettler Toledo). The instrument was equipped with a TSO801R0 autosampler (Mettler Toldeo). The samples were heated in a closed aluminium pan with a heating rate of 10 K/min from 0 °C to 180 °C and then cooled down with the same rate again followed by reheating. The glass transition temperatures were determined from the turning point of the glass stages in the second heating curve.

7.5.5 *Transmission Electron Microscopy (TEM) and Ultramicrotomy*

Bright field TEM was performed using a Zeiss CEM902 transmission electron microscope (**Fig. 7a**) operated at 80 kV and 50 μA beam current. The pictures were captured in the TIF format with a Slow Scan Digital camera (Proscan GmbH), which was equipped with a frame transfer CCD sensor (THX7888). The camera was controlled with the help of the software Vario Visionpro Version 3.2 (LEO). Ultra thin sections of solvent cast films of the block copolymers were cut to ca. 50 nm by means of LEICA Ultra Cut microtome at room temperature.

The acceleration voltage generally is between 50 and 150 kV. The higher it is, the shorter are the electron waves and higher is the power of resolution. However the resolution power of electron microscopy is usually restrained by the quality of the lens system and especially by the technique with which the preparation has been achieved. The accelerated beam of electrons passes a drill-hole at the bottom of the anode. The lens system consists of electronic coils generating an electromagnetic field. The ray is focused by a condenser. It then passes through the object, where it is partially deflected. The degree of deflection depends on the electron density of the object. The greater the mass of the atoms, the greater is the degree of deflection. Block copolymer samples containing

low atomic number atoms namely C, H, N and O have weak contrast. Therefore sometimes it is necessary to treat the thin films with special contrast enhancing staining agents. For example, the polystyrene phases are stained by RuO_4 [260, 261] and polybutadiene phases by OsO_4. [262]

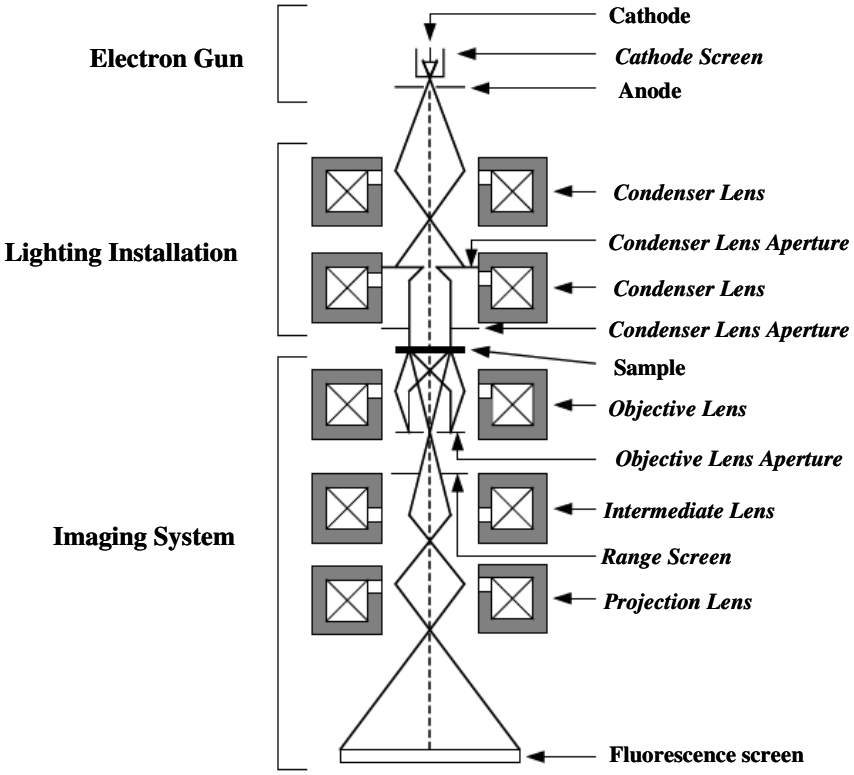

Fig. 7a *Schematic representation of a Transmission Electron Microscope (TEM).*

7.5.6 *Small Angle X-ray Scattering (SAXS)*

SAXS measurements were performed on Beamline A2 of the Hamburger Synchrotronstrahlungslabor (HASYLAB) at the Deutsches Elektronen-Synchrotron (DESY) in Hamburg, where charged positrons accelerated perpendicular to their trajectory delivered monochromatic X-rays (0.1542 nm) on to the sample. A bent, cylindrical mirror focused the X-rays at the detector plane. A two-dimensional charge-coupled device (MarCCD) camera used to collect the scattered X-rays.

The primary experimental ingredient in SAXS is the need for a well-collimated x-ray beam with a small cross-section. Synchrotron radiation sources with their intense

brightness and natural collimation are ideal when we consider the fact that most polymer materials are poor scatterers. The SAXS technique is performed in the transmission mode. In this mode, polymer samples are typically 1-2 mm thick, offering about 63-65 % absorption of the incident X-ray beam. The general relationship between the scattering angle and the size of the object is given by **eq. 7.5.6a**

$$\text{Angle of scattering} \approx 1/\text{object size} \qquad \textbf{7.5.6a}$$

Intense scattering over a range of angles means the structure is ordered on that length scale. Scattering data are represented in the form of intensity measurements as a function of the scattering vector q defined by

$$q = \frac{4\pi \sin\theta}{\lambda} \qquad \textbf{7.5.6b}$$

where λ is the wavelength of the X-ray and θ is half of the scattering angle defined as 2θ. Using Bragg's equation

$$\lambda = 2d_{hkl} \sin\theta \qquad \textbf{7.5.6c}$$

and **eq. 7.5.6b** the d-spacing of the reflection hkl is given by

$$d_{hkl} = 2\pi / q_{hkl} \qquad \textbf{7.5.6d}$$

7.5.7 ***Elemental Analysis***

Elemental analyses were perfomed on a Universal C H N O S Elemental Analyzer (Vario EL III).

7.6 Dielectric Relaxation Spectroscopy (DRS) and Conductivity Measurements

The conductivity measurements were performed by means of Dielectric Relaxation Spectroscopy in a frequency range from 10^{-4} to 10^{7} Hz using a frequency response analysis system. This consisted of a computer-controlled Solatron SI 1260

Impedance/ Gain-Phase Analyzer and a Novocontrol broadband dielectric converter at room temperature.

7.6.1 *Oxidative Doping of Polymers by Iodine*

A doping molar stoichiometry of 1:20 for polymer: iodine (oxidant) was employed in all the homo and block copolymers under investigation. Solution of iodine (0.6 g, 4 mmol) in CH_2Cl_2 (5 mL) was added dropwise to the polymer solution (5 g, 0.2 mmol) in CH_2Cl_2 (50 mL) under aerobic conditions. The mixture was stirred for 24 h and CH_2Cl_2 was removed under reduced pressure. Next the unreacted iodine was removed by sublimation under reduced pressure while heating gently (60 °C) over a period of 24 h that yielded a black powder with around 80 % of all the Fe^{2+} oxidized to Fe^{3+}. Elemental Analysis (PFS), Calculated: ($[Fe(\eta^5\text{-}C_5H_4)_2\ Si(CH_3)_2]_{1.0}[I_3]_{0.82}$): C = 26.01; H = 2.55. Found: C = 26.04; H = 2.57.

7.6.2 *Oxidative Doping of Polymers by Tetracyanoethylene (TCNE)*

A similar methodology with a few modifications as in section **7.6.1** was employed for the doping of polymers with TCNE. The polymers were oxidized under an inert atmosphere using 3 equivalents of the oxidant. After using a similar workup, a black powder was isolated, with a composition having nearly all of the Fe^{2+} sites oxidized to Fe^{3+}. Elemental Analysis (PFS), Calculated: ($[Fe(\eta^5\text{-}C_5H_4)_2\ Si(CH_3)_2]_{1.0}[TCNE]_{0.95}$): C = 58.43; H = 3.88; N = 14.63 . Found: C = 58.45; H = 3.91; N = 14.66.

7.6.3 *Film Preparation and Conductivity Measurements*

The thin-doped polymer film was prepared by solvent evaporation of a (2 % w/v) solution in CH_2Cl_2 in a small flat bottom petridish. This yielded films having thickness of 1mm and diameter of 1-2 cm. The film was carefully removed with the help of tweezers or forceps and sandwiched between two masks. The mask had a circular-shaped hole. Thus, the sample can be sputtered with a gold layer having a round shape (**Fig. 7b**).

The mask ensures that there is no contact between two sides of the sample by gold. The film was sputtered with gold under vacuum (pressure < 0.1 mbar). The film was then transferred to DRS instrument between the two circular copper plates. The size

of the copper plates fit the size of the gold sputtered area of the sample. Then a sinusoidal potential was applied across them and the resultant signal was measured.

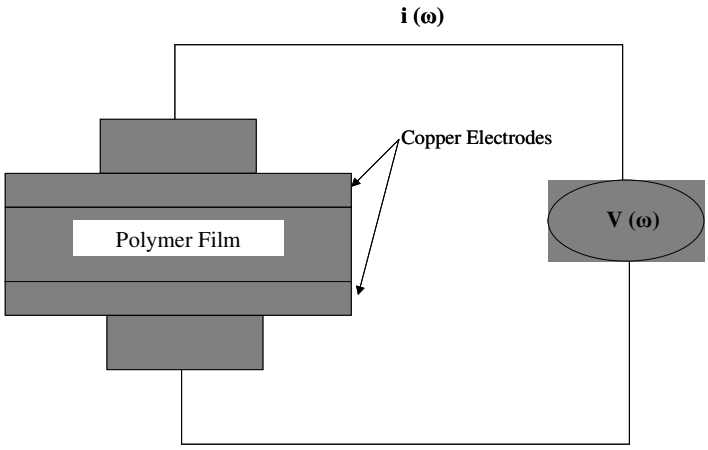

Fig. 7b *Parallel plate sample test cells for dielectric measurement.*

All manipulations regarding the syntheses and solvent degassing/distillation were carried out using either a (Mbraun UNILab) glove box (**Fig. 7c**) equipped with a refrigerator or an all-glass high-vacuum line (**Fig. 7d**) equipped with Teflon valves and a removable five inlet glass reactor (**Fig. 7e**). [26] Both were operated with purified nitrogen (> 99 %). The preparation of polymeric precursors and other reagents/solutions involved the use of ampoules, also equipped with Teflon valves, which can be directly attached to the reactor. The ampoules, schlenk flasks and other glassware were cleaned with dilute HCl followed by THF and preheated in the oven at 150 ºC prior to use. All the reactions including living anionic polymerizations were performed under an inert atmosphere (ultrahigh pure nitrogen), using either high vacuum/schlenk techniques or a vacuum atmosphere glove box.

Fig. 7c *Glove box (Mbraun) with an ultrahigh pure nitrogen atmosphere and a refrigerator maintaining a temperature of –20 °C.*

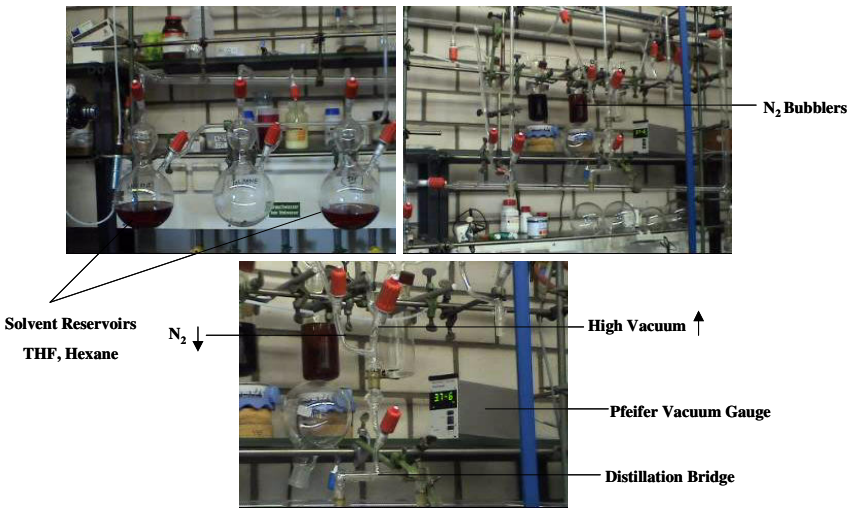

Fig. 7d *High vacuum line equipped with teflon (red) valves and an ultra high pure nitrogen supply for solvent distillation, monomer and block copolymer syntheses.*

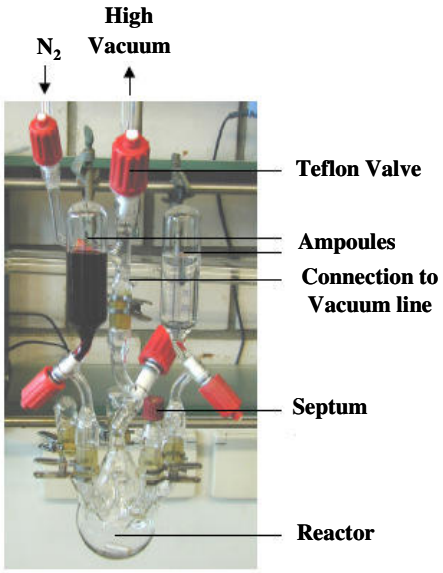

Fig. 7e *Five-inlet glass reactor (250 mL) used for the synthesis of block copolymers.*

8. References

(1) The Physics of Block Copolymers, Ikan. W. Hamley, Oxford University Press, **1998**.

(2) N. Hadjichristidis, Y. Paulos, A. Avgeropoulos, *Macromol. Symposia.* **1998**, *132*, 207.

(3) M. Pitsikalis, S. Pispas, J. W. Mays, N. Hadjichristidis, *Adv. Polym. Sci.* **1998**, *135*, 1.

(4) N. Hadjichristidis, M. Pitsikalis, S. Pispus, H. Iatrou, *Chem. Rev.* **2001**, *101*, 3747.

(5) M. Miyamoto, M. Sawamoto, T. Higashimura, *Macromolecules*, **1984**, *17*, 265.

(6) J. P. Kennedy, N. Meguriya, B. Keszler, *Macromolecules*, **1991**, *24*, 6572.

(7) T. Higashimura, S. Aoshima, M. Sawamoto, *Makromol. Chem. Macromol. Symp.* **1998**, *13/14*, 457.

(8) R. Faust, T. D. Shaffer, *Cationic Polymerization: Fundamentals and Applications, ACS Symposium Series*, **1997**, Vol. 665, Washington D.C.

(9) K. Matyjaszewski, *Cationic Polymerization: Mechanism, Synthesis and Application*, Marcel & Dekker, **1996**, New York.

(10) M. Sawamoto, *Prog. Polym. Sci.* **1991**, *16*, 111.

(11) G. Odian, *Principles of Polymerization*, **1981**, J. Wiley & Sons, New York.

(12) K. Matyjaszewski, J. L. Wang, T. Grimaud, D. Shipp, *Macromolecules*, **1998**, *31*, 1527.

(13) G. Moad, E. Rizzardo, D. H. Solomon, *Macromolecules*, **1982**, *15*, 909.

(14) M. K. Georges, R. P. N. Veregin, P. M. Kazmaier, G. K. Hamer, *Macromolecules,* **1993**, *26*, 2987.

(15) J. S. Wang, K. Matyjaszewski, *J. Am. Chem. Soc.* **1995**, *117*, 5614.

(16) J. S. Wang, K. Matyjazewski, *Macromolecules,* **1995**, *28*, 7901.

(17) B. B. Wayland, G. Poszmik, S. L. Mukerjee, M. Fryd, *J. Am. Chem. Soc.* **1994**, *116*, 7943.

(18) M. Kato, M. Kamigaito, M. Sawamoto, T. Higashimura, *Macromolecules,* **1995**, *28*, 1721.

(19) O. W. Webster, W. R. Hirtler, D. Y. Sogah, W. B. Farnham, T. V. Rajan Babu, *J. Am Chem. Soc.* **1983**, *105*, 5706.

(20) O. W. Webster, *Makromol. Chem. Symp.* **1990**, *33*, 133.

(21) W. J. Feast, E. Khasravi, *New Methods in Polymer Synthesis: Chapman & Hall,* **1995**, Vol. 2, Chapter 3.

(22) L. R. Gilliom, R. H. Grubbs, *J. Am. Chem. Soc.* **1986**, *108*, 733.

(23) R. H. Grubbs, W. Tumas, *Science,* **1989**, *243*, 907.

(24) M. Szwarc, *Nature,* **1956**, *178*, 1168.

(25) M. Szwarc, M. Levy, R. Milkovich, *J. Am. Chem. Soc.* **1956**, *78*, 2656.

(26) N. Hadjichristidis, H. Iatrou, S. Pispas, M. Pitsikalis, *J. Polym. Sci. Part A: Polym. Chem.* **2000**, *38*, 3211.

(27) M. Szwarc, *Carbanions: Living Polymers and Electron Transfer Processes*, Interscience, New York, **1968**.

(28) P. J. Flory, *J. Am. Chem. Soc.* **1940**, *62*, 1561.

(29) J. F. Henderson and M. Szwarc, *J. Polym. Sci., Macromol Rev.* **1968**, *3*, 317.

(30) J. W. Mays and Hadjichristidis, *Polym. Bull.* **1989**, *22*, 471.

(31) J. C. Chen and L. J. Fetters, *Polym. Eng. Sci.* **1987**, *27*, 1300.

(32) D. A. Conlon, J. V. Crivello, J. L. Lee and M. J. O' Brien, *Macromolecules*, **1989**, *22*, 509.

(33) I. Konigsberg and J. Jagur-Grodzinski, *J. Polym. Sci. Polym. Chem. Ed.* **1983**, *21*, 2649.

(34) P. Chaumont, G. Beinert, J. E. Herz and P. Rempp, *Makromol. Chem.* **1982**, *183*, 1181.

(35) O. Okay and W. Funke, *Macromolecules*, **1990**, *23*, 2623.

(36) Y. Nagasaki, H. Ito and T. Tsuruta, *Makromol. Chem*, **1986**, *187*, 23.

(37) D. H. Richards, *Chem. Soc. Rev.* **1977**, *6*, 235.

(38) K. F. Elgert and W. Ritter, *Makromol. Chem.* **1976**, *177*, 2021.

(39) D. Blondin, J. Regis and J. Prudhomme, *Macromolecules*, **1974**, *7*, 187.

(40) T. Suzuki, Y. Tsuji, Y. Takegami and H. J. Harwood, *Macromolecules*, **1979**, *12*, 234.

(41) S. K. Varshney, X. F. Zhong and A. Eisenberg, *Macromolecules*, **1993**, *26*, 701.

(42) D. Freyrs, P. Rempp and H. Benoit, *Polym. Lett.* **1964**, *2*, 217.

(43) D. M. Wiles and S. Bywater, *Polym. Lett.* **1964**, *2*, 1175.

(44) B. C. Anderson, G. D. Andrews, P. Arthur, H. W. Jacobson, L. R. Melby, A. J. Playtis and W. H. Sharkey, *Macromolecules*, **1981**, *14*, 1599.

(45) S. K. Varshney, J. P. Hautekeer, R. Fayt, R. Jerome, *Macromolecules*, **1990**, *23*, 2618.

(46) D. Kunkel, A. H. E. Muller, M. Janata, Makromol. Chem., *Macromol. Symp.* **1992**, *60*, 315.

(47) K. Hatada. T. Kitayama and K. Ute, *Prog. Polym. Sci.* **1988**, *13*, 189.

(48) F. W. Stanely and coworkers, *Ind. Eng. Chem.* **1956**, 778.

(49) M. Szwarc, *Adv. Polym. Sci*, **1983**, *49*, 1.

(50) H. L. Hsieh and O. F. Mc Kinney, *Polym. Lett.* **1966**, *4*, 843.

(51) M. Szwarc, Carbanions, *Living Polymers and Electron Transfer Processes, Wiley Interscience*, New York, **1968**.

(52) G. Beinert, P. Lutz, E. Franta and P. Rempp, *Makromol. Chem.* **1978**, *179*, 551.

(53) P. Lutz, E. Franta and P. Rempp, *Polymer*, **1982**, *23*, 1953.

(54) F. Bandermann, H. D. Speikamp and L. Weigel, *Makromol. Chem.* **1985**, *186*, 2017.

(55) S. Penczek, P. Kulusa and R. Szymanski, Makromol. Chem., Rapid Commun. **1991**, *12*, 77.

(56) M. Szwarc, *Adv. Polym. Sci.* **1983**, *49*, 1.

(57) H. L. Hsieh and W. H. Glaze, *Rubber Chem. Technol.* **1970**, *43*, 22.

(58) H. L. Hsieh and C. F. Wofford, *J. Polym. Sci.*, *Part A*, **1969**, *7*, 449.

(59) M. Van Beylen, S. Bywater, G. Smets, M. Szwarc and D. J. Worsfold, *Adv. Polym. Sci.* **1988**, *86*, 87.

(60) M. Y. Darensbourg, B. Y. Kimura, G. E. Hartwell and T. L. Brown, *J. Am. Chem. Soc.* **1970**, *92*, 1236.

(61) I. A. Alexander and S. Bywater, *J. Polym. Sci. Part A*, **1968**, *6*, 3407.

(62) T. Altares, D. P. Wyman and V. R. Allen, *J. Polym. Sci. Part A*, **1964**, *2*, 4533.

(63) L. J. Fetters and M. Morton, *Macromol. Syn.* **1972**, *4*, 77.

(64) Ph. Teyssie, R. Fayt, J. P. Hautekeer, C. Jacobs, R. Jerome, *Makromol. Chem., Macromol. Symp.* **1990**, *32*, 61.

(65) D. M. Wiles and S. Bywater, *Trans. Faraday Soc.* **1965**, *61*, 150.

(66) F. G. Bordwell, *Acc. Chem. Res.* **1988**, *21*, 456.

(67) L. Lochmann, M. Rodova and J. Trekoval, *J. Polym. Sci., Polym. Chem. Ed.* **1974**, *12*, 2091.

(68) D. Garg, S. Höring and J. Ulbricht, *Makromol. Chem., Rapid Commun.* **1984**, *5*, 615.

(69) P. E. M. Allen and D. R. G. Williams, *Ind. Eng. Chem.* **1985**, *24*, 334.

(70) Ian Manners, *Can. J. Chem.*, **1998**, *76*, 371.

(71) Ian Manners, *Advances in Organometallic Chemistry*, **1995**, *37*, 131.

(72) I. Manners, *Chem. Br.* **1996**, *32*, 46.

(73) U. T. Mueller-Westerhoff, *Angew. Chem. Int. Ed.* **1986**, *25*, 702.

(74) W. H. Morrison, D. N. Hendrickson, *Inorg. Chem.* **1975**, *14*, 2331.

(75) J. A. Kramer, D. N. Hendrickson, *Inorg. Chem.* **1980**, *19*, 3330.

(76) H. Rosenberg and E. W. Neuse, *J. Organometal. Chem.* **1966**, *6*, 76.

(77) M. Burkelaing, K. N. Trueblood, *Acta Crystallogr.* **1965**, *19*, 373.

(78) H. L. Lentzner, W. E. Watts, *Tetrahedron*, **1971**, *27*, 4343.

(79) K. Yasufuku, K. Aoki, H. Yamzaki, *Inorg. Chem.* **1977**, *16*, 624.

(80) E. W. Neuse, F. B. D. Khan, *Macromolecules*, **1986**, *19*, 269.

(81) E. W. Neuse, L. Bednarik, *Macromolecules*, **1979**, *12*, 187.

(82) R. Knapp, U. Velten, M. Rehahn, *Polymer*, **1998**, *39*, 5827.

(83) C. U. Pittman, J. C. Lai, D. P. Vanderpool, M. Good, R. Prado, *Macromolecules*, **1970**, *3*, 746.

(84) J. C. Lai, T. Rounsfell, C. U. Pittman, *J. Polym. Sci. A-1*, **1971**, *9*, 651.

(85) C. Aso, T. Kunitake, T. Nakashima, *Makromol. Chem.***1969**, *124*, 234.

(86) A. Togni, T. Hayashi, *Ferrocenes*, Weinheim, New York, Basel, Cambridge, Tokyo, **1995**.

(87) D. Albagli, G. Bazan, M. S. Wrighton, R. R. Schrock, *J. Am. Chem. Soc.* **1992**, *114*, 4150.

(88) K. J. Watson, J. Zhu, S. B. Nguyen, C. A. Mirkin, *J. Am. Chem. Soc.* **1999,** *121,* 462.

(89) H. R. Allcock, A. J. Dodge, I. Manners, G. H. Riding, *J. Am. Chem. Soc.* **1991**, *113*, 9596.

(90) K. H. Pannell, J. M. Rozell, J. M. Ziegler, *Macromolecules*, **1988**, *21*, 276.

(91) T. Inagaki, H. S. Lee, T. A.Skotheim, Y. J. Okamoto, *J. Am. Chem. Soc. Chem. Commun.* **1989**, 1181.

(92) P. D. Hale, T. Inagaki, H. I. Karan, Y. Okamaoto, T. A. Skotheim, *J. Am. Chem. Soc.* **1989**, *111*, 3482.

(93) G. P. Kittlesen, H. S.White, M. S. Wrighton, *J. Am. Chem. Soc.* **1985**, *107*, 7373.

(94) J. J. Bishop, A. Davidson, M. L. Katcher, D. W. Lichtenberg, R. E. Merrill, J. C. Smart, *J. Organomet. Chem.* **1971**, *27*, 241.

(95) I. R. Butler, W. R. Cullen, *Organometallics*, **1986**, *5*, 2537.

(96) A. G. Osborne and R. H. Whiteley, *J. Organomet. Chem.* **1975**, *101*, C27.

(97) H. Stoeckli-Evans, A. G. Osborne and R. H. Whiteley, *Helv. Chim. Acta.* **1976**, *59*, 2402.

(98) A. G. Osborne, R. H. Whiteley and R. E.Meads, *J. Organomet. Chem.* **1980**, *193*, 345.

(99) I. Manners, *Adv. Organomet. Chem.* **1995**, *37*, 131.

(100) D. A. Foucher, B. Z. Tang and I. Manners, *J. Am. Chem. Soc.* **1992**, *114*, 6246.

(101) M. Cypryk, Y. Gupta and K. Matyjaszewski, *J. Am. Chem. Soc.* **1991**, *113*, 1046.

(102) E. Fossum and K. Matyjaszewski, *Macromolecules*, **1995**, *28*, 1618.

(103) L. Wang, Y. Ko, G. Manuel and W. P. Weber, *Macromolecules*, **1992**, *25*, 2828.

(104) N. Yizeng, R. Rulkens, J. K. Pudelski and I. Manners, *Macromol. Rapid. Commun.* **1995**, *16*, 637.

(105) N. P. Reddy, H. Yamashita and M. Tanaka, *Chem. Soc. Chem. Commun.* **1995**, 2263.

(106) M. MacLachlan, M. Ginzberg, N. Coombs, T. W. Coyle, N. P. Raju, J. E. Greedan, G. A. Ozin, I. Manners, *Science*, **2000**, *287*, 1460.

(107) J. Massey, K. N. Power, I. Manners, M. A. Winnik , *J. Am. Chem. Soc.* **1998**, *120*, 9533.

(108) J. Massey, K. N. Power, I. Manners, M. A. Winnik, *Adv. Mater.* **1998**, *10*, 1559.

(109) A. B. Fischer, J. B. Kinney, R. H. Staley and M. S. Wrighton, *J. Am. Chem. Soc.* **1979**, *101*, 6501.

(110) R. Rulkens, A. J. Lough and I. Manners, *J. Am. Chem. Soc.* **1994**, *116*, 797.

(111) P. Gomez-Elipe, P. M. Macdonald and I. Manners, *Angew. Chem. Int. Ed. Engl.* **1997**, *36*, 762.

(112) P. F. Brandt and T. B. Rauchfuss, *J. Am. Chem. Soc.* **1992**, *114*, 1926.

(113) D. L. Compton, P. F. Brandt, T. B. Rauchfuss, D. F. Rosenbaum and C. F. Zukoski, *Chem. Mater.* **1995**, *7*, 2342.

(114) D. A. Foucher, I. Manners, *Makromol. Chem., Rapid Commun.* **1993**, *14*, 63.

(115) H. P. Withers, D. Seywerth, J. D. Fellmann, P. E. Garrou, S. Martin, *Organometallics*, **1982**, *1*, 1283.

(116) J. M. Yu, P. Dubois, P. Teyssié, R. Jérôme, *Macromolecules*, **1996**, *29*, 6090.

(117) J. M. Yu, P. Dubois, P. Teyssié, R. Jérôme, *Polymer,* **1997**, *38*, 3091.

(118) R. S. Benson, Q. Wu, A. R. Ray, D. J. Lyman, *J. Polym. Sci. Polym. Chem. Ed.* **1985**, *23*, 399.

(119) J. C. Chen, L. J. Fetters, *J. Vinyl Technol.* **1987**, *9*, 1300.

(120) F. S. Bates, G. H. Fredrickson, *Annu. Rev. Phys. Chem.* **1990**, *41*, 525.

(121) H. A. Klok, S. Lecommandoux, *Adv. Mater.* **2001**, *13*, 1217.

(122) A. C. Edrington, A. M. Urbas, N. Hadjichristidis, *Adv. Mater.* **2001**, *13*, 421.

(123) I. W. Hamley, *The Physics of Block Copolymers*, Oxford University Press, Oxford **1999**.

(124) P. Mansky, P. Chaikin, E. L. Thomas, *J. Mater. Sci.* **1995**, *30*, 1987.

(125) M. Park, C. Harrison, D. H. Adamson, *Science*, **1997**, *276*, 1401.

(126) J. Raez, I. Manners, M. A. Winnik, *J. Am. Chem. Soc.* **2002**, *124*, 10381.

(127) N. Hadjichristidis, S. Pispas, G. Floudas, "Block Copolymers, Synthetic Strategies, Physical Properties and Applications", Wiley, New Jersey **2003**.

(128) S. Patel, J. W. Goodby, P. L. Finn, *Phys. Rev. Lett.* **1989**, *62*, 1764.

(129) D. D. Ling, B. Friman, G. Grinstein, *Phys. Rev. B*, **1981**, *24*, 2718.

(130) L. Leibler, *Macromolecules*, **1980**, *13*, 1602.

(131) E. L. Thomas, D. B. Alward, D. J. Kinning, D. C. Martin, L. J. Fetters, *Macromolecules*, **1986**, *19*, 2197.

(132) J. D. Litster, R. J. Birgeneau, M. Kaplan, S. Mathiesen, *Phys. Rev. B*, **1980**, *22*, 312.

(133) G. H. Fredrickson and K. Binder, *J. Chem. Phys.* **1989**, *91* (11), 7265.

(134) G. Floudas, G. Fytas, N. Hadjichristidis, M. Pitsikalis, *Macromolecules*, **1995**, *28*, 2359.

(135) G. H. Fredrickson, E. Helfand, *J. Chem. Phys.* **1987**, *87*, 697.

(136) F. S. Bates, J. H. Rosedale, G. H. Fredrickson, *J. Chem. Phys.* **1990**, *92*, 6255.

(137) T. Wolff, C. Burger, W. Ruland, *Macromolecules*, **1993**, *26*, 1707.

(138) G. Floudas, T. Pakula, E. W. Fischer, N. Hadjihristidis, S. Pispas, *Acta. Polym.* **1994**, *45*, 176.

(139) C. D. Han, J. K. Kim, *Macromolecules*, **1989**, *22*, 383.

(140) K. R. Amundson, E. Helfand, S. S. Patel, Z. Quan, S. D. Smith, *Macromolecules*, **1992**, *25*, 1935.

(141) P. J. Flory, *J. Chem. Phys.* **1942**, *10*, 51.

(142) Flory and Huggins, *J. Phys. Chem.* **1942**, *46*, 151.

(143) Flory and Huggins, *J. Am. Chem. Soc.* **1942**, *64*, 1712.

(144) S. Strobel, *The Physics of Polymers*, Springer: Berlin, Heidelberg, New York, **1997**.

(145) R. J. Young, P. A. Lovell: *Introduction to Polymers*, Chapman and Hall: London, Weinheim, New York, **1991**.

(146) D. Leary and M. Williams, *Journal of Polymer Science Part B*, **1970**, *8*, 335.

(147) D. Leary and M. Williams, *Journal of Polymer Science: Polymer Physics*, **1973**, *11*, 345.

(148) D. Leary and M. Williams, *Journal of Polymer Science: Polymer Physics*, **1974**, *12*, 265.

(149) D. J. Meier, *Journal of Polymer Science C*, **1969**, *26*, 81.

(150) E. Helfand and Z. R. Wasserman, *Macromolecules*, **1976**, *9*, 879.

(151) E. Helfand, *Macromolecules*, **1975**, *8*, 552.

(152) E. Helfand, *Journal of Chemical Physics*, **1975**, *62*, 999.

(153) H. Hasegawa, H. Tanaka, K. Yamasaki and T. Hashimoto, *Macromolecules*, **1987**, *20*, 1651.

(154) L. Leibler, *Macromolecules*, **1980**, *13*, 1602.

(155) M. W. Matsen and F. S. Bates, *Macromolecules*, **1969**, *29*, 1091.

(156) M. W. Matsen and M. Schick, *Macromolecules*, **1994**, *27*, 6761.

(157) M. W. Matsen and M. Schick, *Physical Review Letters*, **1994**, *72*, 2660.

(158) E. F. David and K. S. Schweizer, *Journal of Chemical Physics*, **1994**, *100*, 7767.

(159) E. F. David and K. S. Schweizer, *Journal of Chemical Physics*, **1994**, *100*, 7784.

(160) F. S. Bates and G. H. Fredrickson, *Annual Reviews of Physical Chemistry*, **1990**, *41*, 525.

(161) J. M. Seddon, *Biochimica et Biophysica Acta*, **1990**, *1*, 1031.

(162) M. F. Schulz, F. S. Bates, and K. Mortensen, *Physical Review Letters*, **1994**, *73*, 86.

(163) D. A. Hajduk, S. M. Gruner, C. C. Honeker, E. L. Thomas, L. J. Fetters, *Macromolecules*, **1995**, *28*, 2570.

(164) S. Förster, A K. Khandpur, F. S. Bates, I. W. Hamley, *Macromolecules*, **1994**, *27*, 6922.

(165) I. W. Hamley, K. A. Koppi, J. H. Rosedale, F. S. Bates, K. Mortensen, *Macromolecules*, **1993**, *26*, 5959.

(166) C. Auschra, R. Stadler, *Macromolecules*, **1993**, *26*, 2171.

(167) W. Zheng, Z. G. Wang, *Macromolecules*, **1995**, *28*, 7215.

(168) U. Breiner, U. Krappe, R. Stadler, *Macromolecular Rapid Communications*, **1996**, *17*, 567.

(169) U. Breiner, U. Krappe, V. Abetz, R. Stadler, *Macromolecular Chemistry and Physics*, **1997**, *198*, 1051.

(170) U. Krappe, R. Stadler, I. Voigt-Martin, *Macromolecules*, **1995**, *28*, 4558.

(171) R. Stadler, C. Auschra, J. Beckmann, U. Krappe, I. Voigt-Martin, *Macromolecules*, **1995**, *28*, 3080.

(172) V. Abetz in *Comprehensive Polymer Science*, Vol. 3, G. Allen, J. C. Bevington (Hrsg.), Pergamon: Oxford, **2003**, *3*, 482 .

(173) J. M. Halls, C. A. Walsh, A. B. Holmes, *Nature*, **1995**, *376*, 498.

(174) M. Grandstrom, K. Petritsch, R. H. Friend, *Nature*, **1998**, *395*, 257.

(175) S. A. Chen, Y. Fang, *Synth. Met.* **1993**, *60*, 215.

(176) E. M. Genies, M. Lapkowski, *Synth. Met.* **1988**, *24*, 69.

(177) P. K. Shen, Z. Q. Tian, *Electrochim. Acta*, **1989**, *34*, 1611.

(178) P. A. Kilmartin, G. A. Wright, *Electrochim. Acta*, **1998**, *43*, 3091.

(179) Y. Greenwald, J. Poplawski, S. Speiser, *Synth. Met.* **1997**, *85*, 1353.

(180) O. A. Semenikhin, Z. A. Rotenberg, E. V. Kazarinov, *J. Electroanal. Chem.* **1999**, *463*, 190.

(181) S. Jin, G. Xue, *Appl. Phys. A.* **1996**, *63*, 397.

(182) C. K. Chiang, A. J. Heeger, A. G. MacDiarmid, *Phys. Rev. Lett.* **1977**, *39*, 1098.

(183) Ito, H. Shirakawa, S. Ikeda, *J. Polym. Sci. Polym. Chem. Ed.* **1974**, *12*, 11.

(184) C. K. Chiang, C. R. Fischer, H. Shirakawa, A. G. MacDiarmid, *Phys. Rev. Letters*, **1977**, *39*, 1098.

(185) M. A. Druy, S. C. Gau, A. J. Heeger, Y. W. Park, H. Shirakawa, *J. Am. Chem. Soc.* **1978**, *100*, 1013.

(186) Y. M. Paushkin, T. P. Vishnyakova, A. F. Lunin, S. A. Nizova, Organic Polymeric Semiconductors (Translated from Russian by R. Kondor), John Wiley & Sons, **1974**, p 10

(187) T. Yamamoto, K. Sanechika, A. Yamamoto, *Inorganica Chimica Acta*, **1983**, *73*, 75.

(188) K. Sanechika, T. Yamamoto, A. Yamamoto, *Polym. J.* **1981**, *13*, 225.

(189) J. C. W. Chien, R. D. Gooding, C. P. Lillya, *Polym. Mater. Sci. Eng.* **1993**, *49*, 107.

(190) T. Yamamoto, K. Sanechika, A. Yamamoto, M. Katada, *Inorg. Chim. Acta.* **1983**, *73*, 75.

(191) C. LeVanda, D. O. Cowan, C. Leitch, K. Bechgaard, *J. Am. Chem. Soc.* **1974**, *96*, 6788.

(192) T. Hirao, K. Mamoru, K. Aramaki, H. Nishihara, *J. Chem. Soc., Dalton Trans*, **1996**, *14*, 2929.

(193) J. Chien, R. Gooding, C. Lillya, *Polym. Mater. Sci. Eng.* **1993**, *49*, 107.

(194) B. C. Crandall, J. Lewis, *Nanotechnology: Research and Perspectives*, *The MIT Press: Cambridge, MA*, **1992**.

(195) D. Gatteschi, O. Kahn, J. S. Miller, *Magnetic Molecular Materials, Series E: Applied Sciences; Kluwer Academic Press: Dordrecht, The Netherlands*, **1991**; *Vol. 198.*

(196) C. Kloninger, M. Rehahn, *Macromolecules*, **2004**, *37*(5), 1720.

(197) C. Kloninger, D. Knecht, M. Rehahn, *Polymer*, **2004**, *45*(25), 8323.

(198) C. Kloninger, M. Rehahn, *Macromolecules*, **2004**, *37*(22), 8319.

(199) U. Datta, M. Rehahn, *Macromol. Rapid Commun.* **2004**, *25*, 1615.

(200) Y. M. Paushkin, T. P. Vishnyakova, A. F. Lunin, S. A. Nizova, *Organic Polymeric Semiconductors (Translated from Russian by R. Kondor). John Wiley & Sons Ltd., Chichester*, **1974**, p 30

(201) M. S. Wrighton, M. C. Palazzotto, A. B. Bocarsly, J. M. Bolts, A. F. Fischer, L. Nadjo, *J. Am. Chem. Soc.* **1978**, *11*, 7264.

(202) K. H. Ahn, C. W. Cho, H. H. Baek, J. Park, S. Lee, *J. Org. Chem.* **1996**, *61*, 4937.

(203) N. Yizeng, R. Rulkens, I. Manners, *J. Am. Chem. Soc.* **1996**, *118*, 4102.

(204) B. Bildstein, M. Malaun, H. Kopacka, K. Wurst, M. Mitterbock, *Organometallics*, **1999**, *18*, 4325.

(205) G. Osborne and R. H. Whiteley, *J. Organomet. Chem.* **1975**, 101, C27.

(206) H. L. Hsieh, R. P. Quirk: *Anionic Polymerization: Principles, Practice and Applications*, Marcel Dekker: New York, 1996.

(207) R. G. H. Lammertink, M. A. Hempenius, E. L. Thomas, G. J. Vancso, *J. Polym. Sci., Part B: Polym. Phys.* **1999**, *37*, 1009.

(208) H. C. Wang, C. Levin, M. Szwarc, *J. Am. Chem. Soc.* **1978**, *100*, 3969.

(209) L. I. Denisovich, S. P. Gubin, *J. Organomet. Chem.* **1973**, *75*, 109.

(210) F. G. Bordwell, H. E. Fried, *J. Org. Chem.* **1981**, *46*, 4327.

(211) D. M. Wiles, S. Bywater, *J. Phys. Chem.* **1964**, *68*, 1983.

(212) J. M. Yu, P. Dubois, R. Jérôme, *Macromolecules*, **1997**, *30*, 4984.

(213) Christian Kloninger, *Ph.D. Dissertation, Dem Fachbereich Chemie der Technischen Universität Darmstadt*, **2004**.

(214) M. S. Gordon, J. A. Boatz, R. Walsh, *J. Phys. Chem.* **1989**, *39*, 1584.

(215) K. Matsumoto, H. Yamaoka, *Macromolecules*, **1995**, *28*, 7029.

(216) R. K. Sheikh, K. Tharanikkarasu, I. Imae, Y. Kawakami, *Macromolecules*, **2001**, *34*, 4384.

(217) F. S. Bates, *Science*, **1991**, *251*, 898.

(218) M. Morton, *"Anionic Polymerisation: Principles and Practice"*, Academic Press, New York **1983**, p.21.

(219) U. Johnsen, *Kolloid-Zeitschrift and zeitschrift fur polymere*, **1961**, 178.

(220) J. Wang, R. Jérôme, R. Warin, P. Teyssié, *Macromolecules*, **1993**, *26*, 5984.

(221) J. Brandrup, E. H. Immergut, *Polymer Handbook*, 3rd edition, Wiley, New York **1989**.

(222) R. A. Register, *Nature*, **2003**, *Vol 424*, 378.

(223) S. O. Kim, H. H. Solak, M. P. Stoykovich, P. F. Nealey, *Nature*, **2003**, *Vol 424*, 411.

(224) T. Inuoe, T. Soen, T. Hashimoto, H. Kawai, *J. Polym. Sci. A2*, **1969**, *7*, 1283.

(225) T. Inoue, T. Soen, H. Kawai, M. Fukatsu, M. Kurata, *J. Polym. Sci. B*, **1968**, *6*, 75.

(226) M. Shibayama, T. Hashimoto, H. Kawai, *Macromolecules*, **1982**, *15*, 16.

(227) Y. Isono, H. Tanisugi, K. Endo, T. Fujimoto, H. Hasegawa, T. Hashimoto, H. Kawai, *Macromolecules*, **1983**, *16*, 5.

(228) Y. Miyaki, M. Iwata, Y. Fujita, H. Tanisugi, Y. Isono, T. Fujimoto, *Macromolecules*, **1984**, *17*, 1907.

(229) S. Takahashi, K. Matsumura, M. Toda, T. Fujimoto, H. Hasegawa, Y. Miyaki, *Polym. J.*, **1986**, *18*, 41 .

(230) G. Scatchard, *Chem. Rev.* **1931**, *8*, 321.

(231) D. M. Koenhen, C. A. Smolders, *J. Appl. Polym. Sci.* **1975**, *19*, 1163.

(232) U. Siemann, *Eur. Polym. J.* **1992**, *28*, 293.

(233) C. Marco, A. Bello, J. Garza, *Makromol. Chem.* **1986**, *187*, 177.

(234) A. J. Ashworth, G. J. Price, *Macromolecules*, **1986**, *19*, 362.

(235) Y. Yagi, H. Inomata, S. Saito, *Macromolecules*, **1992**, *25*, 2997.

(236) K. Kulbaba, E. B. Evans, I. Manners, *Macromol. Chem. Phys.* **2001**, *202*, 1768.

(237) I. C. McNeill, *Comprehensive Polymer Science*, Pergamon: Oxford, **1988**, S. 387.

(238) B. Z. Tang, R. Peterson, D. A. Foucher, A. Lough, R. Sodhi, I. Manners, *J. Chem. Soc. Chem. Commun.* **1993**, 523.

(239) R. Peterson, D. A. Foucher, B. Z. Tang, A. Lough, N. P. Raju, J. E. Greedan, I. Manners, *Chem. Mater.* **1995**, *7*, 2045.

(240) S. Varshney, C. Jacobs, J. P. Hautekeer, P. Bayard, R. Jérôme, *Macromolecules*, **1991**, *24*, 4997.

(241) *Encyclopedia of Polymer Science and Engineering*, 2nd ed. John Wiley & Sons, Inc. New York, **1987**, *Vol. 16*, p 1.

(242) A. Noshay, J. E. McGrath, *Block Copolymers, Overview and Critical Survey*, Academic Press: New York, **1977**, p 187.

(243) U. Breiner, U. Krappe, E. L. Thomas, R. Stadler, *Macromolecules*, **1998**, *31*, 135.

(244) K. J. Hanley and T. P. Lodge, *Macromolecules*, **2000**, *33*, 5918.

(245) U. Breiner, U. Krappe, T. Jakob, V. Abetz, R. Stadler, *Polym. Bull.* **1998**, *40*, 219.

(246) G. Reiss, M. Schlienger, S. J. Marti, *J. Macromol. Sci. Phys.* **1989**, *B17*, 355.

(247) R. Stadler, C. Auschra, J. Beckmann, U. Krappe, I. Voigt-Martin, L. Leibler, *Macromolecules*, **1995**, *28*, 3080.

(248) W. Stocker, J. Beckmann, R. Stadler, J. P. Rabe, *Macromolecules*, **1996**, *29*, 7502.

(249) O. Glatter, O. Kratky, *Small Angle X-ray Scattering*, New York: Academic Press, **1982**.

(250) K. I. Winney, E. L. Thomas, L. J. Fetters, *Macromolecules*, **1992**, *25*, 422.

(251) T. Hashimoto, H. Tanaka, H. Hasegawa, *Macromolecules*, **1990**, *23*, 4378.

(252) H. Tanaka, H. Hasegawa, T. Hashimoto, *Macromolecules*, **1991**, *24*, 240.

(253) H. Tanaka, T. Hashimoto, *Macromolecules*, **1991**, *24*, 5713.

(254) T. A. Witten, L. Leibler, P. A. Pincus, *Macromolecules*, **1992**, *25*, 422.

(255) S. Koizumi, H. Hasegawa, T. Hashimoto, *Makromol. Chem. Macromol. Symp.* **1992**, *62*, 75.

(256) J. Raez, Y. Zhang, L. Cao, S. Petrov, K. Erlacher, I. Manners, M. A. Winnik, *J. Am. Chem. Soc.* **2003**, *125*, 6010.

(257) A. R. Blythe, *Electrical Properties of Polymers*, *Cambridge University Press*, **1979**.

(258) P. Park, A. J. Lough, D. A. Foucher, *Macromolecules*, **2002**, *35*, 3810.

(259) Y. H. Kang, K. Kim, *Tetrahedron*, **1999**, *55*, 4271.

(260) J. S. Trent, J. I. Scheinbein, P. R. Couchman, *Macromolecules*, **1983**, *16*, 589.

(261) R. Vitali, E. Montani, *Polymer*, **1980**, *21*, 1220.

(262) K. Kato, *Polym. Lett.* **1966**, *4*, 35.

CURRICULUM VITAE

Name	UTTAM DATTA
Date and Place of Birth	11th November 1973 (New Delhi)
Nationality	Indian

Educational Profile

1997 - 1999	M.Tech- Chemical Analysis and Control. I. I. T- Delhi, New Delhi (India)
1995 - 1997	M.Sc. Chemistry. I. I. T- Delhi, New Delhi (India)
1992 - 1995	B.Sc. (Hons) Chemistry. University of Delhi, Delhi (India)

Awards and Scholarships

Received a **D.A.A.D** research fellowship from the ***GERMAN ACADEMIC EXCHANGE SERVICE*** to carry out thesis cum research work required for the degree (Master of Technology) in collaboration with *UNIVERSITY OF STUTTGART (INSTITUTE FÜR ORGANISCHE CHEMIE UND ISOTOPANFORSCHUNG)* as a part of networking between the I.I.T's and the German universities for a period of nine months ie. *June 1998 – February 1999*.

Graduate Aptitude Test for Engineering (**GATE-1997**) Scholarship awarded by Indian Institute of Technology, Delhi with the percentile of 99.05. All India Rank 13 out of 10,000 candidates.

Industrial Research Experience

- **Ranbaxy Research Laboratories,** Delhi (India)
  (**Research Associate,** *March 1999 –October 2000*)
  (India's number one Pharmaceutical Company in New Drug Formulations)

- **GE (General Electric) –** JFWTC, Bangalore (India)
  (**Research Scientist,** *November 2000 – May 2002*)
  (GE's First Corporate R & D other than New York, Schenectady, USA)

Publications

- Synthesis and Self-Assembly of Styrene–[1]Dimethylsilaferrocenophane–Methyl Methacrylate Pentablock Copolymers. Uttam Datta, Matthias Rehahn, ***Macromol. Rapid Commun.*** **2004**, *25*, 1615.

- Synthesis and Bulk Morphology of Styrene-Ferrocenylsilane-Methyl Methacrylate Tri- and Pentablock Copolymers. Christian Kloninger, Uttam Datta and Matthias Rehahn. ***ACS Symposium Series 2005*** **(Submitted)**.

Eidesstattliche Erklärung

Ich erkläre hiermit an Eides statt, dass ich meine Dissertation selbstständig und nur mit den angegebenen Hilfsmitteln angefertigt habe.

Datum:
Ort: Darmstadt

Uttam Datta,
In Der Kirchtanne 27, WG312,
Eberstadt, Darmstadt- 64297

Erklärung

Ich erkläre hiermit, noch keinen Promotionversuch unternommen zu haben.

Datum:
Ort: Darmstadt

Uttam Datta,
In Der Kirchtanne 27, WG312,
Eberstadt, Darmstadt- 64297